AN ABSTRACT OF THE THESIS OF

Paul Eric Bacon for the degree of Master of Science in Chemistry presented on August 21, 1995. Title: Searching for New Niobium Oxide Based Superconductors.

Abstract approved: Redacted for Privacy

Arthur W. Sleight

A new niobium compound, represented by the formula Ca_xNbO_3, with a range of composition has been found. Samples ranging from x = 0.56 to x = 1.00 were prepared and analyzed by powder x-ray diffraction. X-ray data indicated a range of composition from x = 0.66 to x = 0.96. Samples with compositions of x = 0.66 and x = 0.96 were used for Rietveld powder structure determinations. Refined calcium contents indicated a range of composition from 0.66 to 0.86. $Ca_{0.66}NbO_3$ was found, with an R value of 8.75%, to be orthorhombic, Pnma, with lattice parameters of a = 5.518Å, b = 7.824Å, and c = 5.516Å. The $Ca_{0.96}NbO_3$ sample was found, with R = 7.27%, to be monoclinic, $P2_1/m$, with a = 5.520Å, b= 7.884Å, c = 5.608Å, and β = 90.013°. Magnetic susceptibility measurements showed no superconducting transitions for the powders tested. Electron microprobe showed the samples to be several phase mixtures. A single crystal structural determination was also conducted. The single crystal results indicated a cubic, Pm-3m, with a = 7.828Å. The formula refined to $Ca_{0.75}NbO_3$ with eight formula units per unit cell. The R value was 2.26% with a weighted R of 4.09%.

Mixtures of Nb metal and BaO_2 fired in air were analyzed by x-ray diffraction, electron microprobe, and magnetic susceptometry. The products contained NbN and not a new barium niobium oxide as suggested by the literature. Ta was also found to produce a nitride phase when ignited with BaO_2 in air.

An attempt to shed some light on the reaction between $YBa_2Cu_3O_6$ and iodine was made. Samples were reacted with iodine for different lengths of time. Powder x-ray diffraction, electron microprobe and magnetic susceptometry were used to characterize the products. A T_c between 55 and 60K were observed. No impurity lines in the powder patterns could be matched to impurities on file. Due to small particle size and heterogeneous products, electron microprobe was not very enlightening.

Searching for New Niobium Oxide Based Superconductors

by

Paul Eric Bacon

A THESIS

submitted to

Oregon State University

in partial fulfillment of
the requirements for the
degree of

Master of Science

Completed August 21, 1995
Commencement June 1996

Master of Science thesis of Paul Eric Bacon presented on August 21, 1995

APPROVED:

Redacted for Privacy

Major Professor, representing Chemistry

Redacted for Privacy

Chair of Department of Chemistry

Redacted for Privacy

Dean of Graduate School

I understand that my thesis will become part of the permanent collection of Oregon State University libraries. My signature below authorizes release of my thesis to any reader upon request.

Redacted for Privacy

Paul Eric Bacon, Author

Acknowledgment

I would like to thank all of the following:

my major professor: Dr. A. W. Sleight

and my committee: Dr. G. T. Evans, Dr. D. A. Keszler, Dr. M. M. Lerner, Dr. R. T. Mason

people from the Sleight group:
Dr. Laura King, Dr. Ruiping Wang, Dr. Vince Korthuis, Dr. Phong Nguyen, Dr. Sasirekha Kodialam, Dr. Richard Mackay, Dr. Mark Kennard, Dr. Mary Thundathil, Dr. Seung-Tae Hong, Dr. John Evans, Dr. Rolf-Deiter Hoffmann, Dr. Jianguo Hou, Pat Woodward, Matt Hall, Nazy Khosrovani, Mahadevan Thangaraju

people from other groups:
John Lemmon, Steve Sloop, Chris Herring

my mum M. Eileen Bacon
my dad Michael E. Bacon,
my sister Alisa A. Bacon,
my brother and sister in law Neil A. Bacon and Jenny Lee,
and the whole extended family on my mother's side

Anna Marie Wood

all of my friends scattered all around the country
Karen Mitchell, Dave Fernandes, Erin Carr, Brian Kirchner, Rachel Dolan, Glenn Brooks Barton, Adam Conover, Jason Brakeman, Larry Sanker III, the Sanker family, Harry Bancroft, Abigail Pleasure

and the U.S. Air Force for funding my research.

Table of Contents

Table of Contents (Continued)

List of Figures

List of Figures (Continued)

List of Figures (Continued)

List of Tables

Searching for New Niobium Oxide Based Superconductors

I. Introduction

Niobium metal has the highest superconducting transition temperature (T_c), at 9.5 K, of all of the superconducting elements. Compounds of niobium that have been found to superconduct include A-15 intermetallics, carbides, nitrides, borides, and oxides. Despite much research in niobium oxides, the highest T_c found so far is 5.5 K for $Li_{0.45}NbO_2$ [1]. There are many niobium oxides of the A_xNbO_3 type that have been investigated in hopes of finding a higher T_c.

A_xNbO_3 compounds are of interest for several reasons. The first is that the formula A_xNbO_3 suggests structures related to the perovskite ($CaTiO_3$) structure or tungsten bronze type structures(see fig 1.). The perovskite structure type is of interest because related structures are found in some of the high T_c compounds. $YBa_2Cu_3O_7$ for example has a structure that can be viewed as related to the perovskite structure. In the literature some of these A_xNbO_3 compounds are referred to as bronzes because of their similarity to the tungsten bronzes which are highly colored, have a range of composition, metallic luster, and metallic or semiconducting properties.

The compounds that have a range of composition have a variable niobium oxidation state. When A is a +2 cation and x = 1 niobium has to be Nb^{IV} (d^1). If $x < 1$ some of the niobium will be oxidized to Nb^{V} (d^0). At x = 0.5 all of the niobium will be Nb^{V} and no further loss of A cations can occur without the loss of oxygen. This variability of

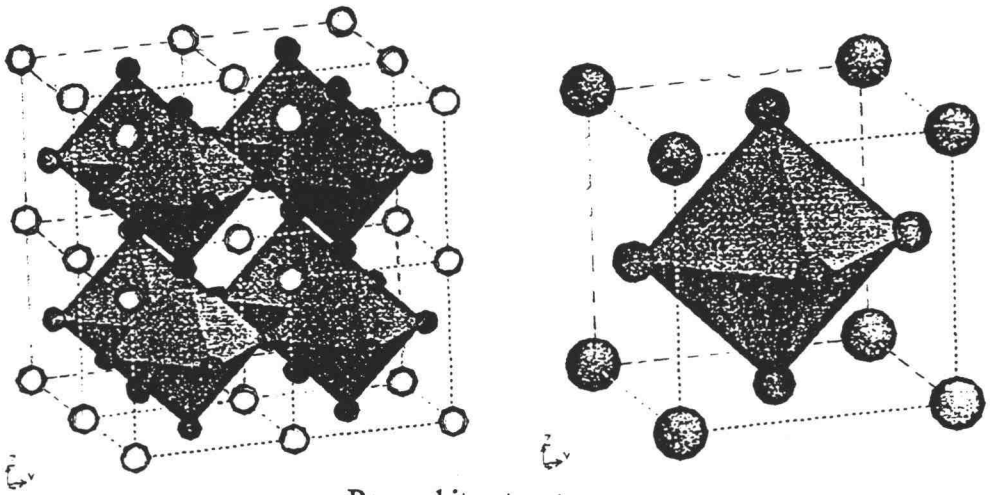

Perovskite structure

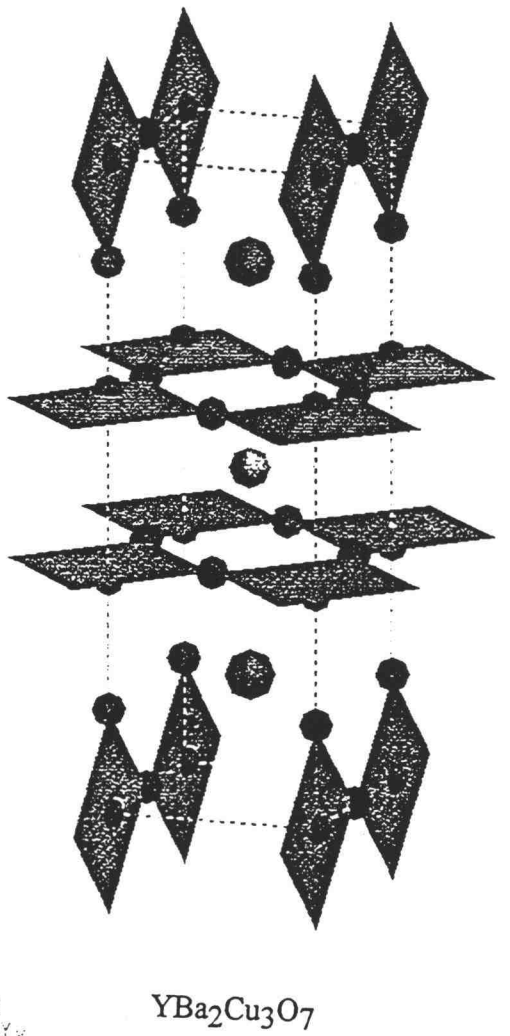

$YBa_2Cu_3O_7$

Figure 1: The Perovskite and $YBa_2Cu_3O_7$ structures

composition allows a variability in the number of electrons and the density of states at the fermi level. In Bardeen, Cooper, and Schrieffer's theory of superconductivity (BCS theory), the T_c is influenced by the density of states (N(0)) at the fermi level : $kT_c = 1.14\hbar\omega\exp[-1/(N(0)V]$ when $kT_c << \hbar\omega$ [2]. When the niobium is all Nb^V (d^0) the d band is empty and the fermi level lies in the band gap between the filled O p band and the empty d band. The density of states at the fermi level is zero and the compound is an insulator. With the reduction of some of the niobium the d band begins to fill and the fermi level is then within a band giving $N(0) > 0$. The largest density of states is at the bottom and top of a band and superconductivity is often observed near an insulator to metal transition.

$LiNbO_3$ has a structure related to the α-Al_2O_3 structure (fig 2) not the perovskite structure [3]. The unit cell consists of a stack of six irregular octahedra sharing faces. This stack is along the trigonal c axis and the cations fill the octahedra in the sequence: Nb, vacancy, Li, Nb, vacancy, Li [4]. Stoichiometric $LiNbO_3$ is an incongruent melter so crystals are made by equilibrating no stoichiometric crystals from the melt with Li vapor. Crystals grown from the melt have the composition $Li_{0.942}NbO_{2.971}$. Both crystal structures are in space group R3c with lattice parameters of a = 5.14739Å and c = 13.85614Å for $LiNbO_3$ and a = 5.15052Å and c = 13.86496Å for $Li_{0.942}NbO_{2.971}$ [5]. This material has been extensively studied for its ferroelectric, optoelectric, and nonlinear optic properties.

Li_xNbO_2 compounds have also been studied [1,6]. These are layered structures consisting of a hexagonal niobium arrangement, each niobium being in trigonal prismatic environment of oxygen (fig. 3). The Nb/O layers are separated by Li atoms. These

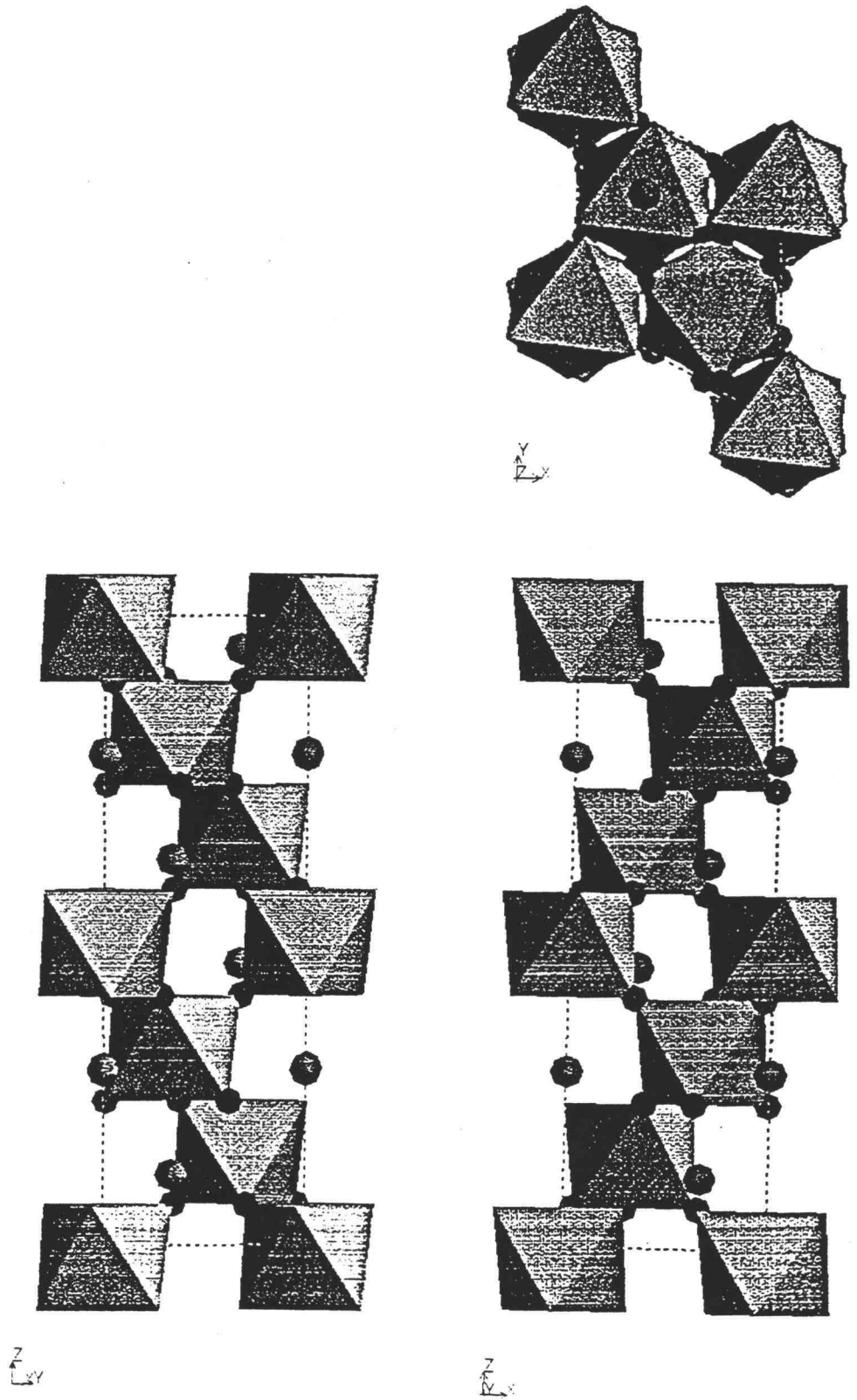

Figure 2: The structure of $LiNbO_3$

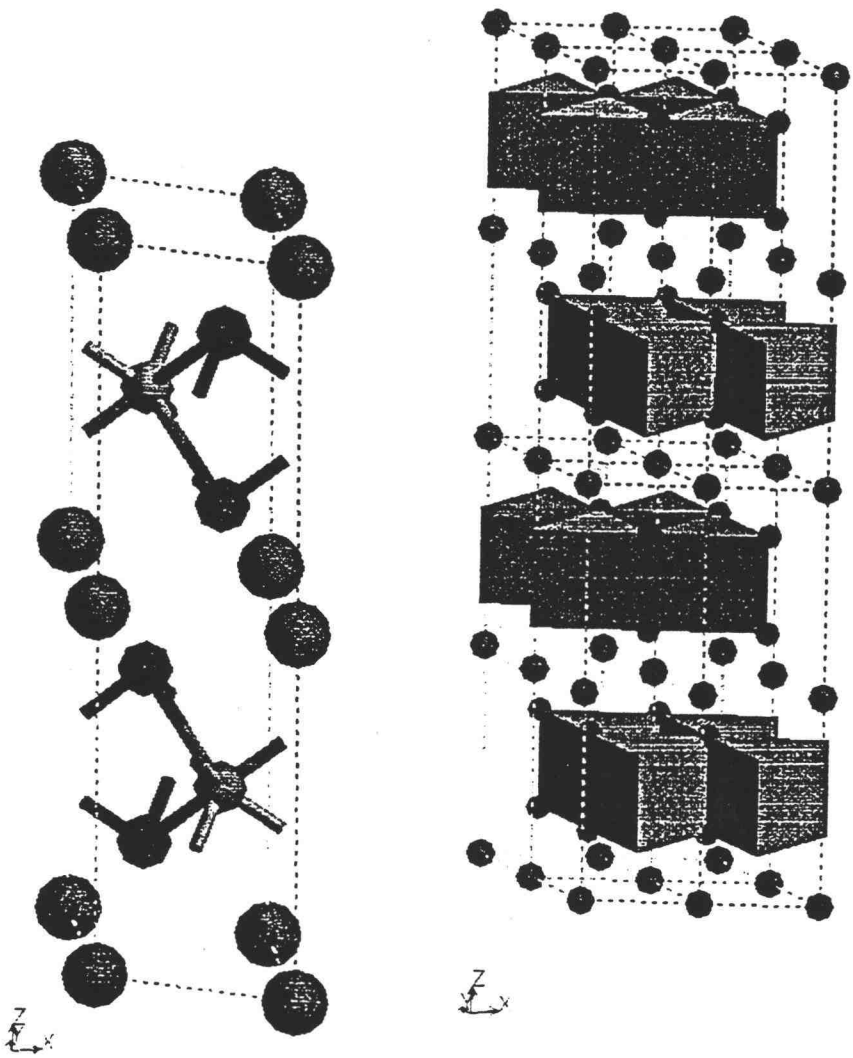

Figure 3: The structure of $LiNbO_2$

compounds have been found to superconduct with a maximum T_c of 5.5 K for the composition $Li_{0.45}NbO_2$ which is in space group $P6_3/mmc$ with lattice parameters of a = 2.9227Å and c = 10.455Å. This is the first layered early transition metal compound to show superconductivity.

$NaNbO_3$ at room temperature is a distorted perovskite in the orthorhombic space group Pbma (fig 4)[7]. The lattice parameters are a = 5.566Å, b = 15.520Å, and c = 5.506Å. The a and c parameters correspond to face diagonals of the simple perovskite unit cell ($\sqrt{2} \cdot a_p$) and b is four times this simple cell edge ($2a_p$). The distortion from the ideal perovskite structure can be visualized as a tilting of the quite regular NbO_6 octahedra. This tilting is by about ten degrees around both the a and b directions. In addition the Nb atoms are off the center of the octahedra. At higher temperatures $NaNbO_3$ undergoes several structural changes that can be described in terms of various tiltings of the NbO_6 octahedra [8,9]. $AgNbO_3$ is known and is isostructural with $NaNbO_3$ [10].

$KNbO_3$ is also perovskite related [11]. The room temperature structure is in the space group Bmm2 with cell parameters a = 5.697Å, b = 3.971Å, and c = 5.721Å (fig. 5). The parameters a and c are face diagonals of the simple perovskite cell. The Nb atoms are displaced off of the center of the nearly regular oxygen octahedra. $KNbO_3$ is ferroelectric and many studies of this compound center around its non-linear optical properties.

$RbNbO_3$ crystalizes in space group $P\bar{1}$ with lattice parameters a = 8.882Å, b = 8.395Å, c = 5.109Å, $\alpha = 94.60°$, $\beta = 95.53°$, and $\gamma = 113.83°$ [12]. The structure consists of Nb with a tetragonal pyramidal coordination by oxygen (fig 6). These tetragonal pyramids share all of their basal oxygens with neighboring pyramids to form long chains. These

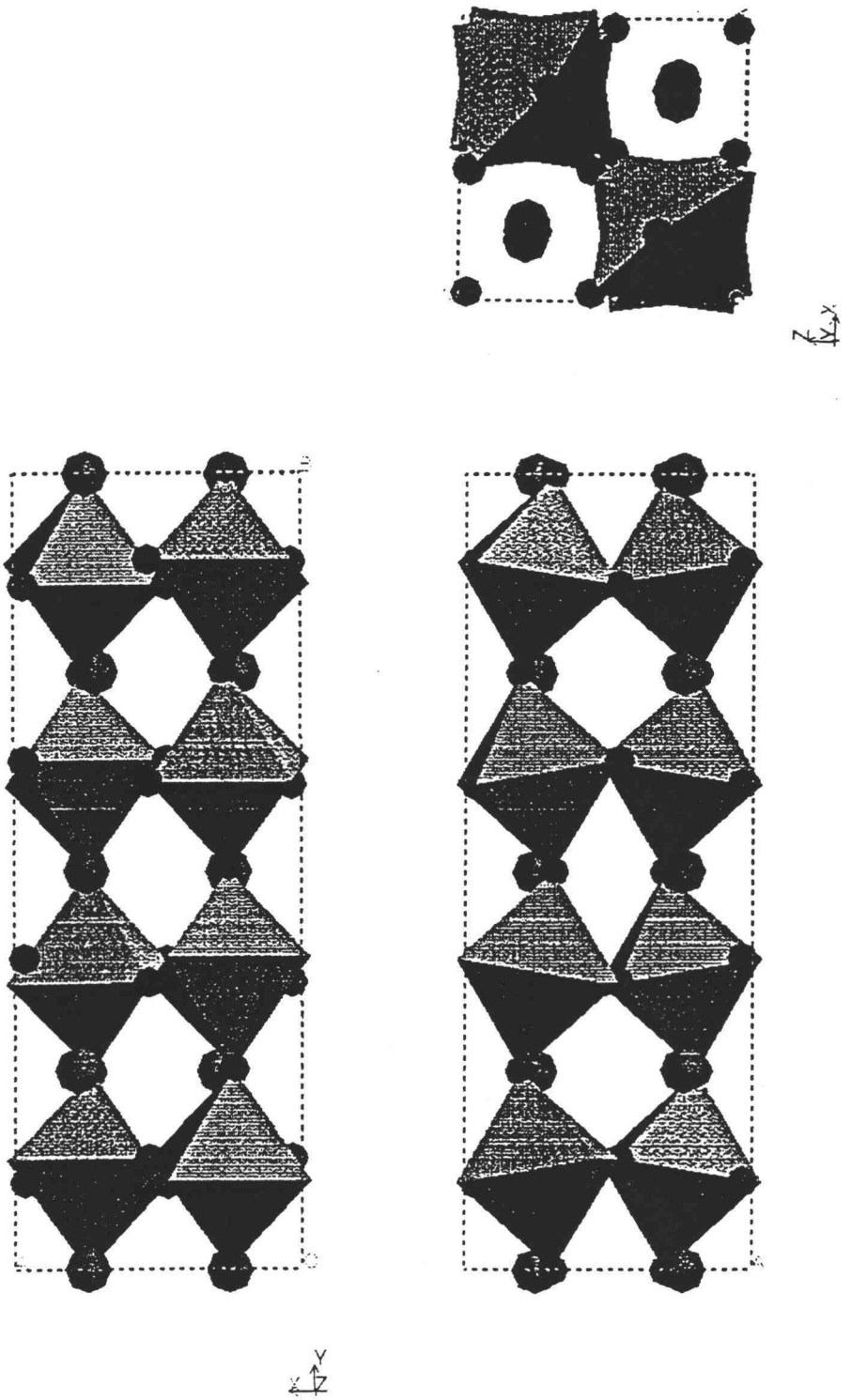

Figure 4: The structure of $NaNbO_3$

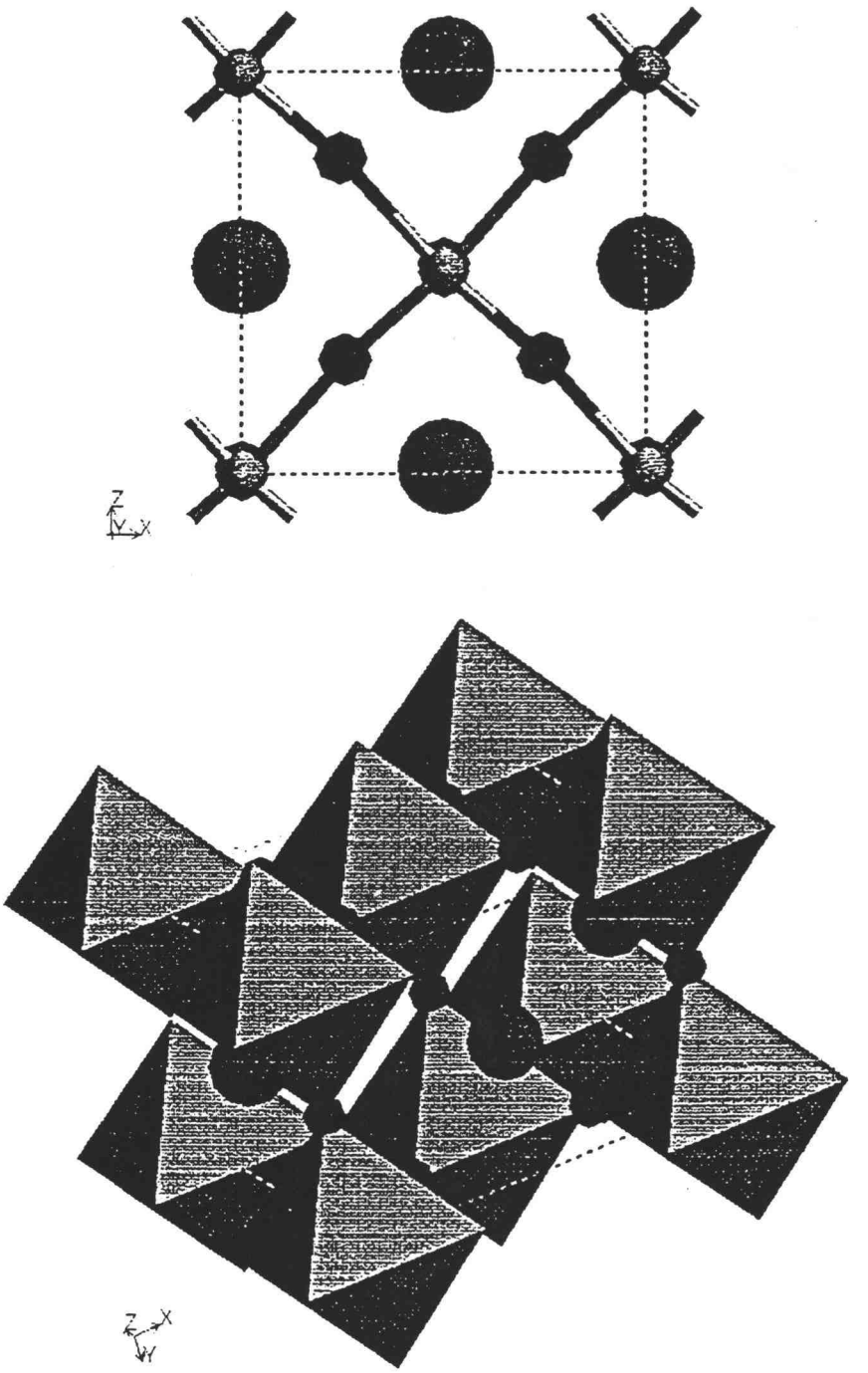

Figure 5: The structure of $KNbO_3$

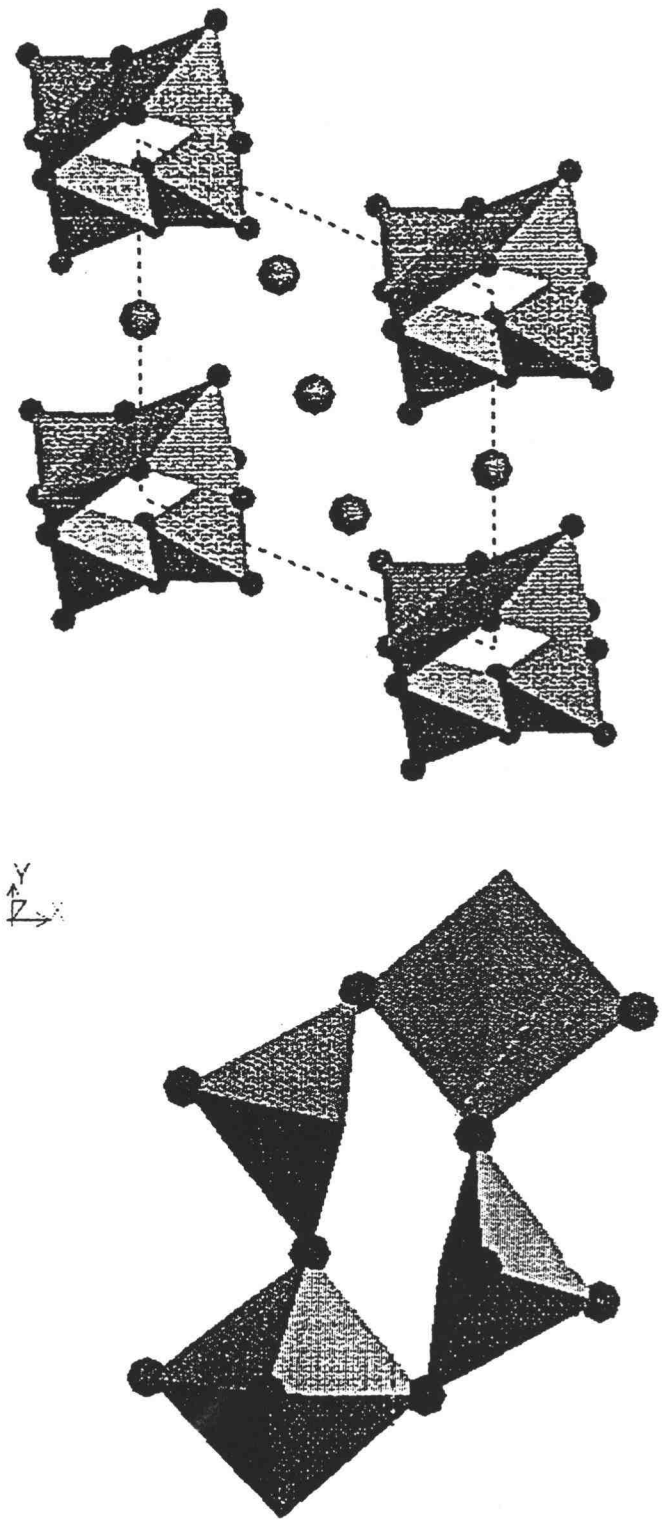

Figure 6: The structure of $RbNbO_3$ with pyramid linkage

chains are held together by Rb^+ . The crystals of this compound are colorless and very moisture sensitive.

$CsNbO_3$ also contains Nb in a tetragonal pyramidal coordination [13, 14]. The authors of the paper on this compound report that four of these pyramids link up to form isolated $[Nb_4O_{12}]$ clusters by sharing two basal oxygens with a neighboring pyramid. However, a computer generated plot of the structure using the given atomic positions reveals the presence of the same type of chains found in $RbNbO_3$ and not the isolated clusters claimed (fig 7). This compound crystalizes in the monoclinic space group $P2_1/c$ with lattice parameters of a = 5.14Å, b = 15.89Å, c = 9.14Å, and β = 93.3°.

The lanthanide elements are generally +3 cations so if x in $A^{III}_xNbO_3$ is one then Nb will have to be +III as well. When $x < 1$ some of the Nb will be oxidized and again the electronic properties will be variable with composition. $LaNbO_3$ for example, is a tetragonaly distorted perovskite with lattice parameters a = 5.554Å and c =7.85Å. It is synthesized from a stoichiometric mixture of La_2O_3, NbO, and NbO_2 at 1400°C in a high vacuum to obtain Nb in such a reduced state[15].

Other compounds of the formula $R_{1+x}Nb_3O_9$ (or $R_{(1+x)/3}NbO_3$) have been synthesized where x = 0-0.15 and R is lanthanum, cerium, or neodymium[16]. These compounds crystallize in space group Pmmm with a = 3.915Å, b = 3.924Å, and c = 7.932Å for $La_{0.38}NbO_3$. The structure can be viewed as a stack of layers in the sequence: $R_{2/3}\square_{1/3}O$ NbO_2 $\square O$ NbO_2 $R_{2/3}\square_{1/3}O$, where $\square$ is a vacancy (fig 8). No diamagnetism was found down to 12 K for these compounds.

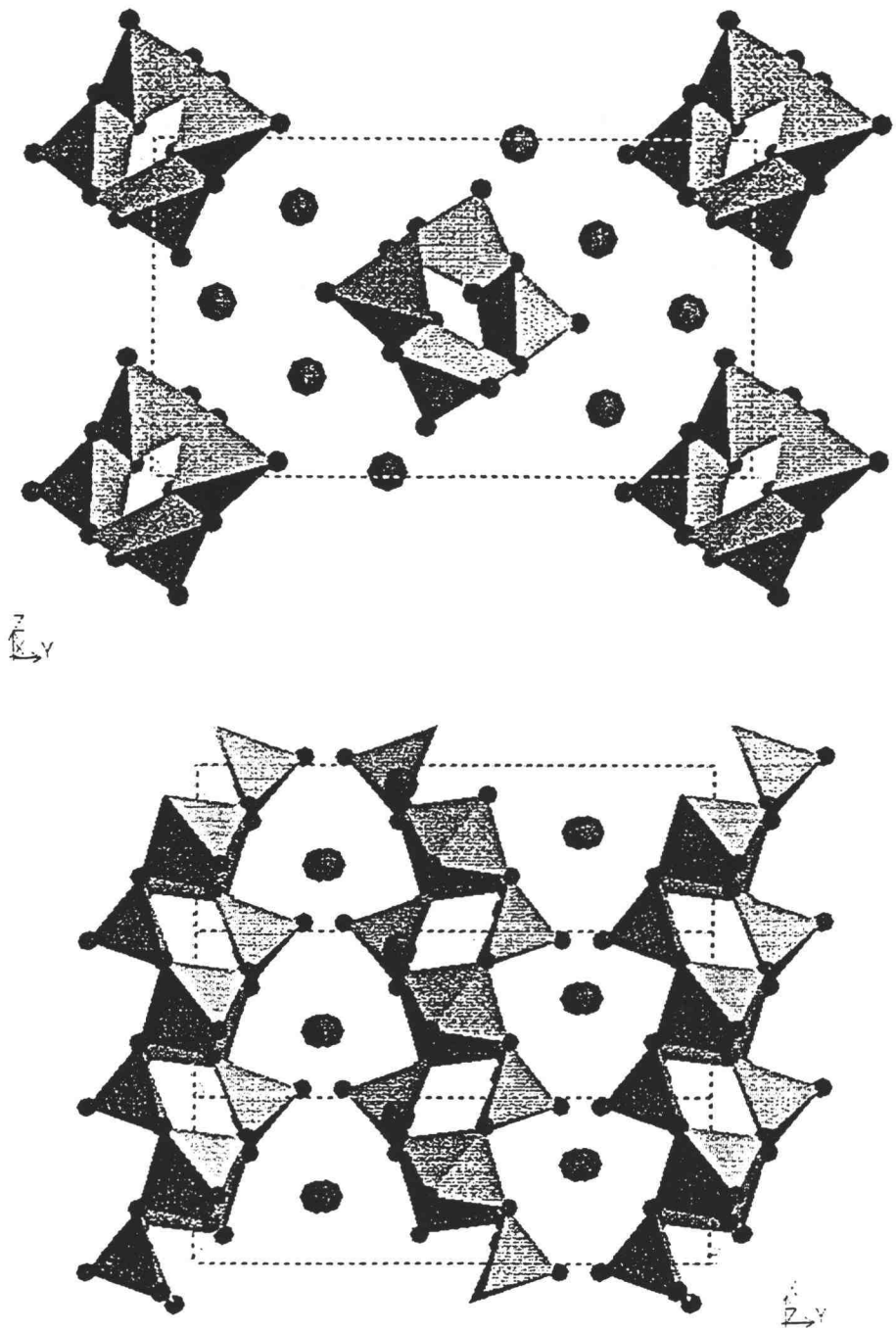

Figure 7: The structure of $CsNbO_3$

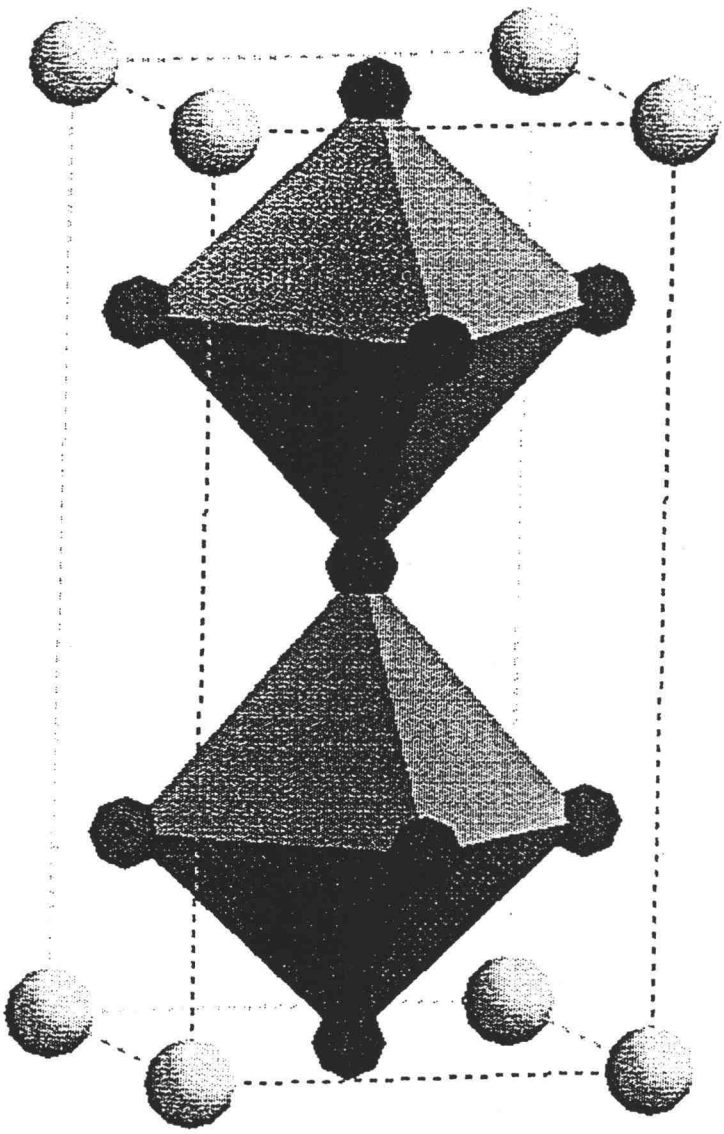

Figure 8: The structure of $R_{1+x}Nb_3O_9$

$LaNb_3O_9$ (or $La_{1/3}NbO_3$) is also reported in space group $P2_1/c$ with lattice parameters a = 5.437Å, b = 7.664Å, c = 16.323Å, and β = 92.198° [17].

In Eu_xNbO_y the Eu is mostly +II but some of it is +III and the amount of oxygen may also vary [18]. When the oxygen site is fully occupied (y = 3), the structure is tetragonal for x = 0.5 - 0.65 and cubic from x = 0.65 to x=1.00. For the tetragonal case the lattice parameters vary from 12.355Å and 3.901 for x = 0.50 to 12.361Å and 3.885 for x = 0.60. The cubic lattice parameter goes from 3.978Å to 4.026Å. If all of the Eu is +2 and all Nb is +4 the compounds are all cubic with lattice parameters varying from 3.982Å for y = 2.30 to 4.026Å for y = 3.00. Tetragonal samples are semiconducting and the cubic samples are metallic conductors.

In the $BaNbO_3$ system it appears that the range of composition is small if there is a range at all. Several studies of this compound have found essentially stoichiometric $BaNbO_3$ [19,20,21]. In one study however a single crystal with the composition of $Ba_{0.95}NbO_3$ was grown from a borate flux [22]. The structures are the perovskite structure in space group Pm3m with a lattice parameter of about 4.08Å.

The Sr_xNbO_3 system has a large range of compositional variability [23, 24]. X varies between 0.70 and 0.95. These compounds are cubic with the perovskite structure. the lattice parameter ranges from 3.981Å to 4.016Å as x increases and the color changes from dark blue to purple. The pressed powders show good conductivities. Above and below the range of x a mixture of products is observed.

There are also many compounds with mixtures of A^I and A^{II} cations [25, 26, 27]. Compounds like lead sodium niobate and sodium strontium cadmium niobate to name just

a few examples. In addition, mixtures of various A^{II} cations like Sr -Ba , Sr - Eu, Sr - Ca and so on are known [28, 29, 30]. Lanthanides and +II cations have also been studied in these systems [31, 32].

In the Ca/Nb/O system there have been some reports of a perovskite related phase [21, 33] and reports of failed attempts to produce a Ca phase [23]. No details of structure or composition range have been given by those who have reported finding a Ca perovskite related phase. In exploratory synthesis work aimed at producing new reduced niobates turned up a new series of compounds in the Ca/Nb/O system. They are highly colored and the lattice parameters from x-ray diffraction data change as a function of the starting composition given by Ca_xNbO_3. The aim of the first part of this thesis is to demonstrate the synthesis of compounds of the type Ca_xNbO_3 with a range of composition and to describe the structure and some properties of these compounds.

The second part of this thesis will deal with the synthesis of niobium nitride by ignition of niobium metal and barium peroxide mixtures in air. A recent paper presents the results of such reactions as a new Ba/Nb/O superconductor [34]. However, electron microprobe and powder x-ray diffraction results indicate that the superconducting phase is NbN.

The last part of this thesis will present some work on the reaction between $YBa_2Cu_3O_6$,an insulator, and iodine that produces a superconducting phase.

References

1.) M. J. Geselbracht, T. J. Richardson, and A. M. Stacy, *Nature*, **345**, 324 (1990).

2.) J.Bardeen, L. N. Cooper, and J. R. Schrieffer, *Phys. Rev.*, **B108**, 1175-1204 (1957).

3.) A. Metha, A. Navrotsky, N. Kumada, and N. Kinomura, *J. Solid State Chem.*, **102,** 213-225 (1993).

4.) M. E. Lines and A. M. Glass, Principles and Applications of Ferroelectrics and Related Materials, Clarendon Press, Oxford, 1977.

5.) S. C. Abrahams and P. Marsh, *Acta Cryst.*, **B42,** 61-68 (1986).

6.) N. Kumada, S. Muramatu, F. Muto, N. Kinomura, S. Kikkawa, and M. Koizumi, *J. Solid State Chem.*, **73,** 33-39 (1988).

7.) A. C. Sakowski-Cowley, K. Lukaszewicz, and H. D. Megaw, *Acta Cryst.*, **B25,** 851-865, (1969).

8.) M. Ahtee, A. M. Glazer, and H. D. Megaw, *Phil. Mag.*, **26,** 995-1014, (1972).

9.) A. M. Glazer and H. D. Megaw, *Phil. Mag.*, **25,** 1119-1135, (1972).

10.) M. H. Francombe and B. Lewis, *Acta Cryst.*, **11,** 175-178, (1958).

11.) L. Katz and H. D. Megaw, *Acta Cryst.*, **22,** 639-648, (1967).

12.) M. Serafin and R. Hoppe, *J. Less-Common Metals,* **76,** 299-316, (1980).

13.) G. Meyer and R. Hoppe, *Z. anorg. allg. Chem.*, **436,** 75-86, (1977).

14.) G. Meyer, R. Hoppe, and M. Jansen, *Naturwissenschaften,* **63,** 386, (1976).

15.) J. Sieler, B. Kreßner, and H. Holzapfel, *Z. Chem.*, **8,** 33, (1968).

16.) A. M. Abakumov, R.V. Shpanchenko, and E.V. Antipov, *Mat. Res. Bull.*, **30,** 97-103, (1995).

17.) J. Sturm and R. Gruehn, *Naturwissenschaften,* **62,** 296, (1975).

18.) K. Ishikawa, G. Adachi, and J. Shiokawa, *Mat. Res. Bull.*, **18,** 653-661, (1983).

19.) M. T. Casais, J. A. Alonso, I. Rasines, and M. A. Hidalgo, *Mat. Res. Bull.*, **30,** 201-208, (1995).

20.) G. Svensson and P. Werner, *Mat. Res. Bull.*, **25,** 9-14, (1990).

21.) R. R. Kreiser and R. Ward, *J. Solid State Chem.*, **1,** 368-371, (1970).

22.) B. Hessen, S. A. Sunshine, T. Siegrist, and R. Jimenez, *Mat. Res. Bull.*, **26,** 85-90, (1991).

23.) D. Ridgley and R. Ward, *Am. Chem. Soc.*, **77,** 6132-6136, (1955).

24.) K. Isawa, J. Sugiyama, K. Matsuura, A. Nozaki, and H. Yamauchi, *Phys. Rev. B,* **47,** 123-127, (1993).

25.) V. J. Tennery, *J. Am. Ceramic Soc.*, **51,** 183-186, (1968).

26.) A. Molak, M. Pawelczyk, and J. Kwapulinski, *J. Phys.:Condens. Matter,* **6,** 6833-6842, (1994).

27.) C. Manolikas, G. Van Tendeloo, and S. Amelinckx, *Solid State Comm.*, **58,** 845-849, (1986).

28.) K. Isawa, R. Itti, J. Sugiyama, N. Koshizuka, and H. Yamamauchi, *Phys. Rev. B.*, **48,** 7618-7623, (1993).

29.) H. Brusset, H. Gillier-Pandraud, and P. Rajaonera, *Mat. Res. Bull.*, **10,** 209-216, (1975).

30.) P. B. Jamieson, S. C. Abrahams, and J. L. Bernstein, *J. Chem. Phys.*, **48,** 5048- 5057, (1968).

31.) J. Akimitsu, J. Amano, H. Sawa, O. Hagase, K. Gyoda, and M. Kogai, *Jpn. J. Appl. Phys.*, **30,** L1155-L1156, (1991).

32.) S. Y. Istomin, O. G. D'yanchenko, E. V. Antipov, *Mat. Res. Bull.*, **29,** 743-749, (1994).

33.) A. Nakamura, *Jpn. J. Appl. Phys.*, **33**, L583-L586, (1994).

34.) V. A. Gasparov, G. K. Strukova, and S. S. Khassanov, *Jour. Exper. Theor. Phys.*, **60,** 440-444, (1994).

II. Synthesis and Electron Microprobe Analysis of Ca_xNbO_3

II.1 Synthesis

Samples with the composition Ca_xNbO_3 were prepared by grinding together appropriate amounts of CaO, Nb_2O_5, and Nb according to the formula: $x\ CaO + (3-x)/5\ Nb_2O_5 + 1-2((3-x)/5)\ Nb \rightarrow Ca_xNbO_3$. The starting materials were weighed out so that the resulting pellets were 1.5 grams each, as this was a convenient size. Values of x ranged from 0.5 to 1.00 in 0.02 increments (0.50, 0.52, 0.54, ... 1.00). In addition some samples, in which the oxygen content was varied, were also prepared ($Ca_{0.66}NbO_y$ and $Ca_{0.96}NbO_y$, where y was 2.90 to 3.10 in 0.05 increments). To grow single crystals, Ca_xNbO_3 samples were prepared as above and heated to higher temperatures.

The CaO was from J. T. Baker Inc. and was heated prior to use to remove any H_2O and CO_2 and then stored in a screw top bottle in a desiccator. The Nb_2O_5 came from the Johnson Matthey Catalog Company and was either 99.9+% or 99.9%. The -325 mesh powdered Nb was from Teledyne Wah Chang Albany.

All samples were fired at about 1500°C in a vacuum of 3 to 4 x 10^{-5} torr for five hours. Samples with low values of x were partially melted and samples of high x had grayish coatings that were removed prior to x-ray diffraction experiments. As x increased, the color of the samples (minus gray coatings) became progressively darker blue. Single crystals were obtained from samples fired at 1600°C for five hours followed by a slow power down of the furnace.

The furnace used in all experiments was a Brew furnace. This furnace consists of a lidded firing chamber composed entirely of tungsten with tungsten heating elements. Samples sit on a tungsten hearth plate surrounded by the three heating elements (see Fig. 9). The firing chamber and power supply are both water cooled and a mechanical pump and diffusion pump provide a high vacuum environment. This eliminates the problem of

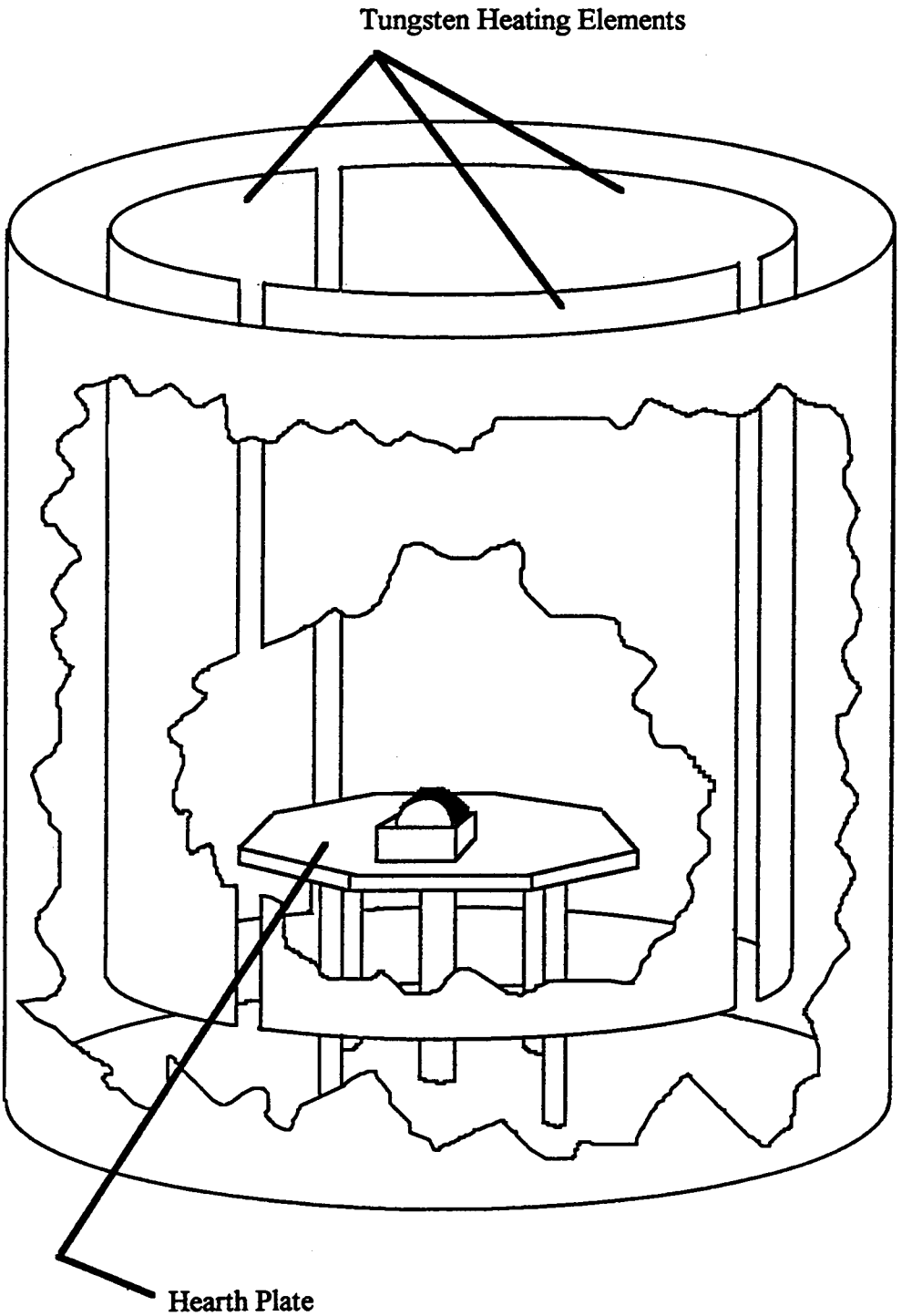

Figure 9: Heating chamber of the Brew furnace

oxidizing the electrodes and thus enables high temperatures to be attained. Approximate temperatures are measured with an optical pyrometer by looking through a window into the heating chamber. This window is normally covered by a shield to prevent deposition of anything that might interfere with these measurements. The temperature can be adjusted by varying the current through the electrodes and monitoring the temperature with the optical pyrometer. Pressure is measured with thermocouple and ionization gauges.

II.2 Electron Microprobe Analysis

Electron microprobe analysis is a technique used to get compositional information about a sample. An electron beam is generated from a hot filament and focused with magnets into a very small region (~ 1-5 μm). The electrons hitting the sample knock core electrons out of the atoms in the sample and when outer shell electrons fall into the resulting holes, characteristic x-rays are generated for each element present. The intensities of the resulting x-rays are measured and compared with standards to determine the amount of each element present. The intensity of the characteristic x-rays for each atom is proportional to the atom's mass concentration in the sample [35] (see Fig. 10).

Four samples were analyzed by R. L. Nielsen of the College of Oceanography and Atmospheric Sciences at Oregon State University. The four samples had the starting compositions $Ca_{0.66}NbO_3$, $Ca_{0.96}NbO_3$, and two of composition $Ca_{0.80}NbO_3$. One of the two x = 0.80 samples was a pellet fired at 1500°C and the other a sample that was heated to 1600°C. The x = 0.66 and x = 0.96 samples were both pellets prepared at 1500°C. The electron microprobe results indicated that the samples were mixtures of phases. The elements, that were analyzed for, were Ca, Nb, O, Ta, W, and Pt, but the elements Ta, W, and Pt were absent from the samples.

In the x = 0.66 sample a total of six measurements were taken at different points in the sample. Three of the points (4,5, and 6)(Numbers refer to Fig. 11) had very similar

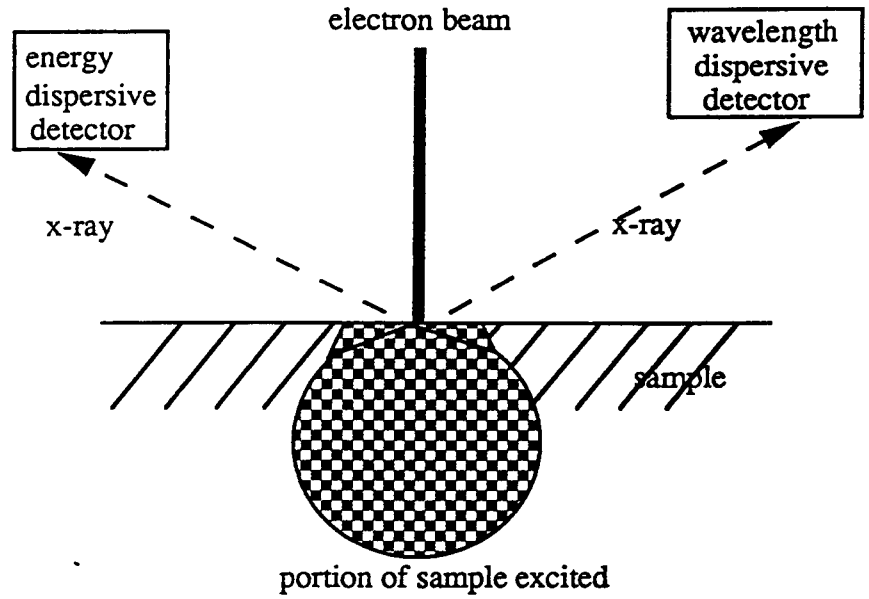

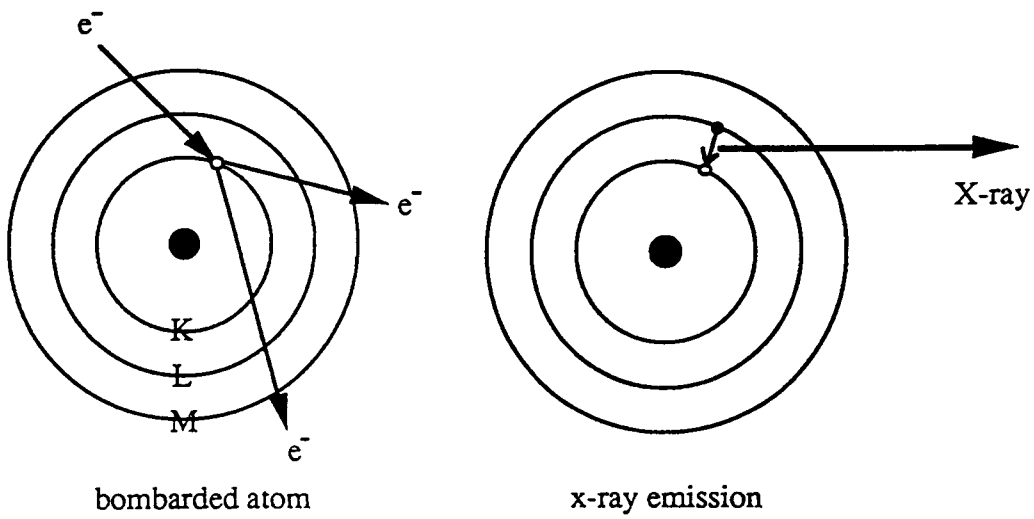

Figure 10: Electron Microprobe Analysis

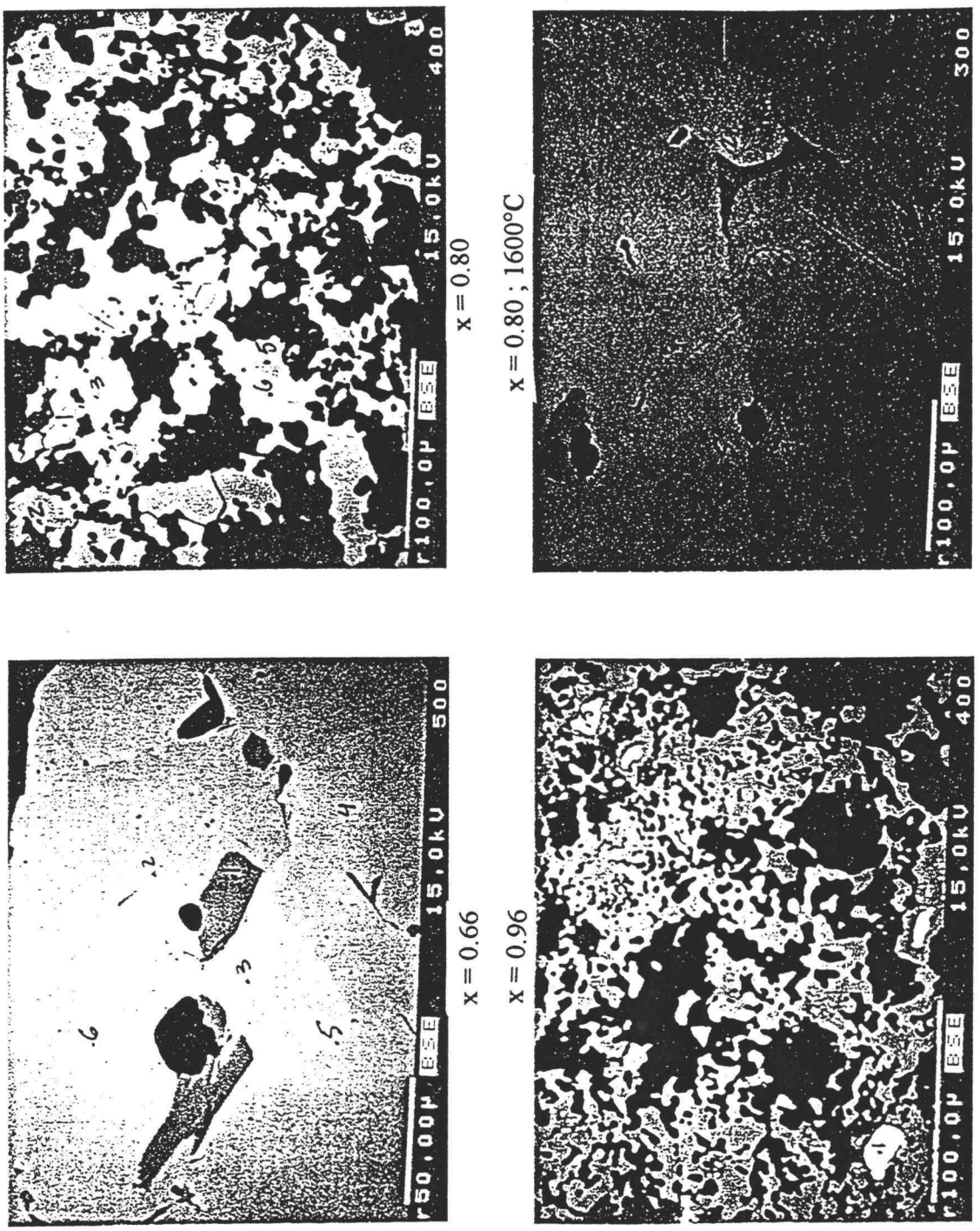

Figure 11: Sample images from electron microprobe analysis

compositions, the average of which was $Ca_{0.27}NbO_{0.43}$. The other three points (1,2, and 3) were all different with compositions of $Ca_{0.93}NbO_{2.85}$, $Ca_{0.62}NbO_{2.51}$, and $Ca_{0.27}NbO_{1.06}$ respectively.

The pellet sample with x = 0.80 had six points (2,4,5,6,7, and 8) of nearly the same composition with an average value of $Ca_{0.74}NbO_{2.57}$. The other two points (1 and 3) gave compositions of $NbO_{0.79}$ and $Ca_{0.31}NbO_{1.07}$ respectively.

In the melted sample with x = 0.80, four points (2,4,5, and 6) gave an average composition of $Ca_{0.72}NbO_{2.57}$ and two points (1 and 3) gave an average of $Ca_{0.94}NbO_{2.90}$.

For x = 0.96 there were four points (2,3,4, and 6) of average composition $Ca_{0.97}NbO_{2.72}$. The other two points (1 and 5) gave about $NbO_{0.10}$ and $NbO_{0.60}$.

References

35.) S. J. Reed, Electron Microprobe Analysis 2nd ed.,Cambridge University Press, 1993.

III. Powder X-Ray Diffraction of Ca_xNbO_3

III.1 Compositional Range

Samples with approximately $x \leq 0.64$ melt and when x is around 0.5 will react with the Nb foil boats holding the sample pellets, making the composition of the products uncertain. Pellets with x values close to 0.64 sag and tend to stick to the bottom of the boats at points of contact. All samples with $x > 0.64$ retained their pellet shape throughout the heating process. The range of composition for which powder x-ray data were taken was from $x = 0.56$ to 1.00 in 0.02 increments.

A portion of each sample was ground with an agate mortar and pestle and packed into a sample holder. Powder x-ray diffraction patterns were obtained for each sample using a Siemens D5000 diffractometer. A variable slit was used during the initial data collection which ranged from $2\theta = 2°$ to 60°. The samples were also measured with some silicon standard packed on top, in order to obtain good lattice parameter measurements, from $2\theta = 2°$ to 90°. In addition a few powder samples were measured with fixed slits from $2\theta = 2°$ to 150° for Rietveld structural determination work.

Figure 12 is a powder pattern of the sample with starting composition $Ca_{0.56}NbO_3$ and figure 13a + b shows the powder patterns of all samples. A search of the powder pattern data base was unable to find any known Ca/Nb/O, Ca/O, or Nb/O compounds that matched. Some of the smaller peaks were matched with NbO and $CaNb_2O_6$ impurities, but no match was found for the strong peaks. The weak peaks grow smaller until by $x = 0.66$ they are absent from the powder pattern (Fig. 14) indicating a

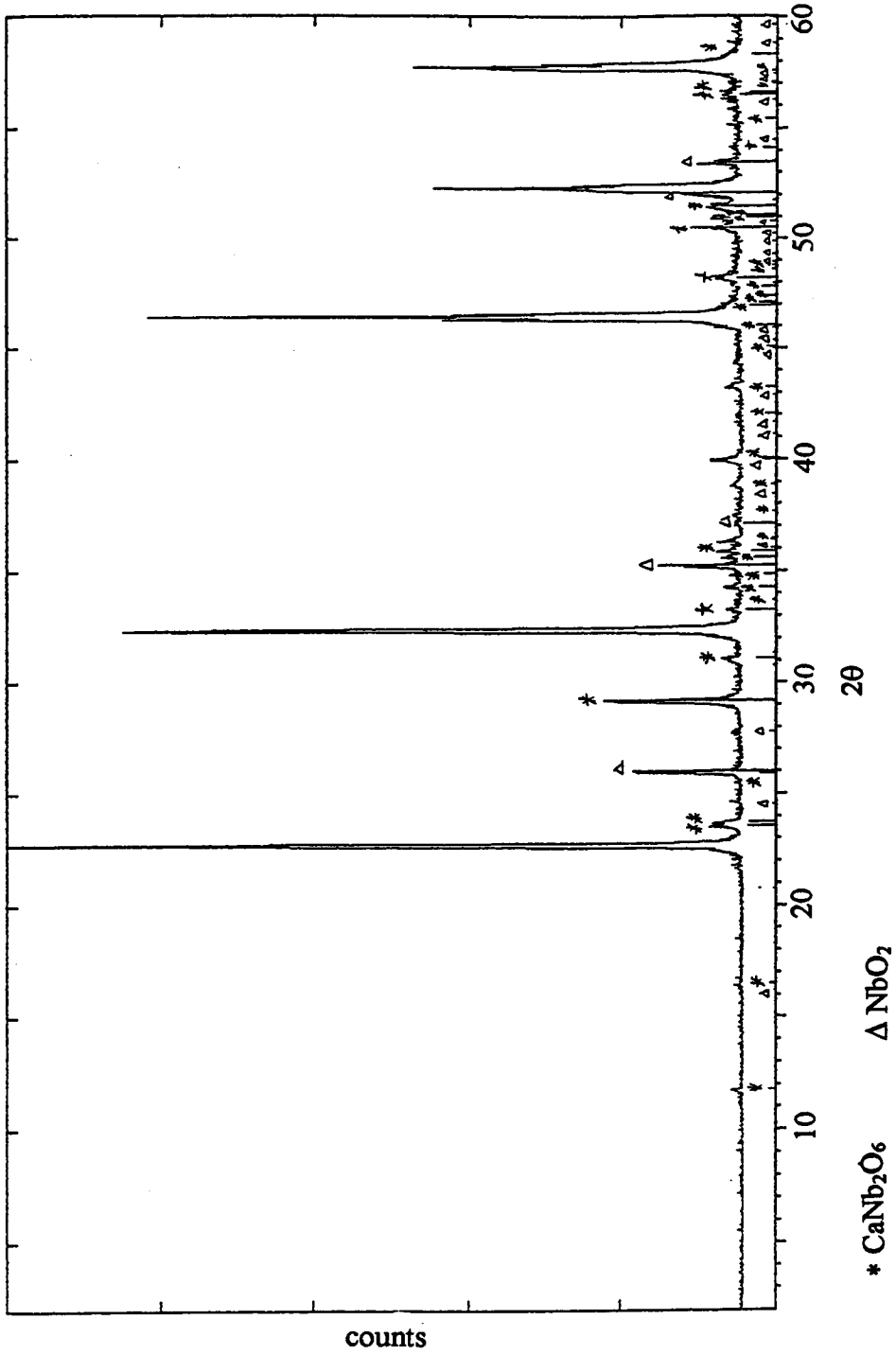

Figure 12: X-ray diffraction (XRD) powder pattern of $Ca_{0.56}NbO_3$

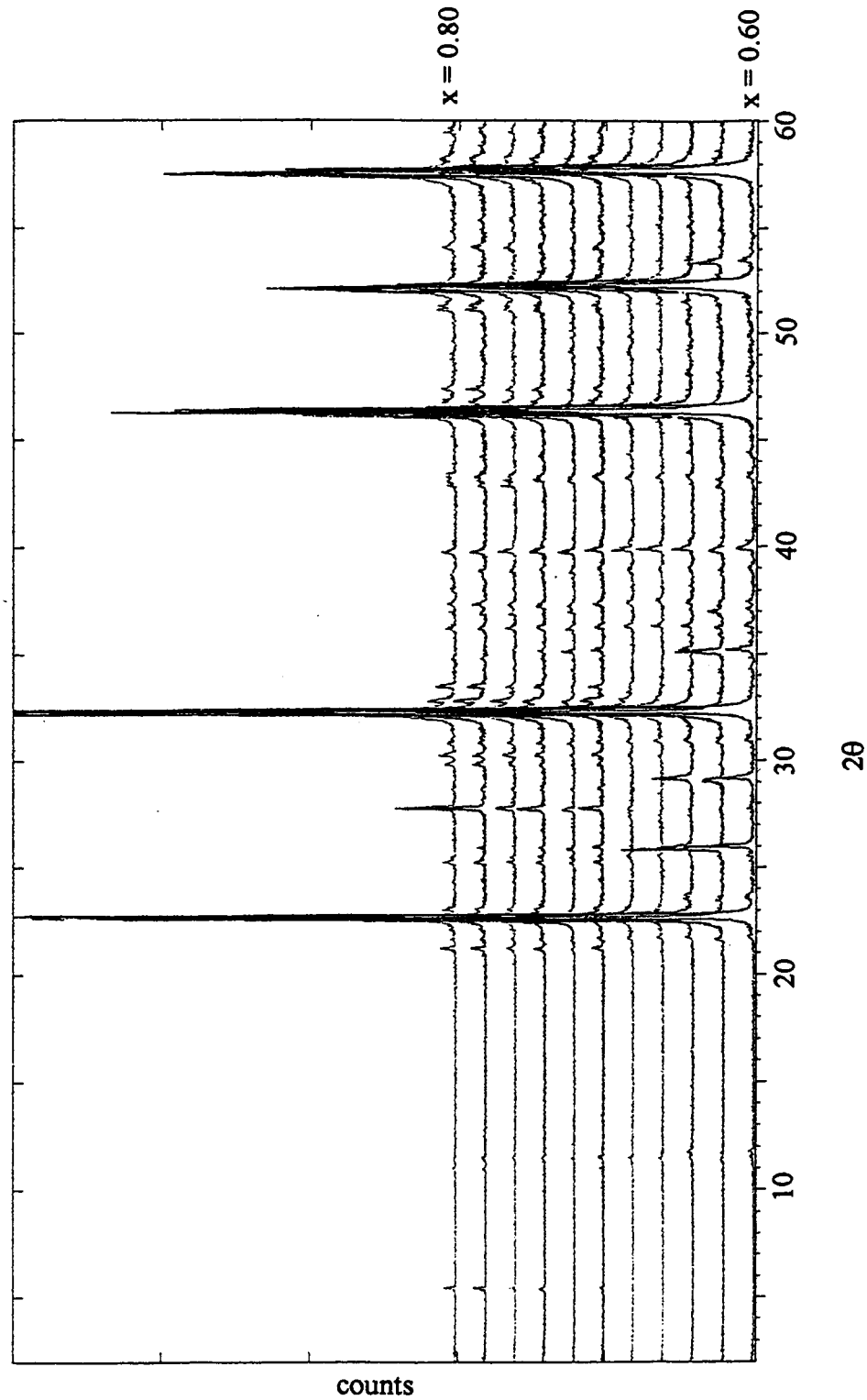

Figure 13a: XRD powder patterns for x = 0.60 to 0.80 in Ca_xNbO_3

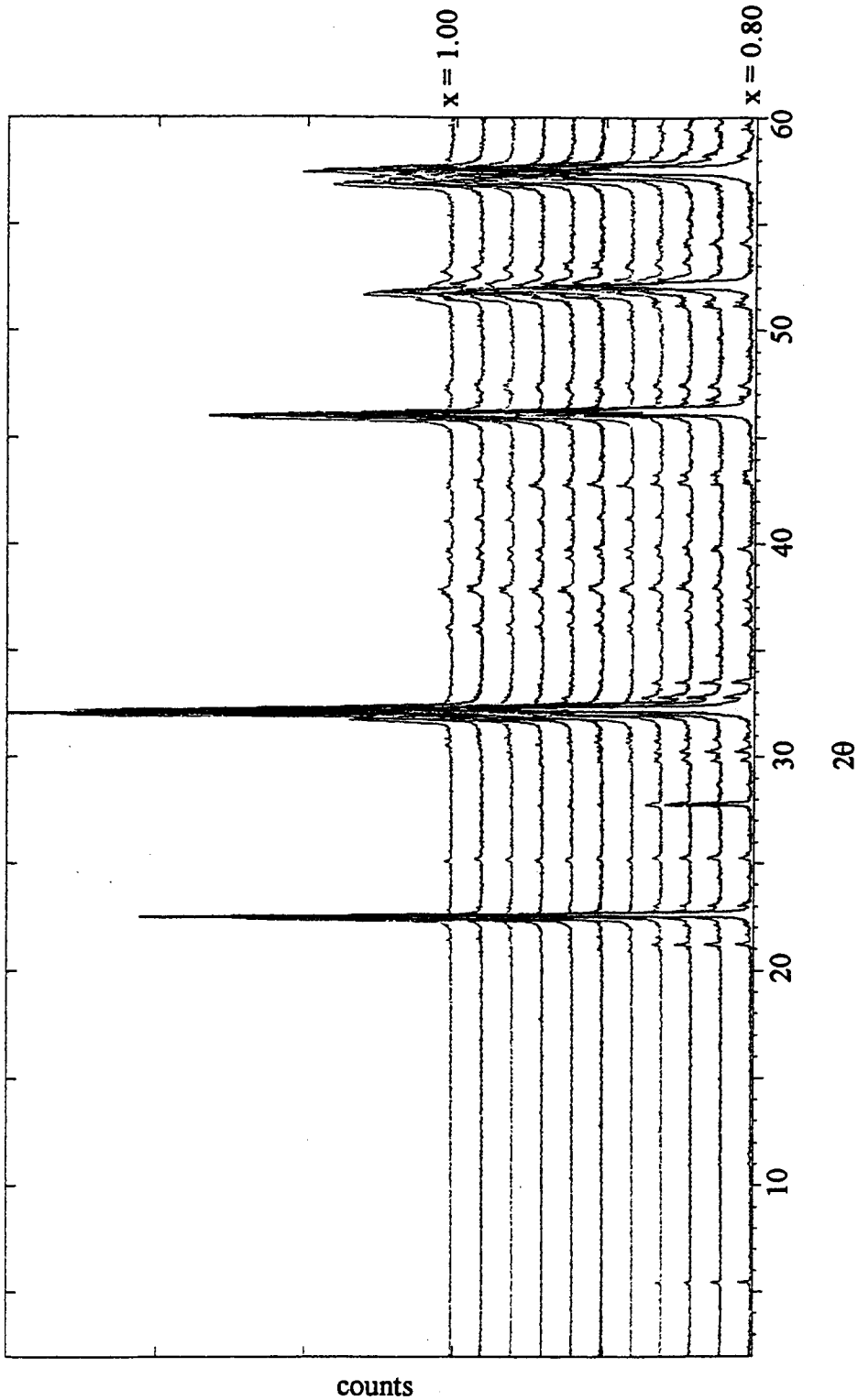

Figure 13b: XRD powder patterns for x = 0.80 to 1.00

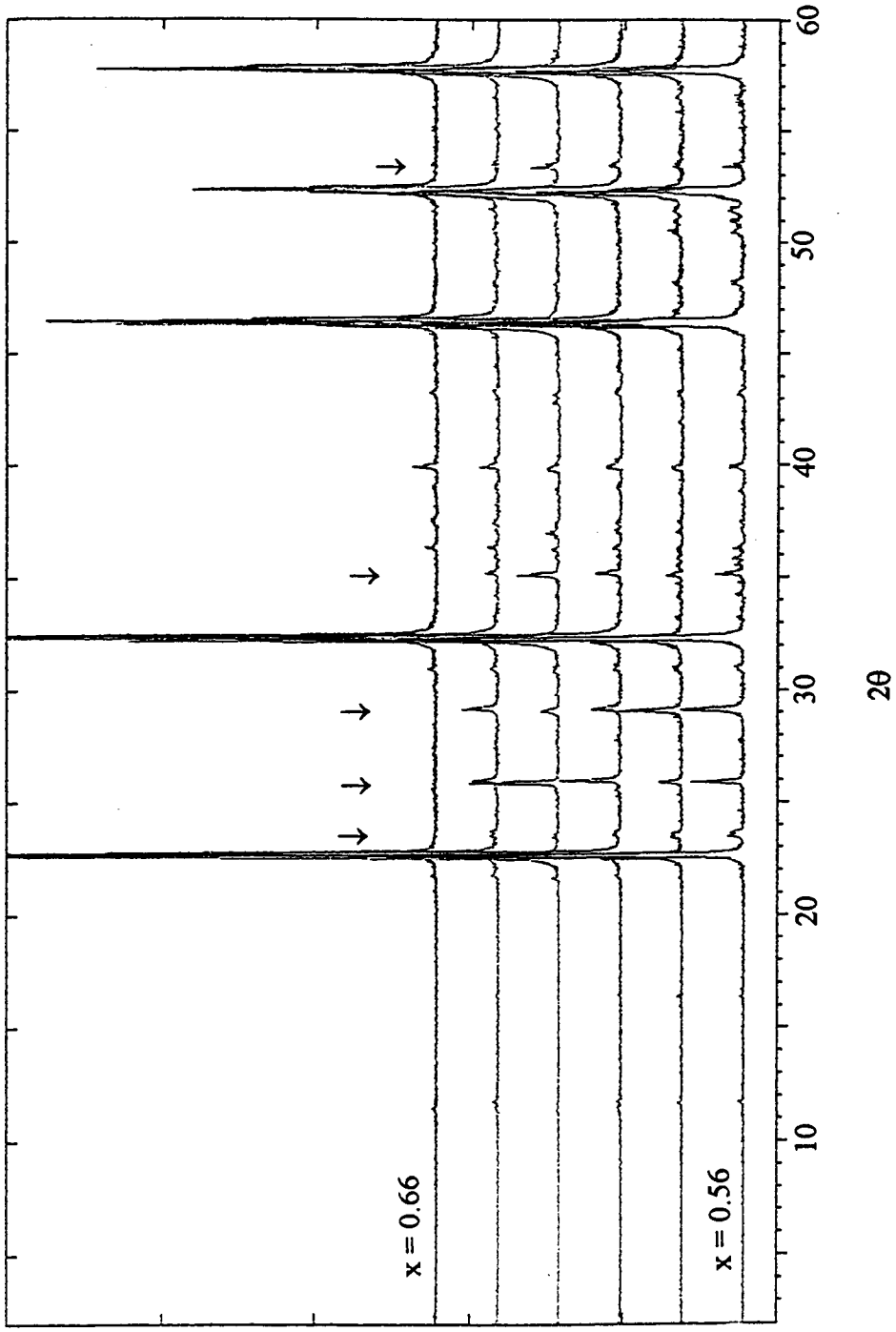

Figure 14: Disappearance of impurity peaks as x increases to 0.66

more or less pure phase and the beginning of the Ca_xNbO_3 compositional range at x = 0.66.

The position of the peaks shifts to lower 2θ values (higher d spacing) as x increases. This can be clearly seen from figure 15, which shows the powder patterns of every third sample. Some of the peaks, as marked, are from the silicon standard used to align the patterns to provide an accurate picture of the peak shifts. After x is about 0.96 the peaks no longer shift position (Fig. 16) indicating the end of the compositional range.

The powder patterns indicate a range of composition from x = 0.66 to 0.96. Figure 17 is a plot of the change in lattice parameter with change in composition.

III.2 Structure Refinements from Powder Data

Three samples of starting composition $Ca_{0.66}NbO_3$, $Ca_{0.80}NbO_3$, and $Ca_{0.96}NbO_3$ were used for structural refinements of powder x-ray diffraction data. These samples represent the beginning, middle, and end of the range of composition in this system. All refinements were carried out using GSAS (the General Structure Analysis System), a least squares refinement program.

At first glance the powder patterns may appear to be cubic (Fig. 18), but on closer examination, the peaks are definitely split, indicating a distortion of some kind. Likely space groups were selected based on several factors. The first was other space groups common to distorted perovskites, namely $GdFeO_3$ [36] reported in space group Pbnm (or in standard setting Pnma). In addition the tilt systems of linked octahedra and their resulting

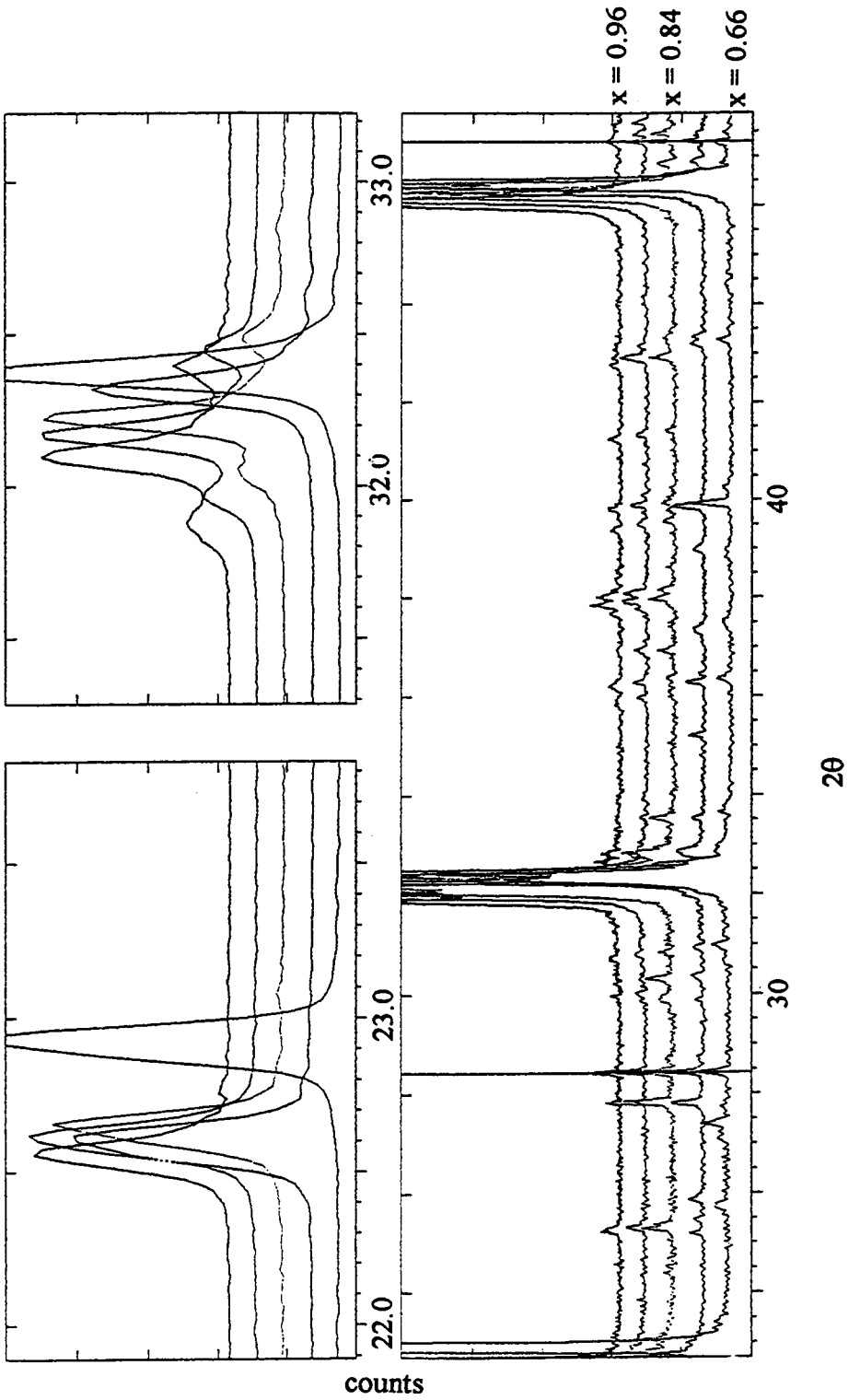

Figure 15: XRD powder patterns with silicon standard

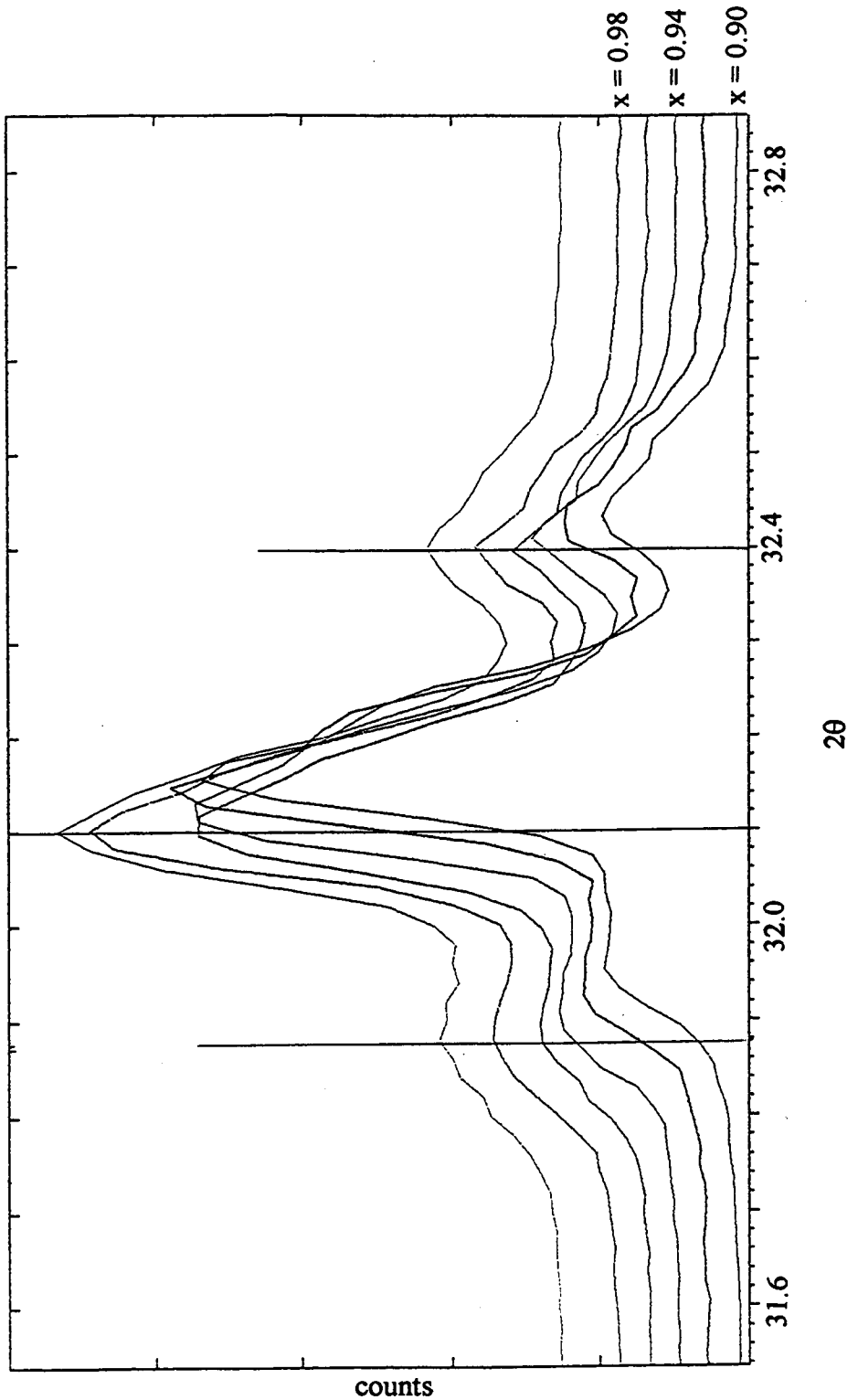

Figure 16: End of peak shifts at high x

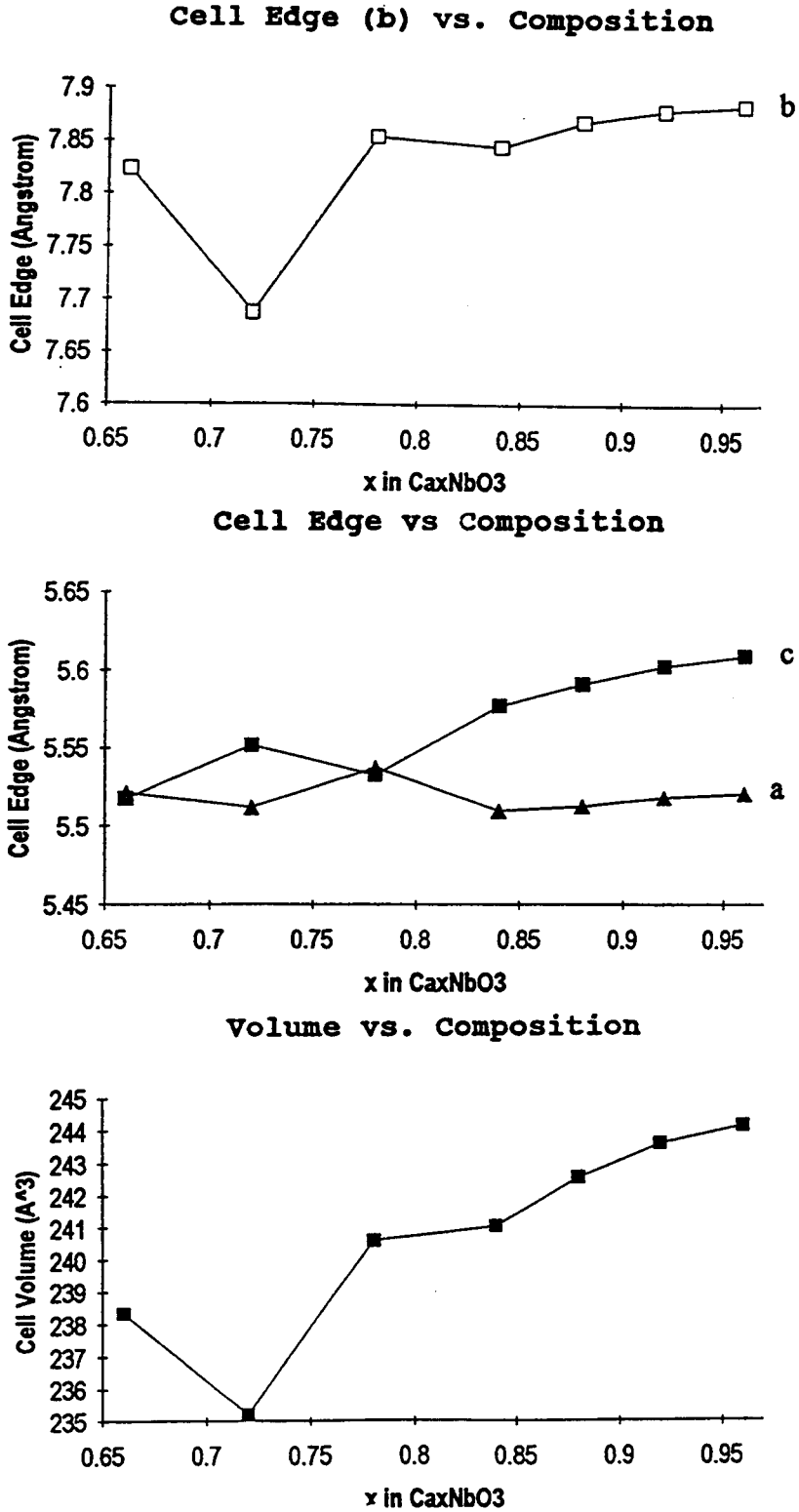

Figure 17: Cell edges and cell volume as a function of x

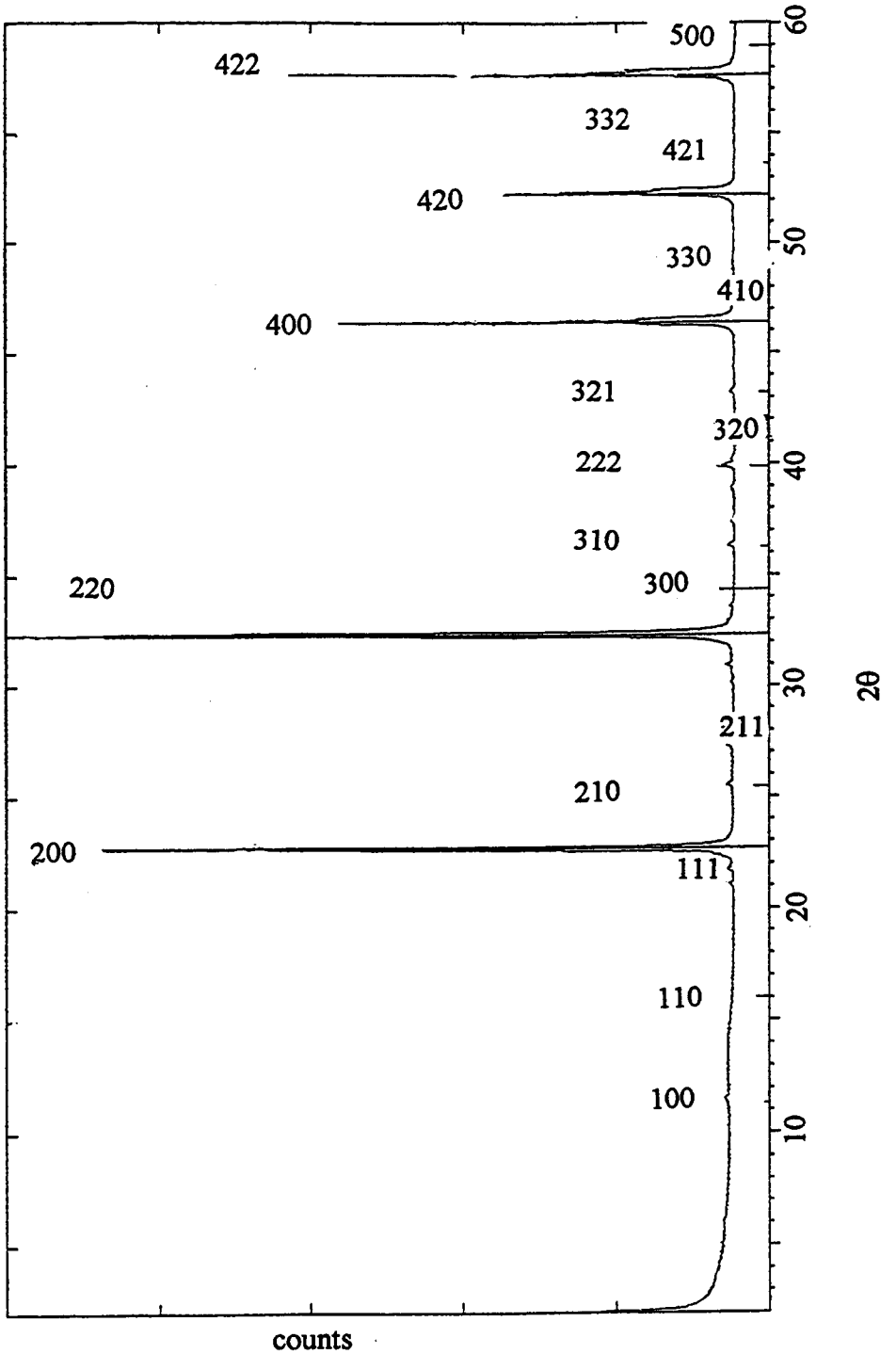

Figure 18: Cubic indexing

space groups were also considered [37,38]. Systematic absences from powder patterns, calculated from high symmetry space groups (Pmmm for example), were also explored.

Small peaks presented a problem in the refinements. From microprobe data it is evident that there are several phases present in the samples so some of the peaks that do not fit are most likely due to impurities. However, finding impurities with matching peaks was not successful as some impurity peaks doubtlessly overlap with intense sample peaks. Alternatively some of the small peaks could be from some type of superstructure and many proposed unit cells were investigated to try account for them. Peaks that were not accounted for were removed from consideration in the final calculations.

$Ca_{0.66}NbO_3$ gave the best R values in the orthorhombic space group Pnma with a unit cell of a = 5.51773 (0.00021)Å, b = 7.824192 (0.00013)Å, and c = 5.516484 (0.00022)Å. In terms of the simple perovskite unit, this cell is doubled along b; a and c are both face diagonals of the simple cell.The calcium content was refined to be 0.66 in agreement with the starting composition. Table 1 summarizes the atomic positions, occupancy, and thermal parameters and table 2 gives various other parameters refined as well as the R values. Figures 19a-i are printouts of the measured and calculated pattern along with the calculated peak positions and a difference plot. Figure 19c shows a section of the pattern in which a peak, marked with an asterisk, is calculated but not observed. This indicates that the space group chosen may not be correct, though it does a good job of matching the rest of the pattern. Figure 20 shows the structure.

The $Ca_{0.80}NbO_3$ sample appears to have some superstructure. The superstructure peaks can be seen to grow in and then disappear as x increases, with a maximum in intensity at x = 0.80 (see figure 13). An attempt to index just these extra peaks with the

Table 1. Atomic Positions and Thermal Parameters ($Ca_{0.66}NbO_3$)

Atom	x	y	z	Frac.	u_{iso}
Ca(1)	0.504824 (0.001402)	0.250000	-0.009495 (0.002522)	0.660 (0.004)	0.02257 (0.078)
Nb(1)	0.000000	0.000000	0.000000	1.000	0.00499 (0.00016)
O(1)	0.203577 (0.004256)	0.015056 (0.001175)	0.271508 (0.003415)	1.000	0.02292 (0.00232)
O(2)	-1.049301 (0.002696)	0.250000	0.999871 (0.002624)	1.000	0.04896 (0.00526)

Table 2. Refinement Summary ($Ca_{0.66}NbO_3$)

Space Group	Pnma
a	5.51773 (0.00021)Å
b	7.824192 (0.00013)Å
c	5.516484 (0.00022)Å
Variables	29
Scale Factor	52.1489 (0.172669)
Zero Point	-0.11 (0.0013)
R_p	0.0875
wR_p	0.1287
Reduced Chi^2	4.070

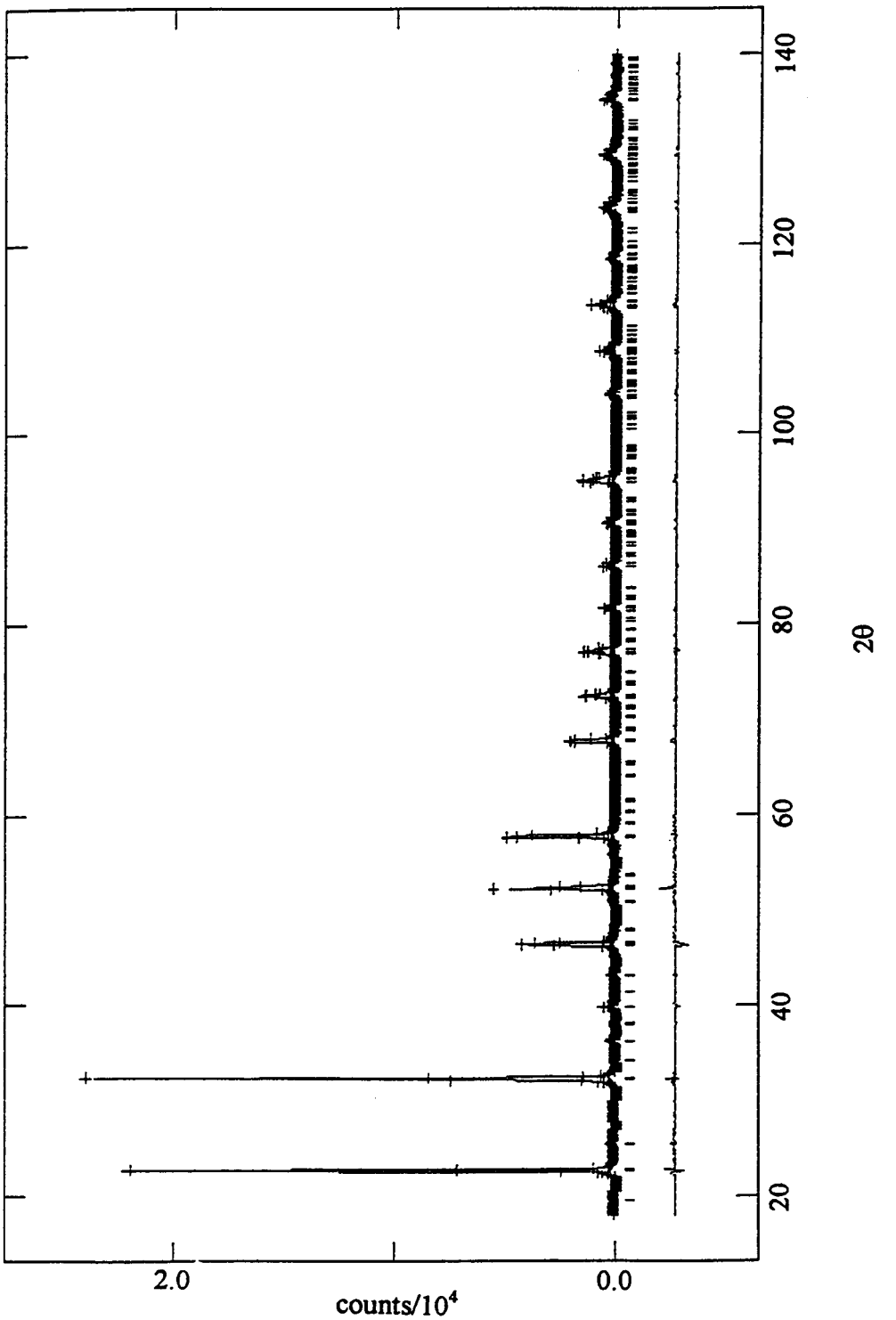

Figure 19a: Calculated and observed powder pattern for $Ca_{0.66}NbO_3$

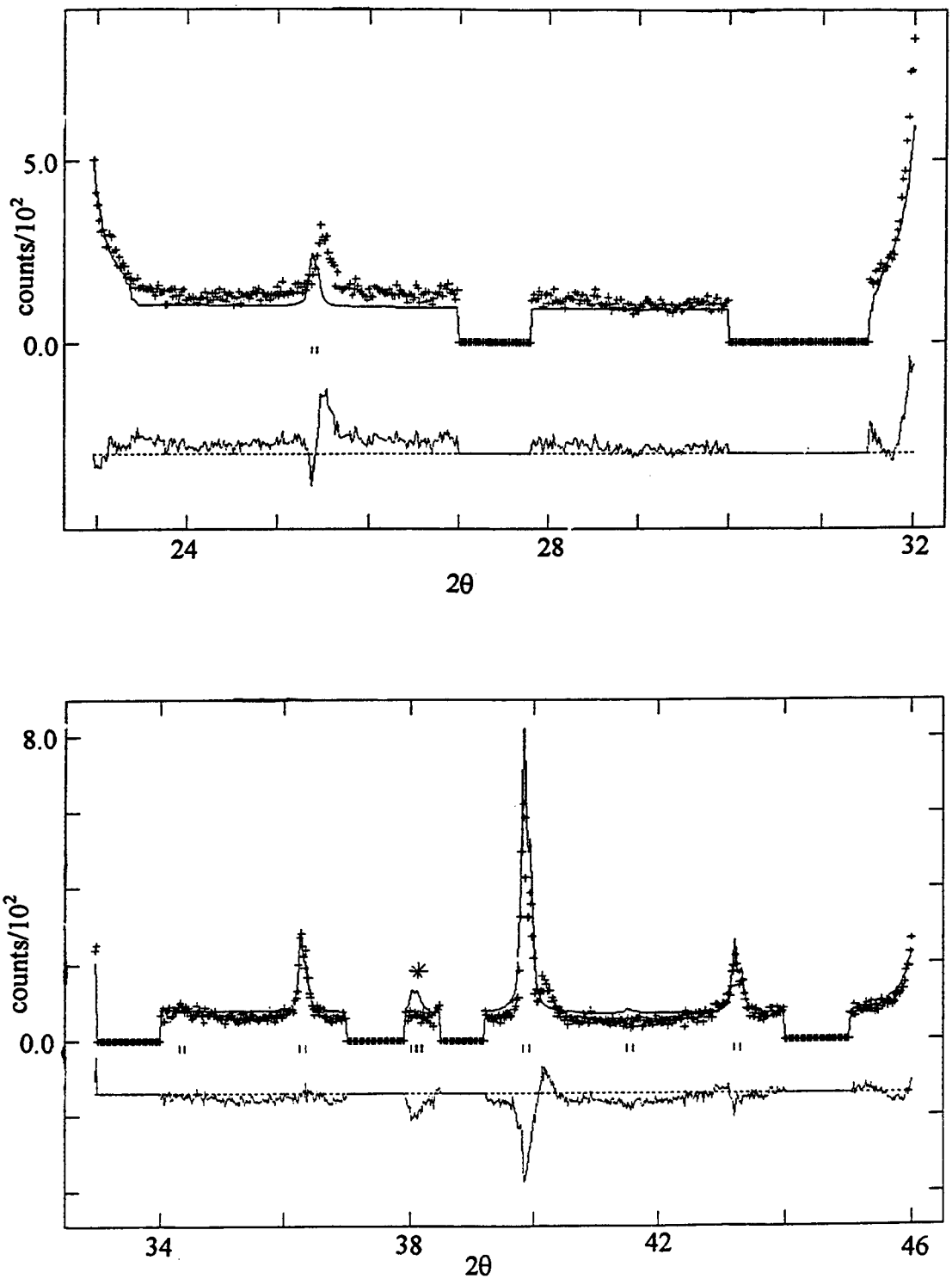

Figure 19b+c: $Ca_{0.66}NbO_3$ pattern from 23 to 32 and 33 to 46 in 2θ

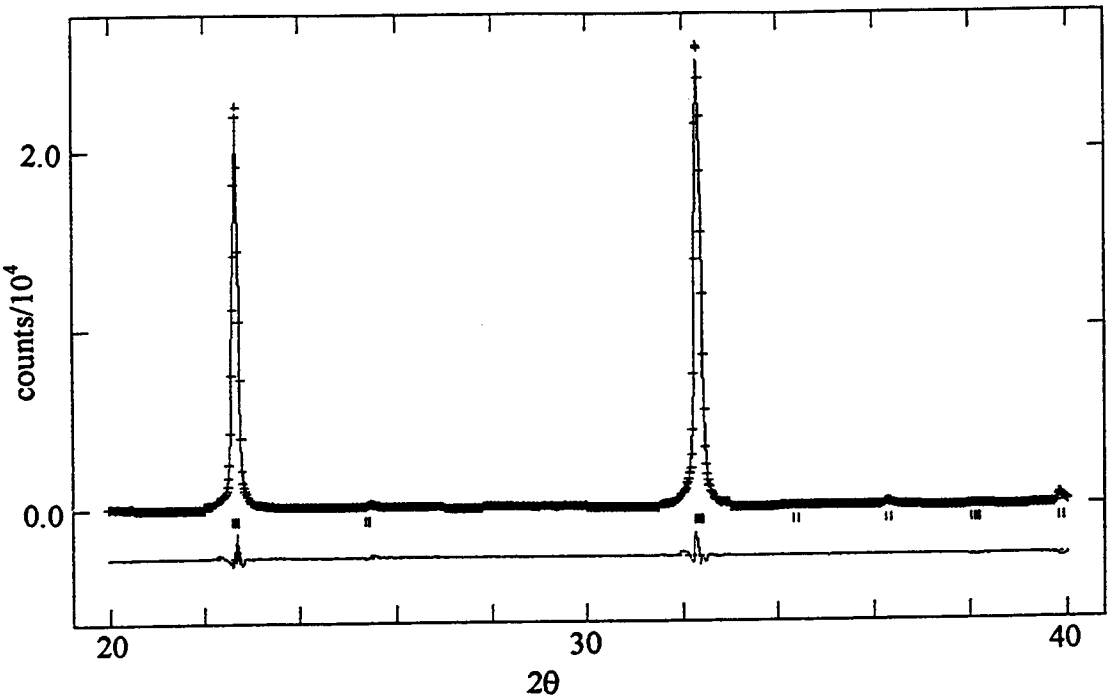

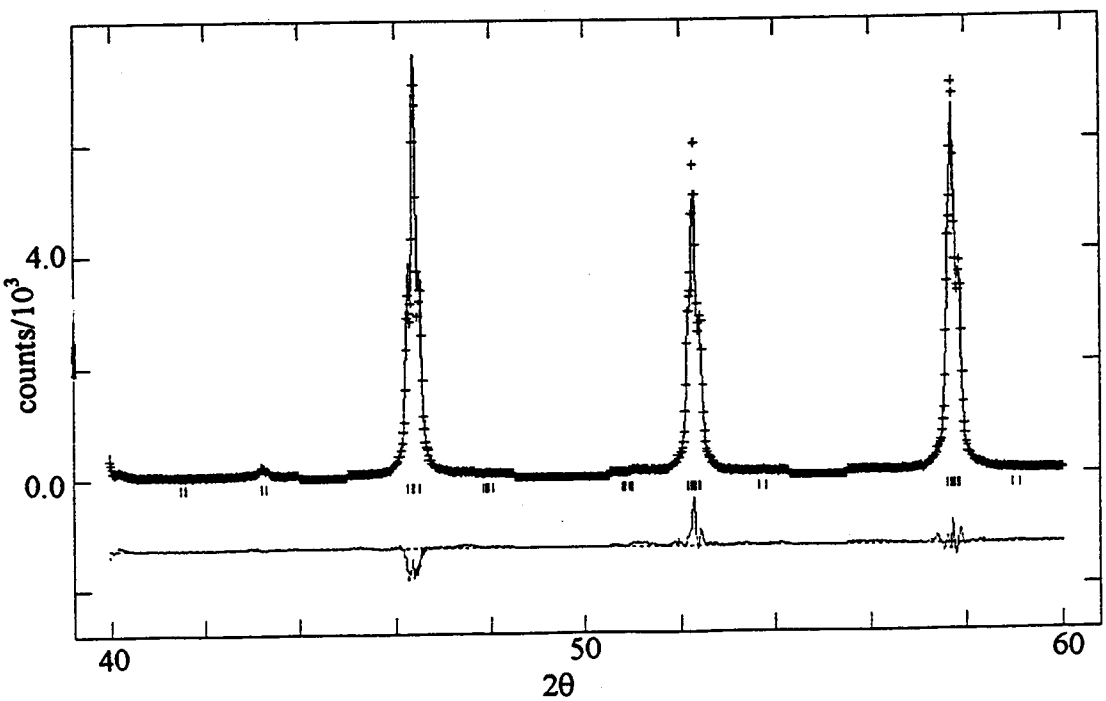

Figure 19d+e: $Ca_{0.66}NbO_3$ pattern from 20 to 40 and 40 to 60 in 2θ

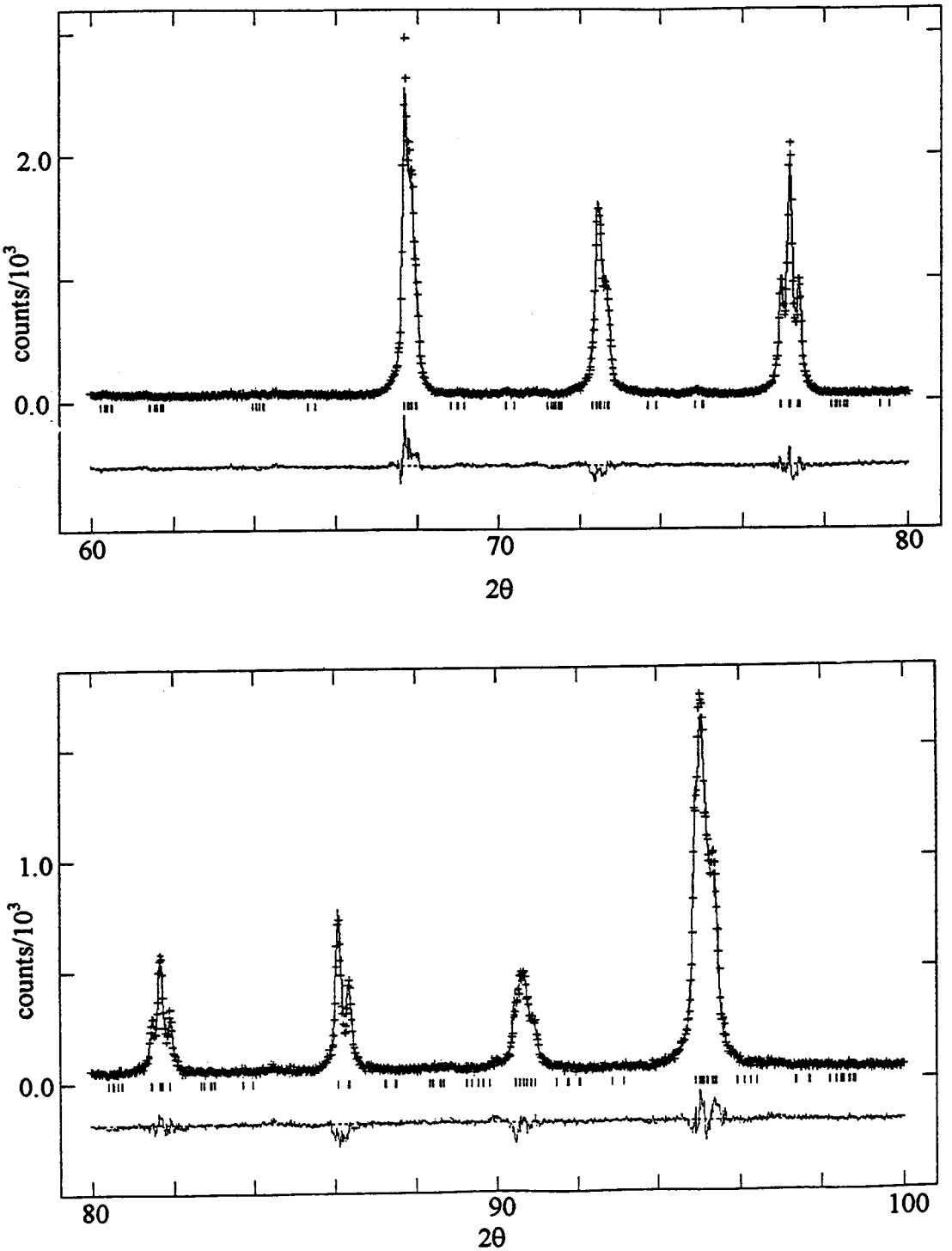

Figure 19f+g: $Ca_{0.66}NbO_3$ pattern from 60 to 80 and 80 to 100 in 2θ

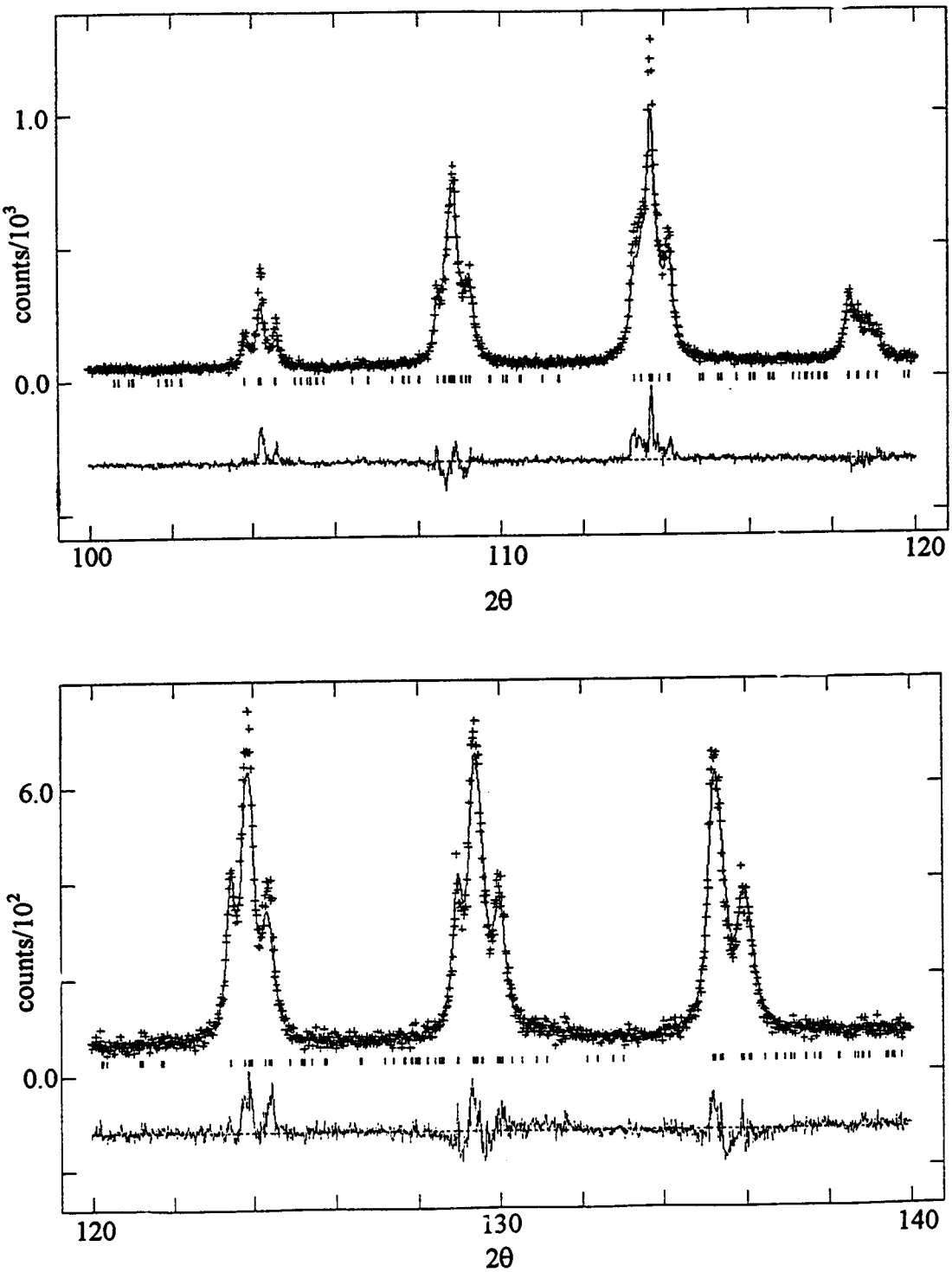

Figure 19h+i: $Ca_{0.66}NbO_3$ pattern from 100 to 120 and 120 to 140 in 2θ

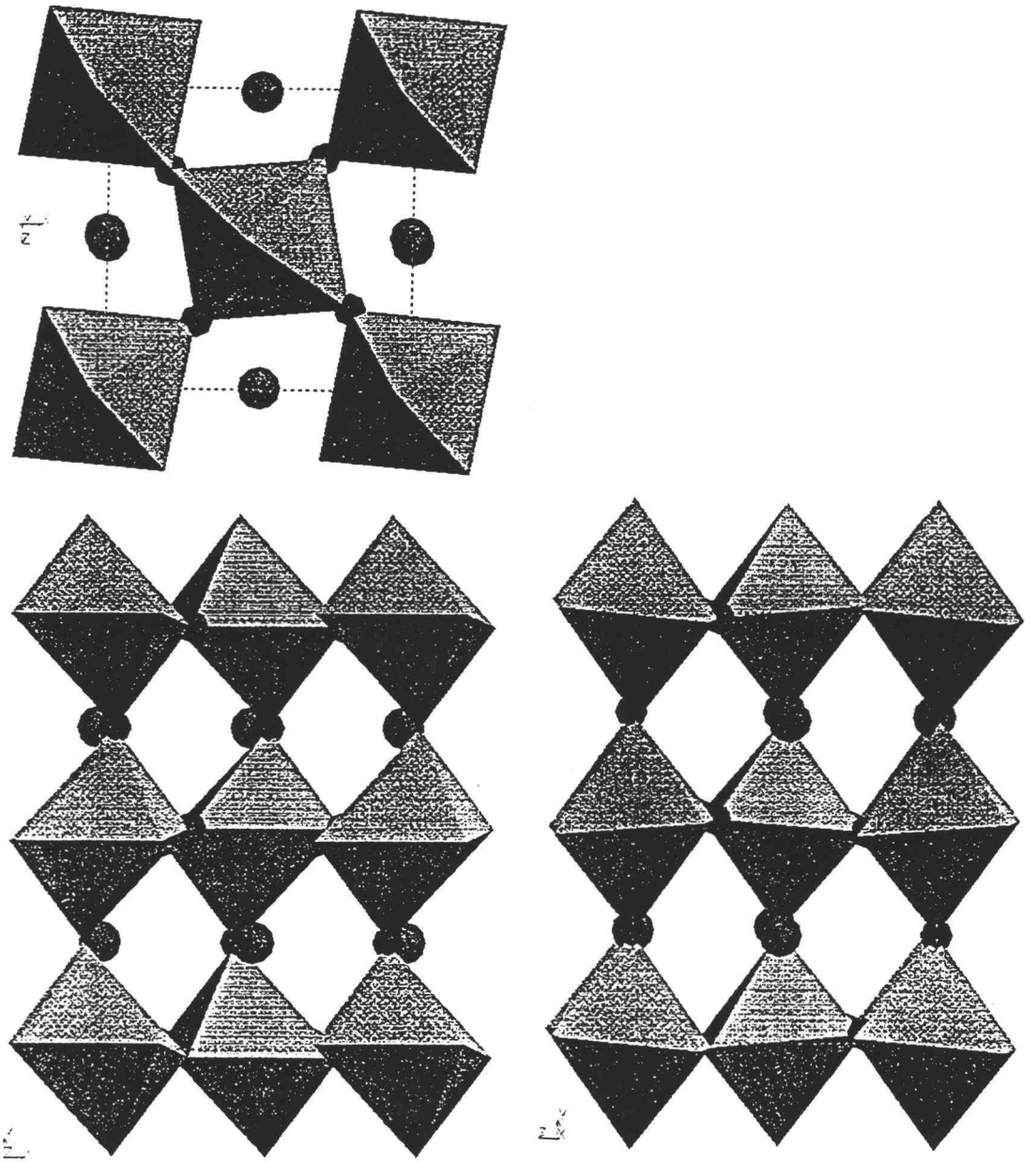

Figure 20: The structure of $Ca_{0.66}NbO_3$

program TREOR gave several possibilities all with rather low goodness of fit. The best ones were orthorhombic with lattice parameters 16.05Å x 11.00Å x 6.41Å and 16.04Å x 6.41Å x 5.50Å.

$Ca_{0.96}NbO_3$ is best fit in space group $P2_1/m$ with lattice parameters a = 5.52040 (0.00012)Å, b = 7.88420 (0.00017)Å, c = 5.60845 (0.00012)Å, and β = 90.013 (0.006)°. This cell is again doubled the simple perovskite cell along b and a and c are face diagonals. The calcium content of this sample refined to a value of 0.86. Figures 21a-i show the measured, calculated, and difference plots of the powder samples as well as the positions of calculated peaks. In table 3 the atomic positions, occupancy, and thermal parameters are given. Table 4 is a list of R values and other refined parameters. Finally, figure 22 shows the structure.

III.3 Additional Powder Work

As mentioned above, some samples had a gray coating that was scraped off prior to x-ray diffraction experiments. This powder was also subjected to x-ray diffraction experiments. The results are shown in figure 23. The peaks from Ca_xNbO_3 are marked with an asterisk and the other peak positions match those of NbO.

Samples with a range of oxygen composition, Ca_xNbO_y were also prepared for x = 0.66 and x = 0.96. These results are shown in figures 24a - b and 25 respectively. in the x = 0.66 case, at y < 3.0 additional peaks attributable to NbO_2 are observed in the pattern. These peaks are essentially gone at y = 3.00. Above y = 3.00 additional peaks from $CaNb_2O_6$ are visible. In the case of x = 0.96, as y increases a few additional weak peaks grow in. Unfortunately, a good match to these few peaks was not found.

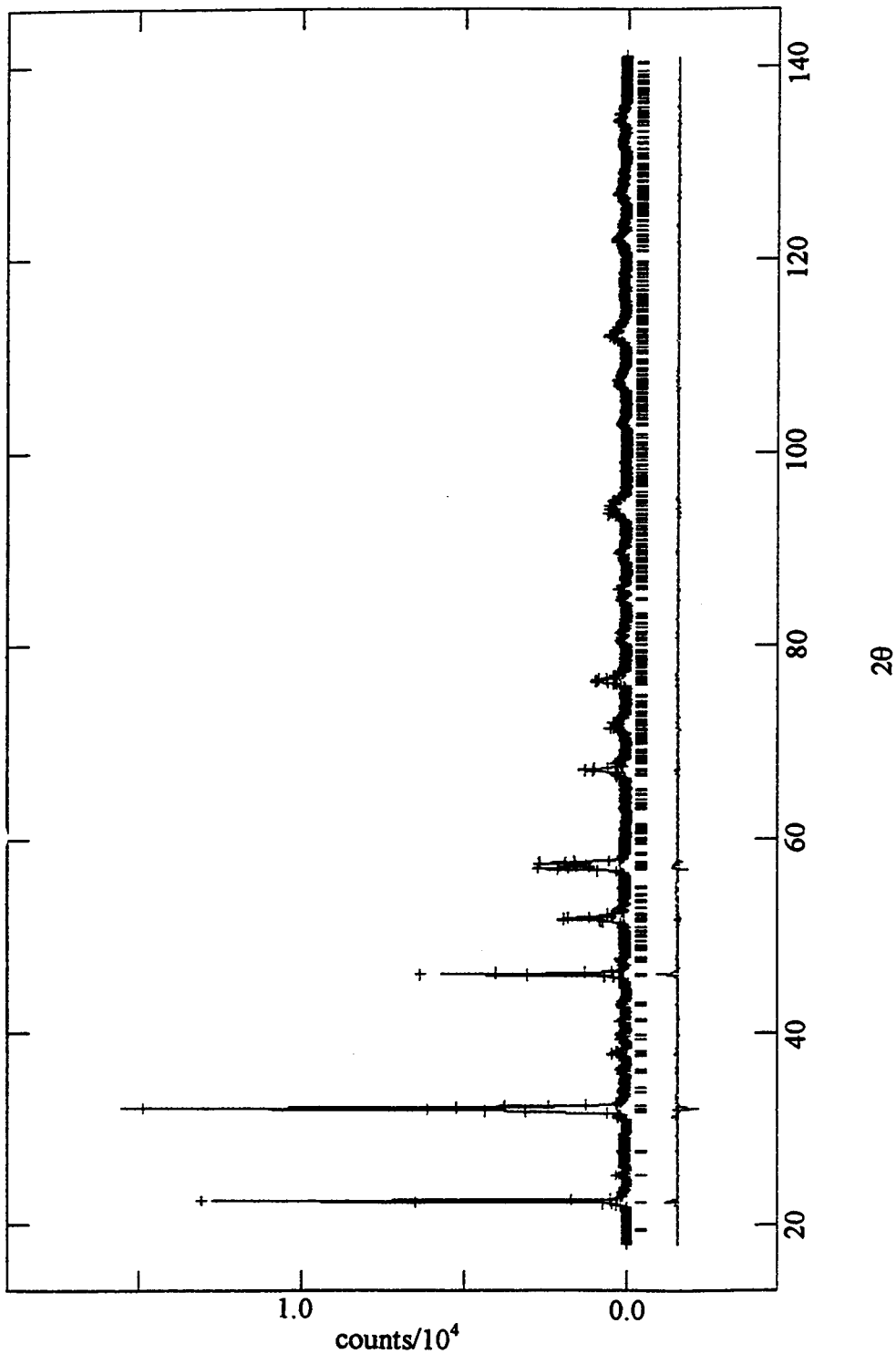

Figure 21a: Calculated and observed powder pattern for $Ca_{0.96}NbO_3$

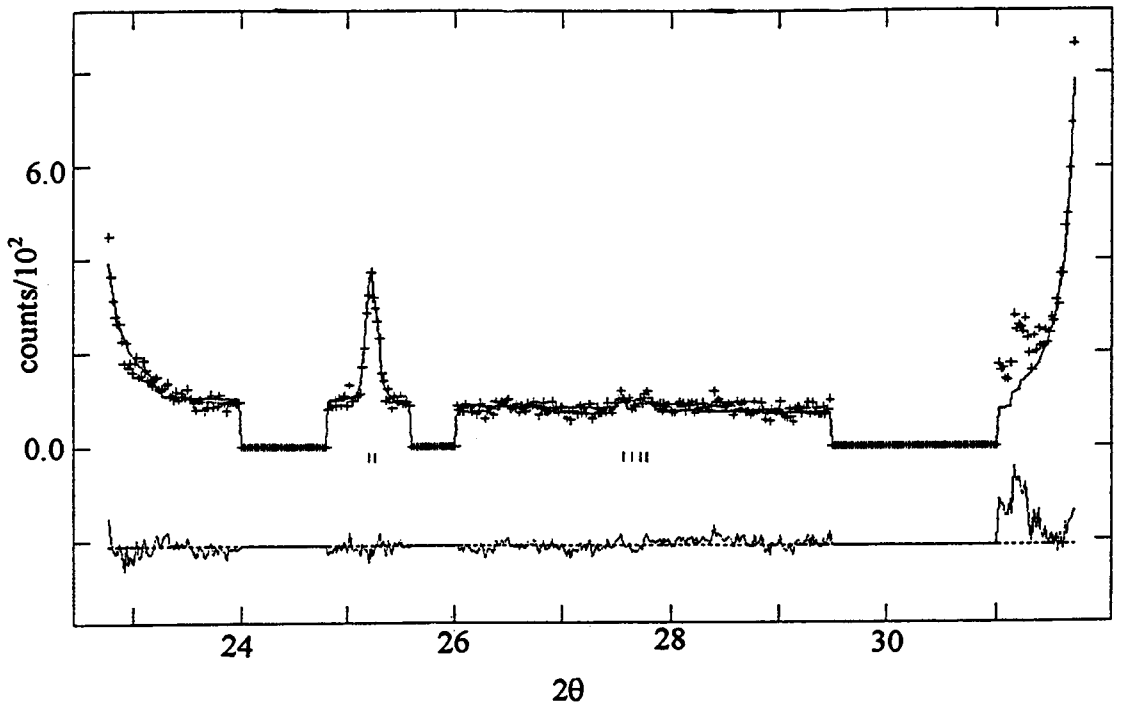

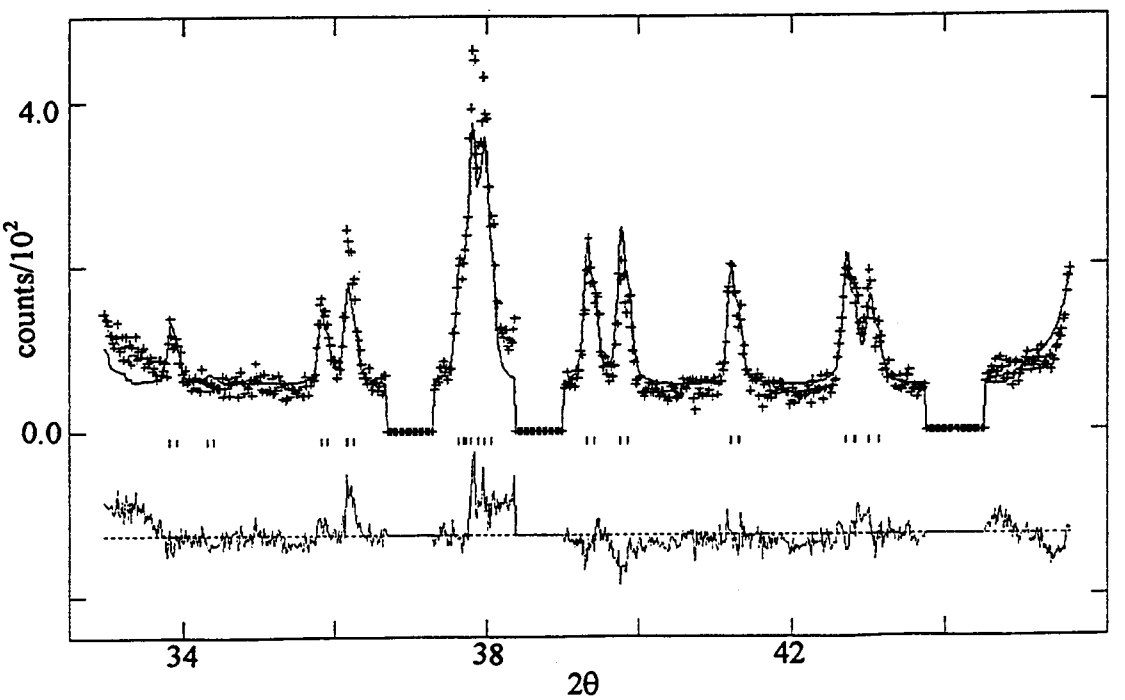

Figure 21b+c: $Ca_{0.96}NbO_3$ pattern from 23 to 32 and 33 to 45 in 2θ

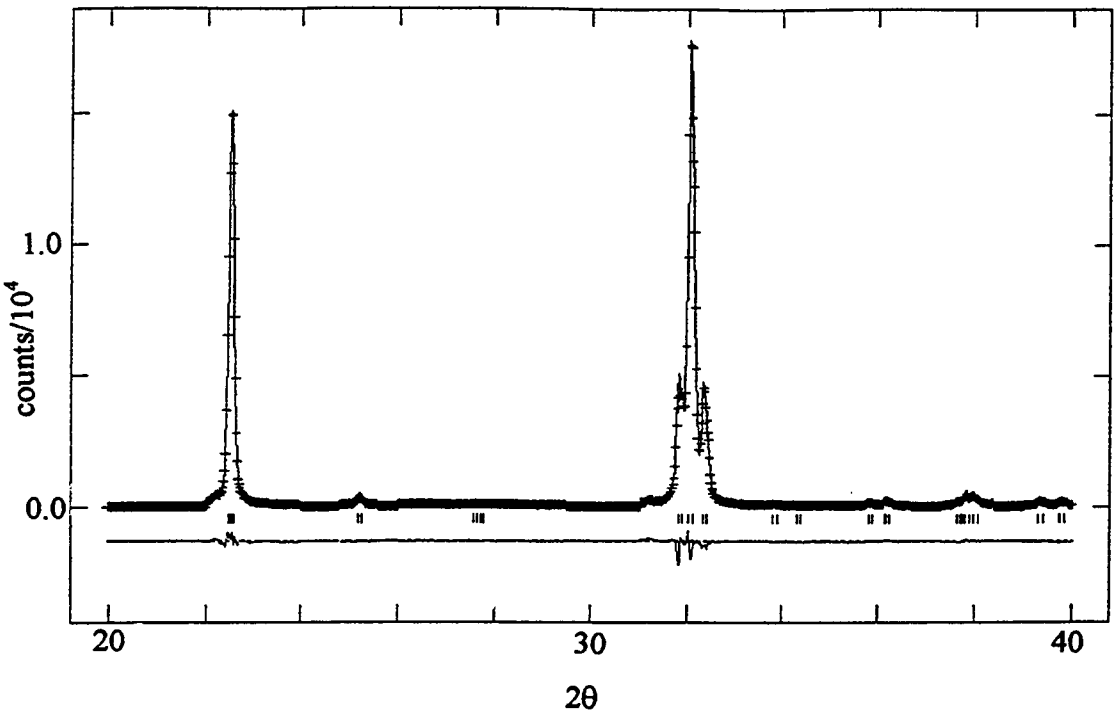

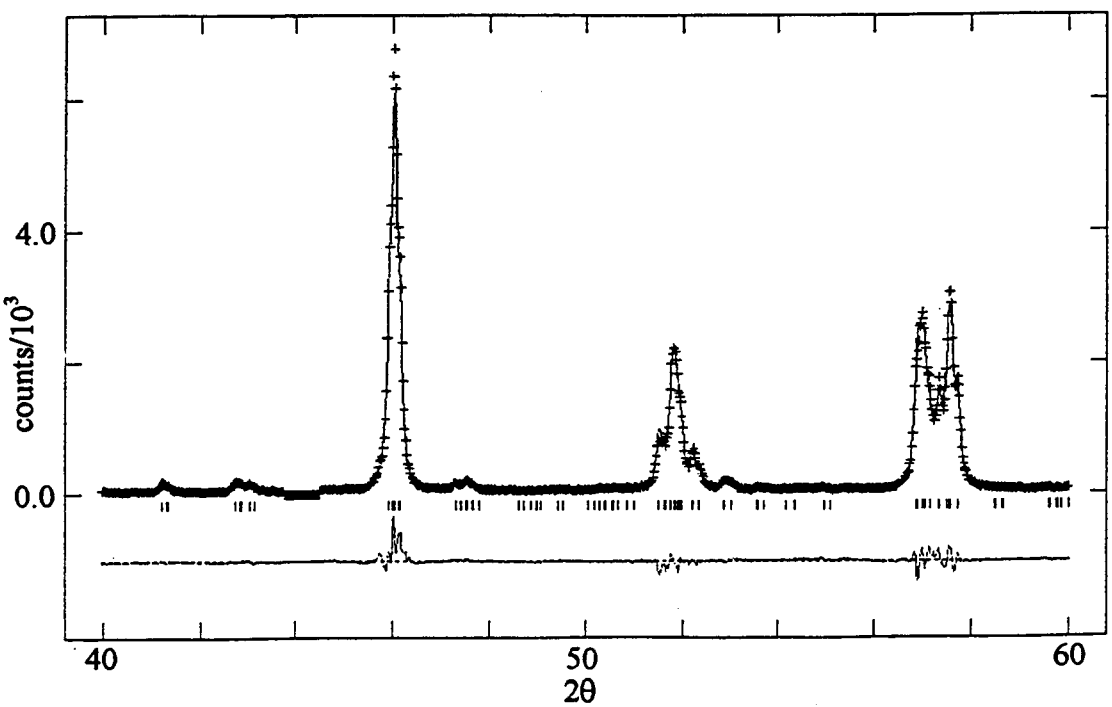

Figure 21d+e: $Ca_{0.96}NbO_3$ pattern from 20 to 40 and 40 to 60 in 2θ

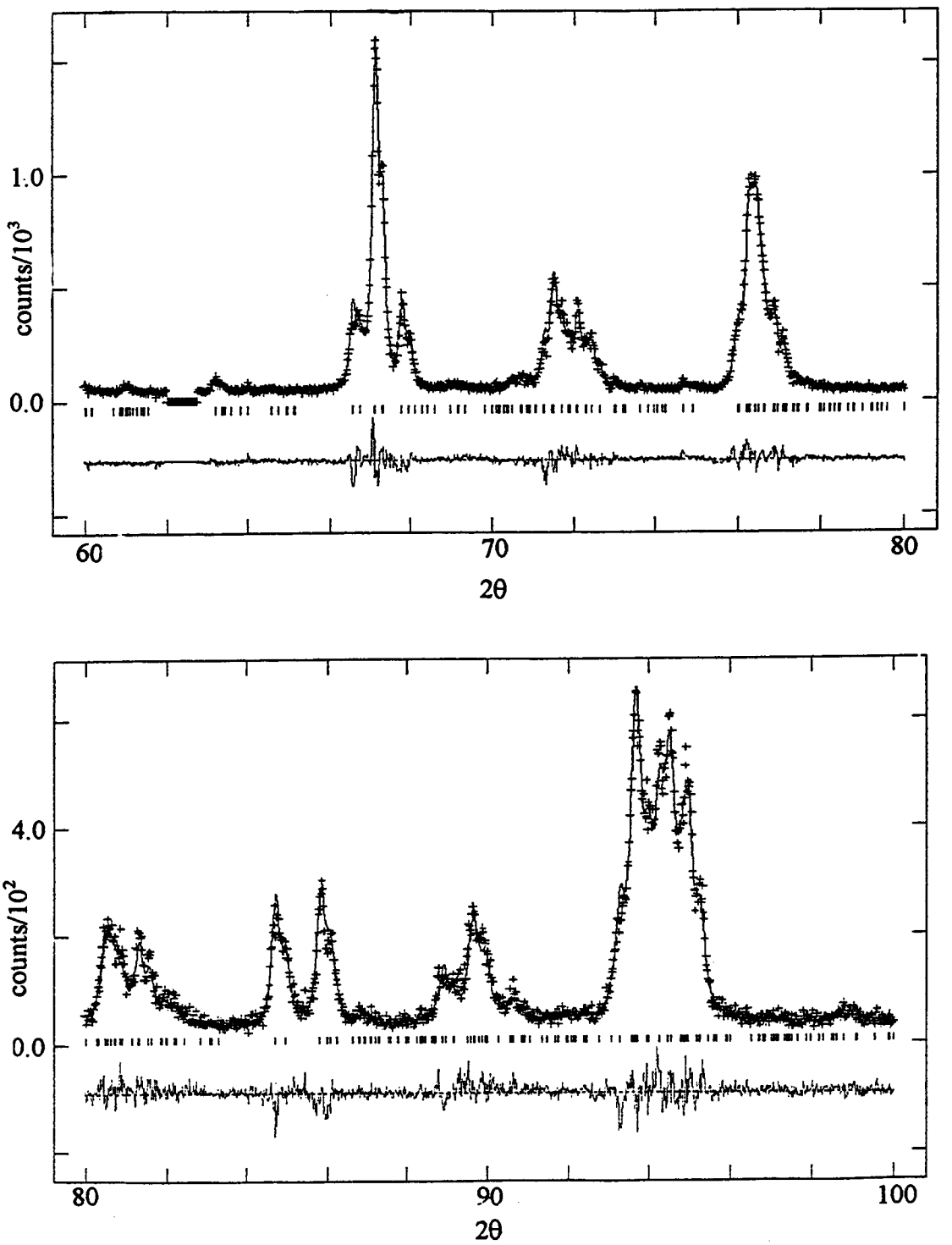

Figure 21f+g: $Ca_{0.96}NbO_3$ pattern from 60 to 80 and 80 to 100 in 2θ

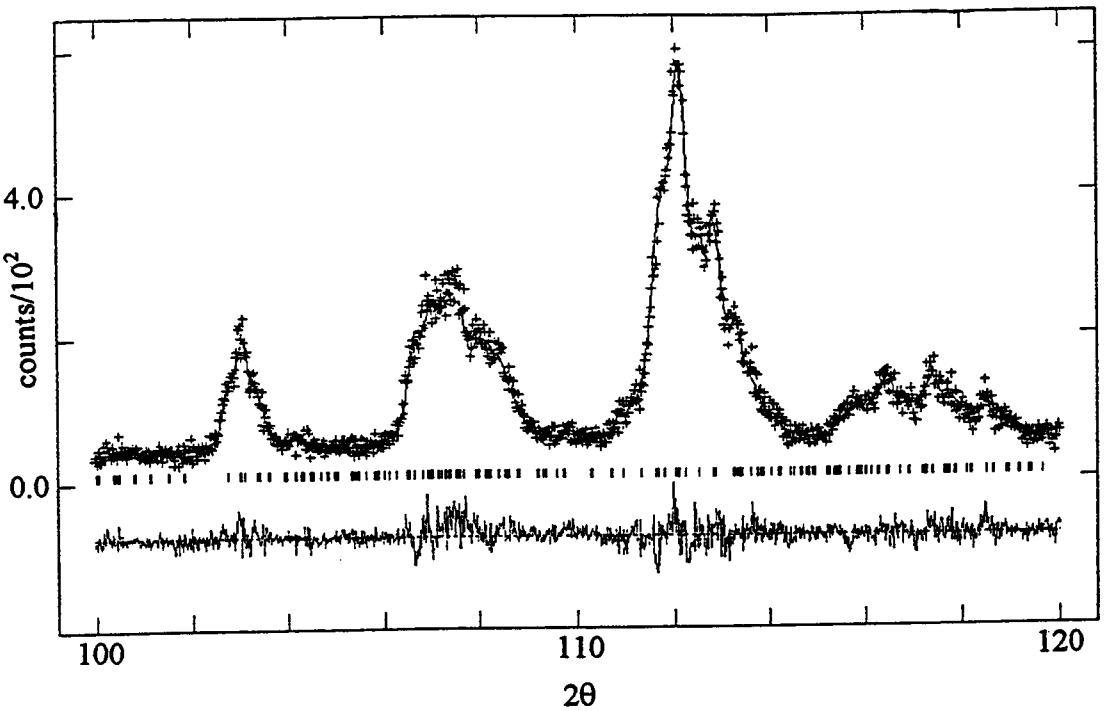

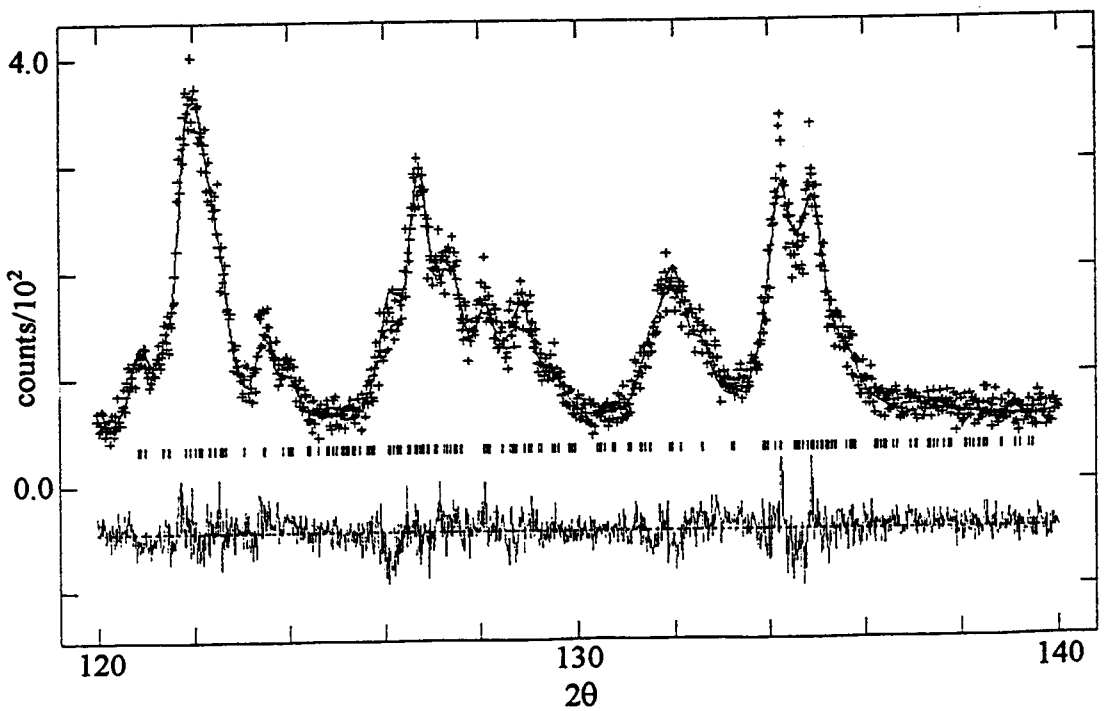

Figure 21h+i: $Ca_{0.96}NbO_3$ pattern from 100 to 120 and 120 to 140 in 2θ

Table 3. Atomic Positions and Thermal Parameters ($Ca_{0.96}NbO_3$)

Atom	x	y	z	Frac.	u_{iso}
Ca(1)	0.501850 (0.001213)	0.250000	-0.032077 (0.001082)	1.000	0.001
Ca(2)	0.024678 (0.001396)	0.250000	0.446029 (0.001461)	0.727 (0.006)	0.00337 (0.00173)
Nb(1)	0.000000	0.000000	0.000000	1.000	0.00121 (0.00065)
Nb(2)	0.500000	0.000000	0.500000	1.000	0.00190 (0.00064)
O(1)	-0.078553 (0.003114)	0.250000	1.043269 (0.002491)	1.000	0.00300
O(2)	0.566689 (0.002892)	0.250000	0.490907 (0.002594)	1.000	0.00300
O(3)	0.299700 (0.002193)	0.033082 (0.002008)	0.204958 (0.002392)	1.000	0.00300
O(4)	0.218061 (0.002341)	0.047323 (0.002002)	0.720715 (0.002637)	1.000	0.00300

Table 4. Refinement Summary ($Ca_{0.96}NbO_3$)

Space Group	$P2_1/m$
a	5.52040 (0.00012)Å
b	7.88420 (0.00017)Å
c	5.60845 (0.00012)Å
β	90.013 (0.006)°
Variables	38
Scale Factor	44.0633 (0.123698)
Zero Point	-0.06 (0.0016)
R_p	0.0727
wR_p	0.1066
Reduced Chi^2	2.468

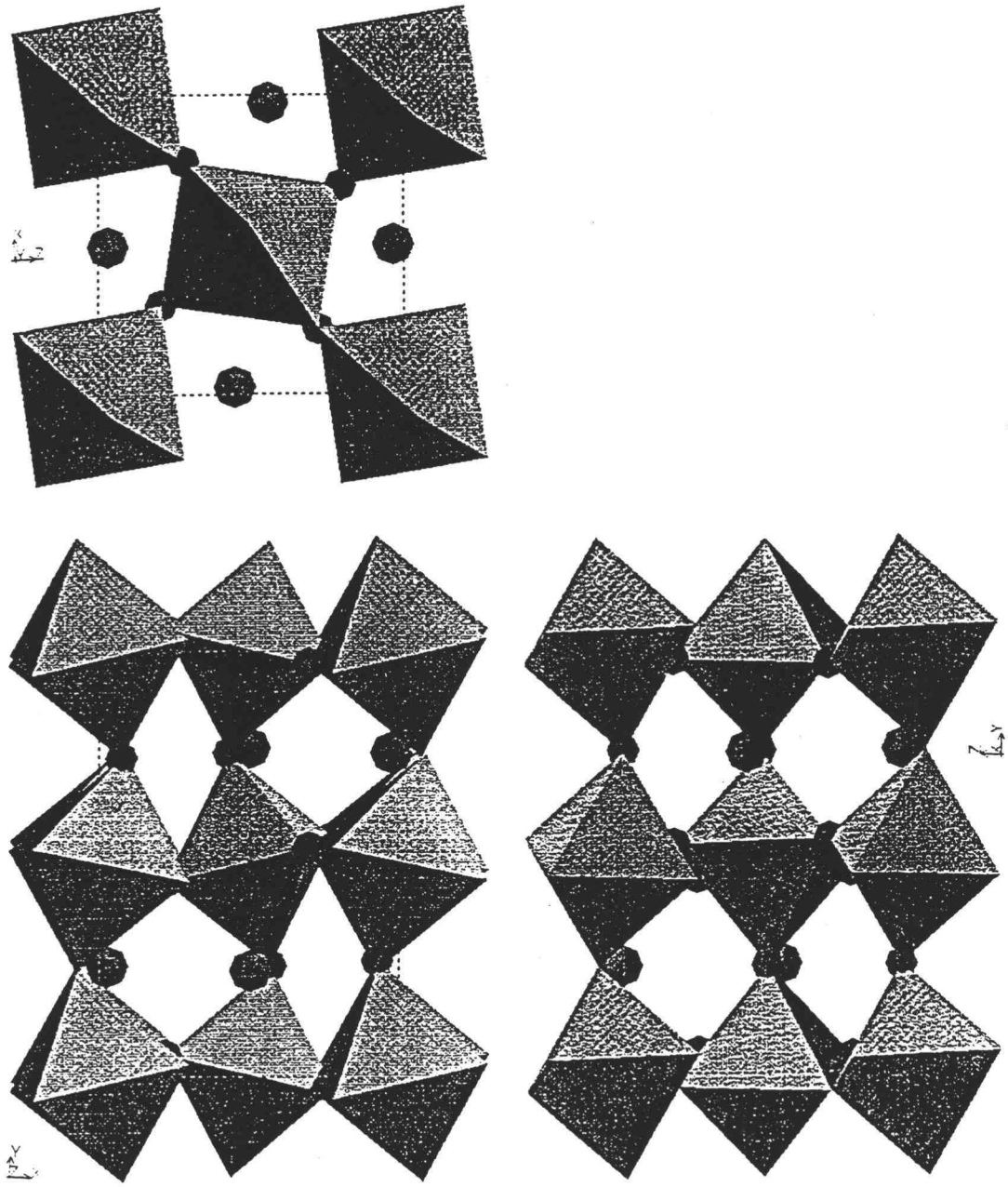

Figure 22: The structure of $Ca_{0.96}NbO_3$

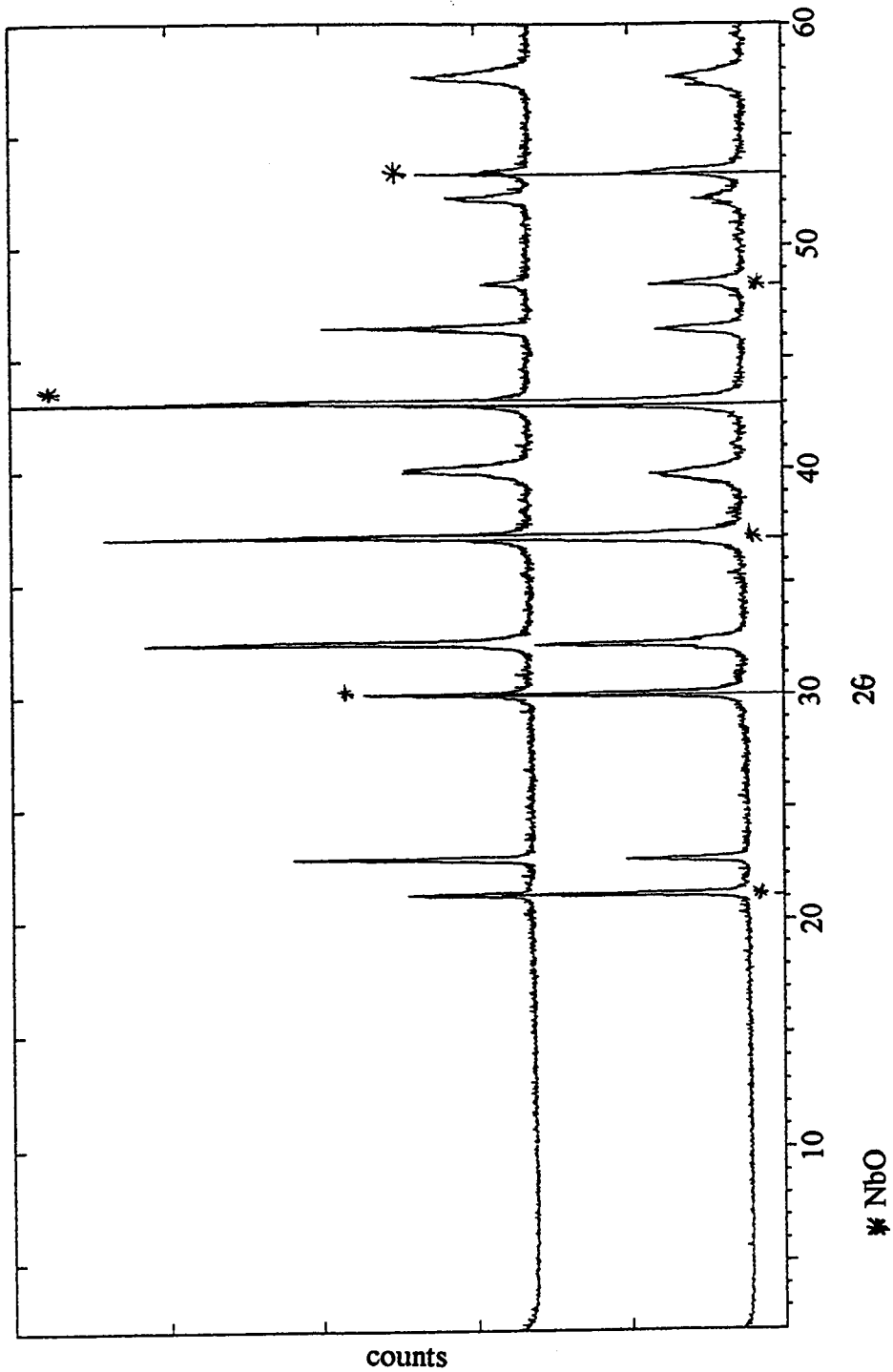

Figure 23: XRD powder pattern of gray pellet coating

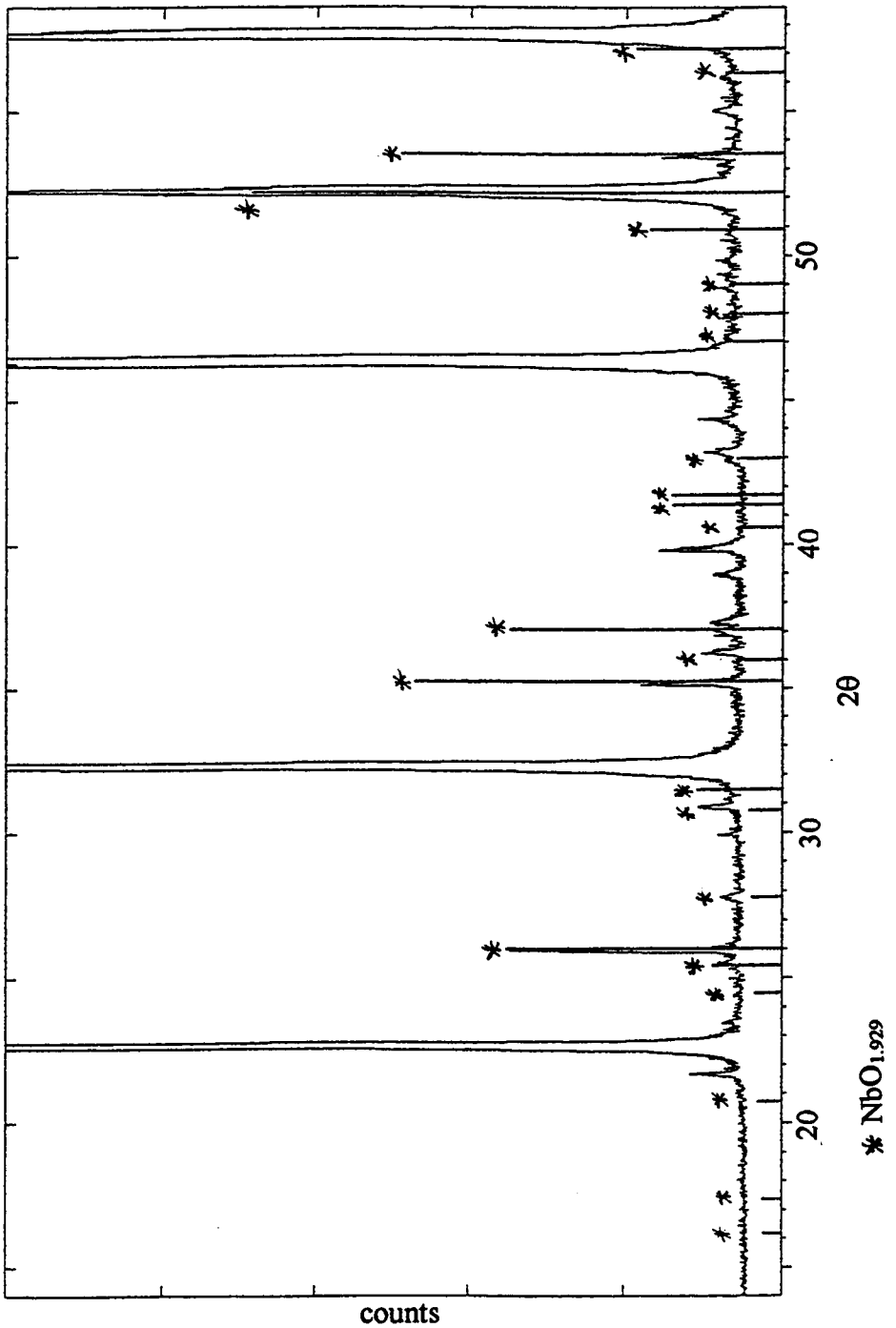

Figure 24a: XRD powder pattern of $Ca_{0.66}NbO_{2.90}$

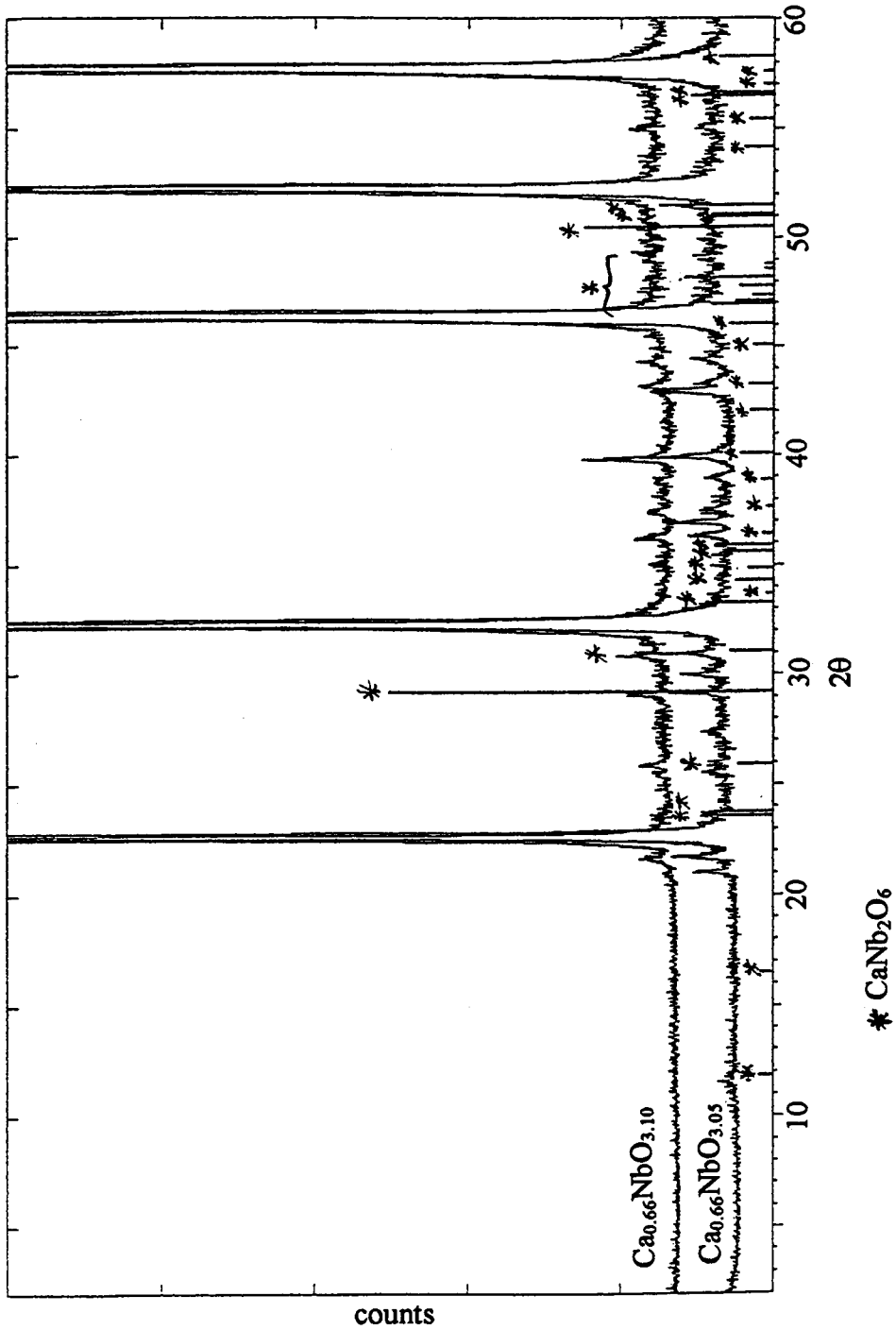

Figure 24b: XRD powder patterns of $Ca_{0.66}NbO_{3.05}$ and $Ca_{0.66}NbO_{3.10}$

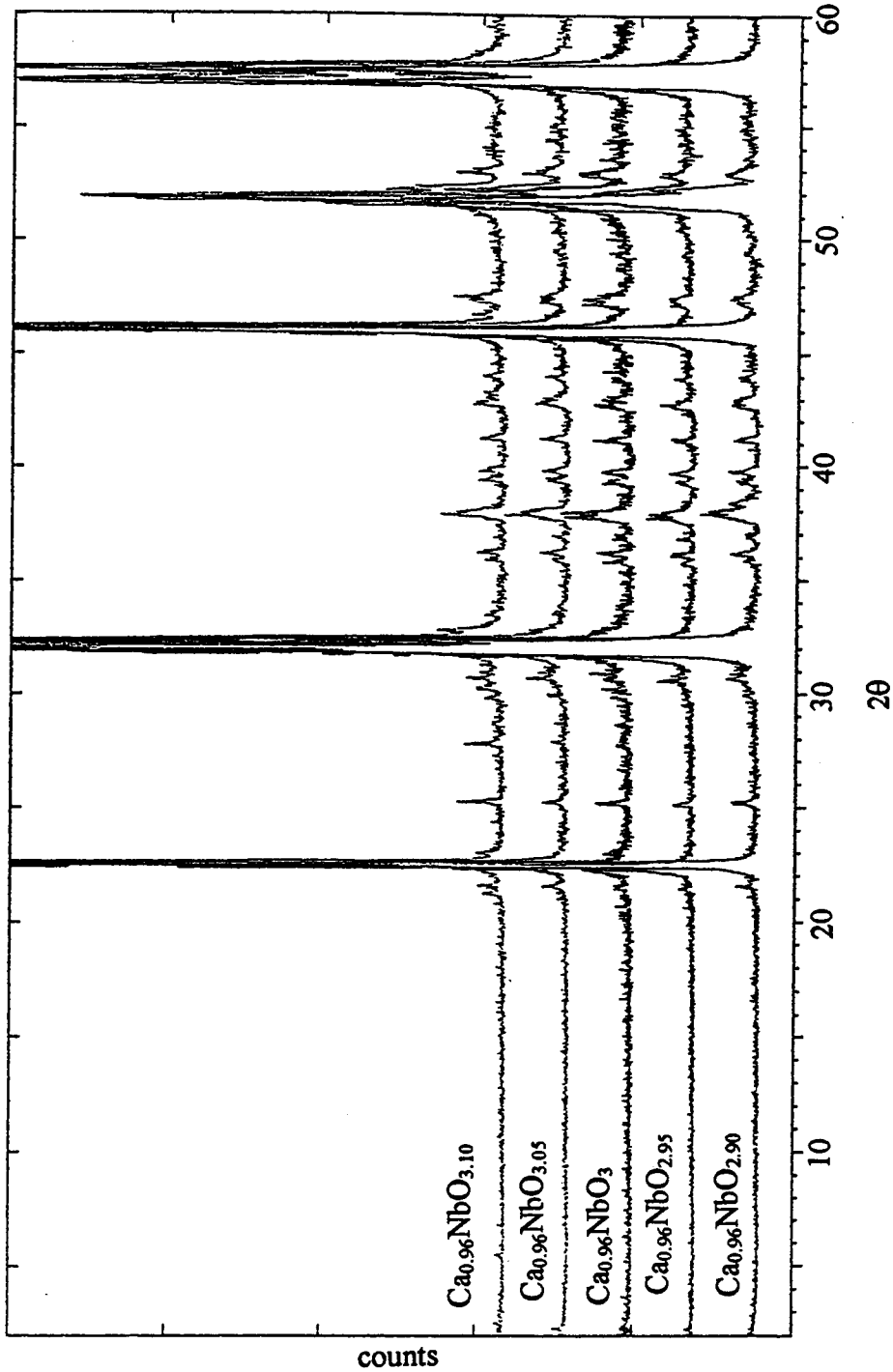

Figure 25: XRD powder patterns of $Ca_{0.96}NbO_y$

References

36.) S. Geller, *J. Chem. Phys.*, **24,** 1236-1239, (1950).

37.) A. M. Glazer, *Acta Cryst.*, **B28,** 3384-3392, (1972).

38.) Suggested modifications of Glazer by Pat Woodward

IV. Single Crystal X-ray Diffraction

Single crystals can be obtained from samples of apparently any composition in the Ca_xNbO_3 system. Samples that have undergone melting often have crystals in small pockets or indentations on the pellets. Even samples of starting composition $Ca_{0.56}NbO_3$ that melt at 1500°C have had small blue crystals inside the pellet in small cavities. The crystals are often cubes or collections of interpenetrating cubes.

A crystal suitable for single crystal diffraction work was found in a sample with starting composition $Ca_{0.76}NbO_3$ that was melted at 1600°C. The crystal was mounted on a glass fiber and photographed with a precession camera. The crystal showed sharp spots indicative of a good quality crystal. A starting lattice parameter of about 3.9Å was also found from the photographs as well as the indication of mirror planes of symmetry in the crystal.

Data was collected on a Rigaku single crystal diffractometer using molybdenum radiation from $2\theta = 2°$ to 100°. A search by the instrument yielded an initial cubic cell with a cell edge of 3.9103Å. When doubling or tripling of the unit cell was investigated, by means of an computer driven search for appropriate peaks, no peaks were found to suggest a superstructure. However, scanning several peak positions revealed very weak intensity present that was lower than the computer's cut off for an observed peak. The final data was collected on a doubled unit cell with a lattice parameter of 7.828Å. The larger cell peaks were counted as observed by the computer in its data collection routine. The data was corrected for absorption with a psi scan.

The structure was refined in space group P m $\bar{3}$ m (#221) with a final R factor of 2.26% and an R_w of 4.09%. A summary of the refinement results is listed in table 5 which is followed by table 6 containing atomic positions, table 7 with thermal parameters, table 8 with atom atom distances, and finally table 9 with the F_{obs} and F_{calc} values.

$Ca_{0.75}NbO_3$ has a double perovskite type structure. There are calcium vacancies on three of the four calcium sites. The calcium site at the origin is completely vacant, whereas the calcium sites at 1/2 1/2 1/2 and 1/2 0 0 are partially vacant and 0 1/2 1/2 is completely filled. Oxygen 1 at 0 0.2170 0.2170 has a rather large thermal ellipsoid with its major axis perpendicular to the face diagonal of the unit cell. Niobium is in a distorted octahedra of three short and three long Nb-O bonds (Fig. 26). This structure contrasts with that of Sr_xNbO_3 (x = 0.72 and 0.86) and $Ba_{0.95}$NbO3, both of which have a simple perovskite unit cell and no ordering of vacancies on the cation site [39].

Ordering of A cations is not very common in perovskite type phases. Other perovskite related compounds that do show A site ordering of vacancies are the $R_{1+x}Nb_3O_9$ (R = La, Ce, Nd) phases [40,41], $La_{2/3}(Mg_{1/2}W_{1/2})O_3$ [42], and $La_{2/3}TiO_3$ [43]. In these structures, the ordering takes the form of alternating A cation layers of all filled and all empty sites. $La_{2/3}(Mg_{1/2}W_{1/2})O_3$ also has an ordering of Mg and W in a rocksalt type arrangement.

More precession film work, subsequent to this crystal solution, has been done. The photographs show a unit cell of at least 32Å along a,b, and c. This corresponds to a cell that is eight times the simple perovskite unit cell. A solution of this cell may account for the large thermal parameters on O(1) through some ordering mechanism.

Table 5. Single Crystal Refinement Summary

Formula	$Ca_{0.75}NbO_3$
Space Group	P m $\bar{3}$ m (#221)
a, Å	7.828
V, Å^3	479.68
d_{cala}, g/cm^3	4.7456
Z	8
Instrument	igaku AFC6R
Scan type	ω 2θ
Radiation(monochromated in incident beam)	MoKα (λ = 0.71069 Å)
Temperature, °C	23
Data collection range	2° ≤ 2θ ≤ 100°
Observations	111
Refined Parameters	12
Refl. with delF/sigF>5.0	6
Largest difference peak, e/Å	1.417
Largest neg. diff. peak, e/Å	-1.820
R	2.26%
R_w	4.09%

Table 6. Atomic Positions

Atom	x	y	z	Occup.
Ca(1)	0.0000	0.0000	0.0000	0.004
Ca(2)	0.5000	0.5000	0.5000	0.769 (0.005)
Ca(3)	0.5000	0.0000	0.0000	0.736
Ca(4)	0.0000	0.5000	0.5000	1.000
Nb(1)	0.2485 (0.0003)	0.2485 (0.0003)	0.2485 (0.0003)	1.000
O(1)	0.0000	0.2170 (0.0024)	0.2170 (0.0024)	1.000
O(2)	0.5000	0.2176 (0.0013)	0.2176 (0.0013)	1.000

Table 7. Thermal Parameters

Atom	u11	u22	u33	u12	u13	u23
Ca)1	0.0165					
Ca)2	0.0165					
Ca)3	0.0161					
Ca)4	0.027					
Nb)1	0.005087	0.005087	0.005087	0.0002	0.0002	0.0002
O)1	0.001	0.05	0.05	0.0	0.0	-0.02
O)2	0.007					

Table 8. Atom-atom Distances

Atom	Atom	Distance	Atom	Atom	Distance	Atom	Atom	Distance
Ca)3	Ca)4	3.9139)5	Ca)4	O)2	2.7907)4	Nb)1	O)1	1.9765)3
Ca)3	Ca)4	3.9139)5	Ca)4	O)2	2.7907)4	Nb)1	O)1	1.9765)3
Ca)3	Ca)4	3.9139)5	Ca)4	O)2	2.7907)4	Nb)1	O)1	1.9765)3
Ca)3	Ca)4	3.9139)5	Ca)4	O)2	2.7907)4	Nb)1	O)2	1.9980)3
Ca)3	Nb)1	3.3830)5	Ca)4	O)2	2.7907)4	Nb)1	O)2	1.9980)3
Ca)3	Nb)1	3.3830)5	Ca)4	O)2	2.7907)4	Nb)1	O)2	1.9980)3
Ca)3	Nb)1	3.3830)5	Ca)4	O)2	2.7907)4	Ca)4	Nb)1	3.3963)5
Ca)3	Nb)1	3.3830)5	Ca)4	O)2	2.7907)4	Ca)4	Nb)1	3.3963)5
Ca)3	Nb)1	3.3830)5	Ca)4	O)1	3.1331)4	Ca)4	Nb)1	3.3963)5
Ca)3	Nb)1	3.3830)5	Ca)4	O)1	3.1331)4	Ca)4	Nb)1	3.3963)5
Ca)3	Nb)1	3.3830)5	Ca)4	O)1	3.1331)4	Ca)4	Nb)1	3.3963)5
Ca)3	Nb)1	3.3830)5	Ca)4	O)1	3.1331)4	Ca)4	Nb)1	3.3963)5
Ca)3	O)1	2.7916)4	Ca)1	O)1	2.4021)3	Ca)4	Nb)1	3.3963)5
Ca)3	O)1	2.7916)4	Ca)1	O)1	2.4021)3	Ca)4	Nb)1	3.3963)5
Ca)3	O)1	2.7916)4	Ca)1	O)1	2.4021)3	Ca)2	O)2	3.1258)4
Ca)3	O)1	2.7916)4	Ca)1	O)1	2.4021)3	Ca)2	O)2	3.1258)4
Ca)3	O)1	2.7916)4	Ca)1	O)1	2.4021)3	Ca)2	O)2	3.1258)4
Ca)3	O)1	2.7916)4	Ca)1	O)1	2.4021)3	Ca)2	O)2	3.1258)4
Ca)3	O)1	2.7916)4	Ca)1	O)1	2.4021)3	Ca)2	O)2	3.1258)4
Ca)3	O)1	2.7916)4	Ca)1	O)1	2.4021)3	Ca)2	O)2	3.1258)4
Ca)3	O)2	2.4093)3	Ca)1	O)1	2.4021)3	Ca)2	O)2	3.1258)4
Ca)3	O)2	2.4093)3	Ca)1	O)1	2.4021)3	Ca)2	O)2	3.1258)4
Ca)3	O)2	2.4093)3	Ca)1	O)1	2.4021)3	Ca)2	O)2	3.1258)4
Ca)3	O)2	2.4093)3	Ca)1	O)1	2.4021)3	Ca)2	O)2	3.1258)4
Ca)3	Ca)1	3.9139)5	Ca)4	Ca)2	3.9139)5	Ca)2	O)2	3.1258)4
Ca)3	Ca)1	3.9139)5	Ca)4	Ca)2	3.9139)5	Ca)2	O)2	3.1258)4
Nb)1	Ca)2	3.4096)5	Nb)1	Ca)1	3.3696)5			

k	l	Fo	Fc	sigF
^^^^^^	h = 0	^^^^^^		
0	2	2207	2152	33
0	6	1116	1099	18
0	8	1821	1832	28
0	12	1027	1051	18
1	-1	83	148	13
2	2	2849	2835	43
2	6	1882	1861	28
4	-14	454	433	9
4	-12	921	935	15
4	0	3686	3650	55
4	2	1685	1657	25
4	4	2690	2660	41
4	6	1080	1059	17
6	-6	1511	1505	23
8	-6	900	905	14
8	-2	1167	1156	18
9	-7	129	102	11
10	-4	671	693	12
10	2	1181	1178	18
10	10	830	810	16
12	10	491	501	10
14	0	436	415	25
16	0	586	592	15
^^^^^^	h = 1	^^^^^^		
0	-3	222	158	12
0	0	89	86	5
1	-2	81	127	8
5	2	100	15	12
^^^^^^	h = 2	^^^^^^		
1	-3	191	165	9
2	-10	817	808	14
2	-6	940	895	15
2	-3	82	163	9
2	2	491	537	10
2	8	1734	1722	27
4	-14	641	648	12
5	-3	171	127	15
6	-12	894	891	15
7	-5	148	128	9
7	-1	138	122	11
8	-4	1014	1017	16
8	6	1338	1331	21
12	-10	593	596	11
14	0	688	683	12
16	-2	653	670	13

k	l	Fo	Fc	sigF
^^^^^^	h = 3	^^^^^^		
0	-5	223	196	14
^^^^^^	h = 4	^^^^^^		
0	-8	1556	1570	24
2	-6	1719	1709	26
2	2	2440	2427	37
3	1	100	109	11
3	5	118	148	8
4	-14	442	438	13
4	-4	2146	2119	33
4	2	1407	1388	22
6	6	1404	1392	22
6	10	978	977	16
10	-4	663	683	14
10	2	1092	1107	17
10	8	612	610	11
10	10	752	739	14
12	-8	631	646	12
12	-6	616	604	11
12	4	845	843	15
12	10	470	466	9
16	-2	455	455	9
^^^^^^	h = 5	^^^^^^		
0	-1	134	82	11
4	2	80	157	11
^^^^^^	h = 6	^^^^^^		
0	-14	658	649	12
2	-14	516	522	10
2	-6	925	910	15
4	4	1002	997	16
6	-10	680	668	13
6	6	839	843	17
6	14	452	458	10
10	-12	502	505	10
10	2	757	753	13
10	8	763	759	13
12	0	675	669	12
12	6	716	724	14
12	8	464	463	9
^^^^^^	h = 7	^^^^^^		
0	5	150	112	14

k	l	Fo	Fc	sigF
^^^^^^	h = 8	^^^^^^		
0	-10	640	644	12
0	-8	1073	1105	18
4	-6	831	830	13
4	-4	1377	1379	22
6	-8	632	658	13
6	6	1087	1088	18
8	-4	986	1004	17
8	-2	726	757	13
8	8	776	777	19
10	2	886	884	14
14	0	444	425	9
^^^^^^	h = 9	^^^^^^		
3	0	142	130	12
^^^^^^	h = 10	^^^^^^		
0	-6	1055	1058	17
0	0	666	680	13
2	-10	611	600	13
6	-10	534	510	13
8	-10	555	563	13
8	8	515	513	12
^^^^^^	h = 11	^^^^^^		
0	0	119	209	19
^^^^^^	h = 12	^^^^^^		
0	-2	808	810	13
0	8	682	695	12
2	-8	499	513	9
2	2	1142	1134	19
4	2	713	710	12
8	-8	531	529	13
^^^^^^	h = 13	^^^^^^		
0	2	109	114	16
^^^^^^	h = 14	^^^^^^		
2	-9	104	49	17
2	-2	547	564	14
6	-4	588	601	11
8	-4	428	410	8
8	2	515	528	10
^^^^^^	h = 16	^^^^^^		
0	2	535	523	11
0	4	549	528	11

Table 9. F_{obs} vs. F_{calc}

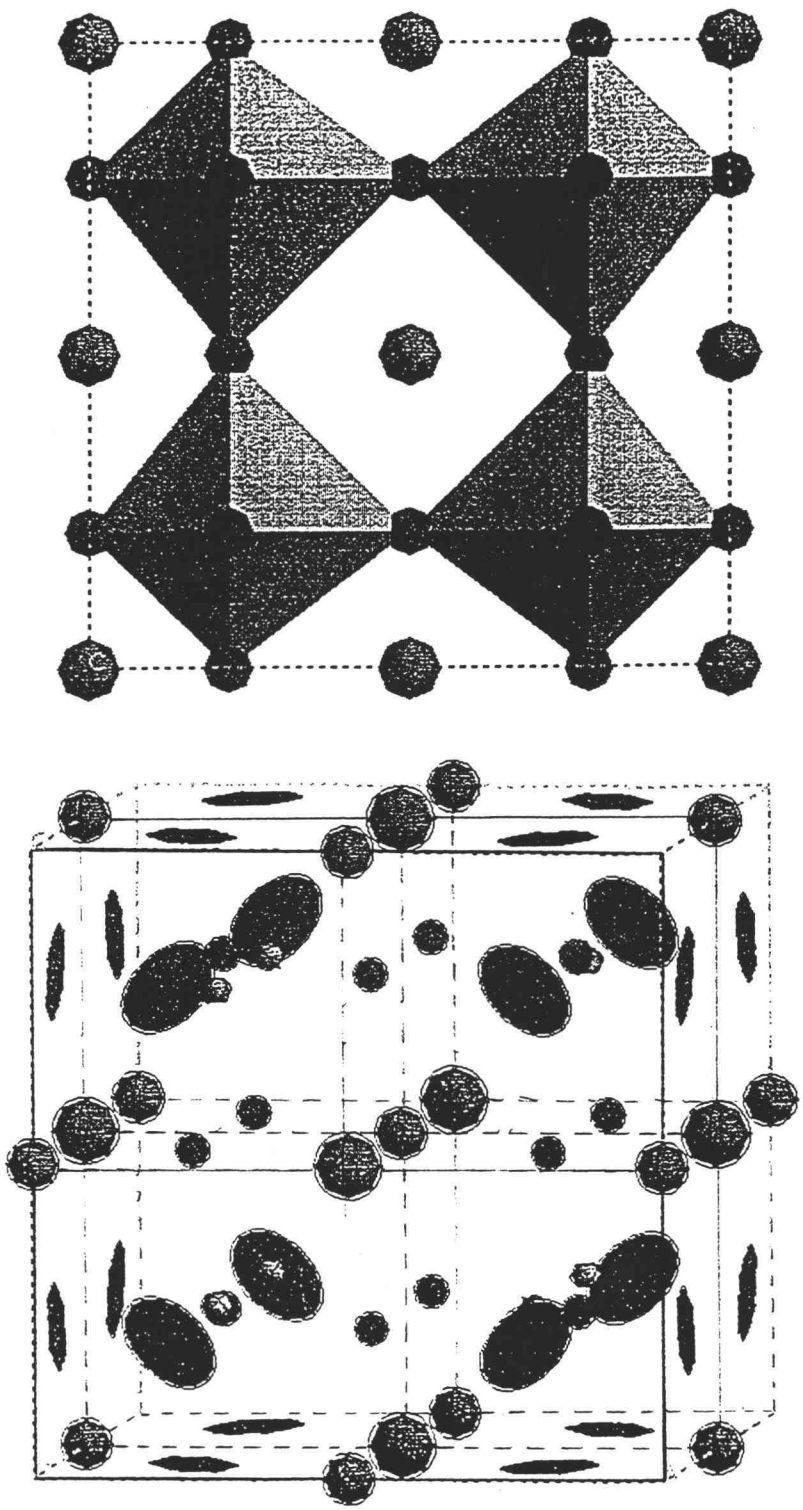

Figure 26: Structure of $Ca_{0.75}NbO_3$ from single crystal XRD

References

39.) B. Hessen, S. A. Sunshine, T. Siegrist, and R. Jimenez, *Mat. Res. Bull.*, **26,** 85-90, (1991).

40.) A. M. Abakumov, R. V. Shpanchenko, and E. V. Antipov, *Mat. Res. Bull.*, **30,** 97-103, (1995).

41.) P. N. Iyer and A. J. Smith, *Acta Cryst.*, **23,** 740-746, (1967).

42.) Y. Torii, *Chem. Lett.*, **1979,** 1215-1218.

43.) M. Abe and K. Uchino, *Mat. Res. Bull.*, **9,** 147-156, (1974).

V. Magnetic Susceptibility Measurements

An important property of superconductors, other than zero resistance to electrical flow, is that below the critical temperature a superconductor is a perfect diamagnet. In such a state, all magnetic field is excluded from the interior of the superconductor. Because of this property, the T_c can be determined by plotting the magnetic susceptibility of a sample as a function of temperature. Such a plot shows a decrease in magnetic susceptibility below T_c.

To measure magnetic susceptibility a sample of about 0.4g is loaded into a small sample holder at the end of a long probe. When the probe is in place in the instrument, the sample sits inside several coils of wire and surrounded by two nested dewers of liquid He and liquid N_2. The sample is initially very close to liquid He temperature and is then warmed up by a resistive heater in a controlled manner (see Fig. 27).

The coils of wire around the sample are used to measure the magnetic susceptibility. The outer coil is the primary and generates an alternating magnetic field. This field is picked up by the sensing coils, which are two coils with opposite winding that are connected in series. This arrangement of the sensing coils cancels out the voltages induced by the ac field and any outside sources. Ideally, when no sample is present inside the coils no voltage will be detected. Placing a sample in one of the coils disrupts this balance and causes a voltage to be read. This voltage is proportional to the magnetic susceptibility[44].

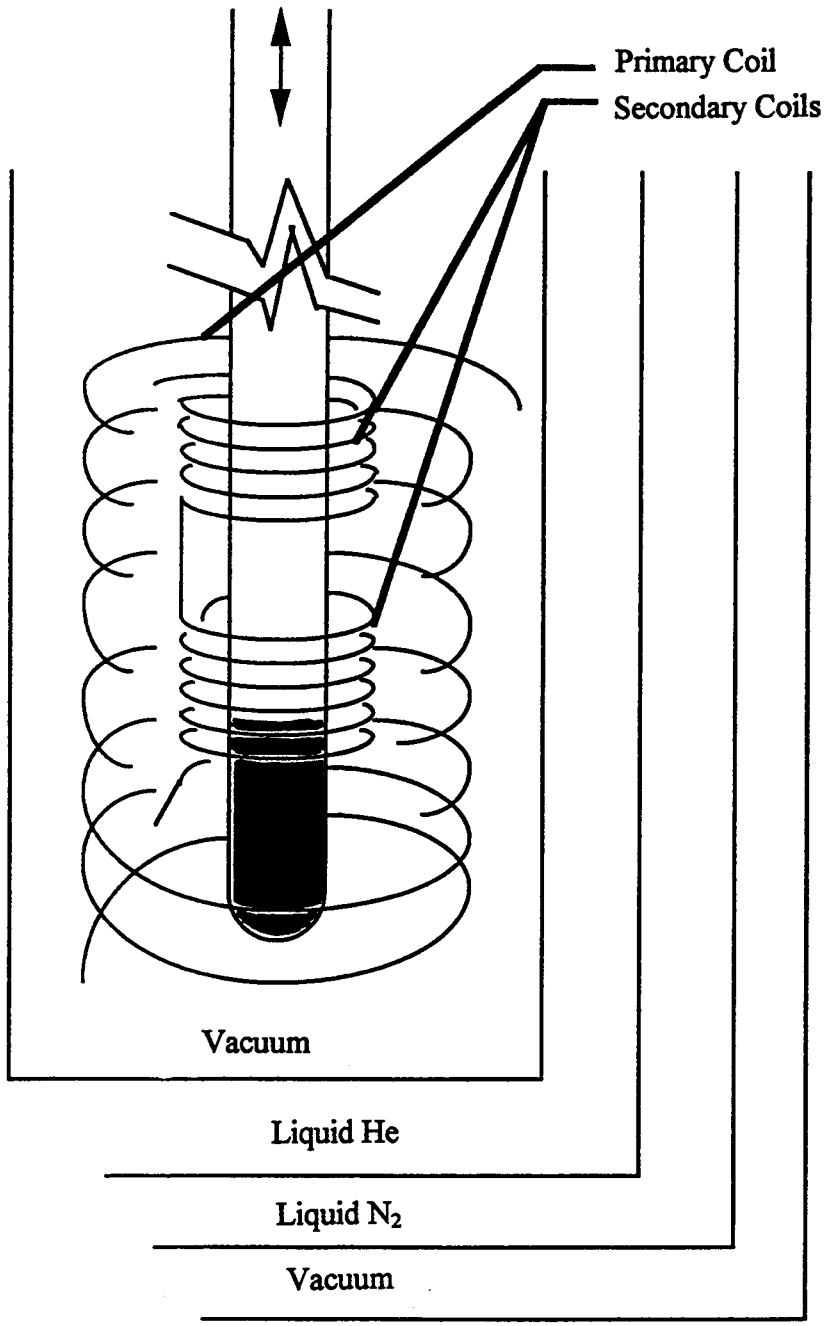

Figure 27: Magnetic susceptibility measurements

In practice the sample is moved between the two sensing coils at each temperature point to insure that the offset voltage (the voltage that arises from two nonidentical coils) is compensated. If coil one gives a voltage $V_1 = V + V_{offset}$ and coil two gives $V_2 = -V + V_{offset}$ then the true voltage V can be found by $V = (V_1 - V_2)/2$ [44].

All measurements were taken using the Model 7000 AC Susceptometer made by Lake Shore Cryotronics, Inc.

The three samples measured were $Ca_{0.66}NbO_3$, $Ca_{0.80}NbO_3$, and $Ca_{0.96}NbO_3$. None of these samples showed any transition to a superconducting state.

References

44.) Instruction Manual, Model 7000 AC Susceptometer, 1989, Lake Shore Cryotronics, Inc.

VI. NbN Formation by Ignition in Air[45]

It has been reported by Gasparov et al. that a Ba/Nb/O phase, with T_c about 20K and an fcc (face centered cubic) structure of lattice parameter 4.40Å, has been found in mixtures of Nb metal powder and BaO_2 reacted at around 600°C in air[46]. This was of interest because the highest T_c for Nb oxide compounds so far found is only 5.5K for $Li_{0.45}NbO_3$ [47]. For this reason, an investigation of these results was undertaken.

Mixtures of Nb metal powder and BaO_2 in a $0.33BaO_2$:1Nb ratio were ground together in an agate mortar. The resulting powder was pressed into a pellet and placed in an alumina boat. The samples were then loaded into a muffle furnace, preheated to 600°C. When the samples became red hot they were removed immediately or after about five seconds. Other experiments of this type using SrO_2 instead of BaO_2, Nb by itself, or Ti \ Zr \ Mo \ W \ Ta in place of Nb were also carried out. These reactions produced a mixture of phases in most cases.

When BaO_2 was used with Nb the x-ray diffraction patterns showed the presence of $Ba_4Nb_2O_9$, $Ba_6Nb_3O_{13.5}$, and the fcc phase (Fig. 28). SrO_2 and Nb mixtures produced $Sr_4Nb_2O_9$, $SrNb_2O_6$, and again the fcc phase (Fig. 29). Both reactions yielded products that also contained unreacted niobium metal. The face centered cubic phase in both cases had a lattice parameter of 4.392 ± 0.002Å. This indicates that Ba and Sr are probably not in the structure since their size difference would likely show up as a difference in lattice parameter. In addition, the size of the cell edge for this fcc phase is the same as that

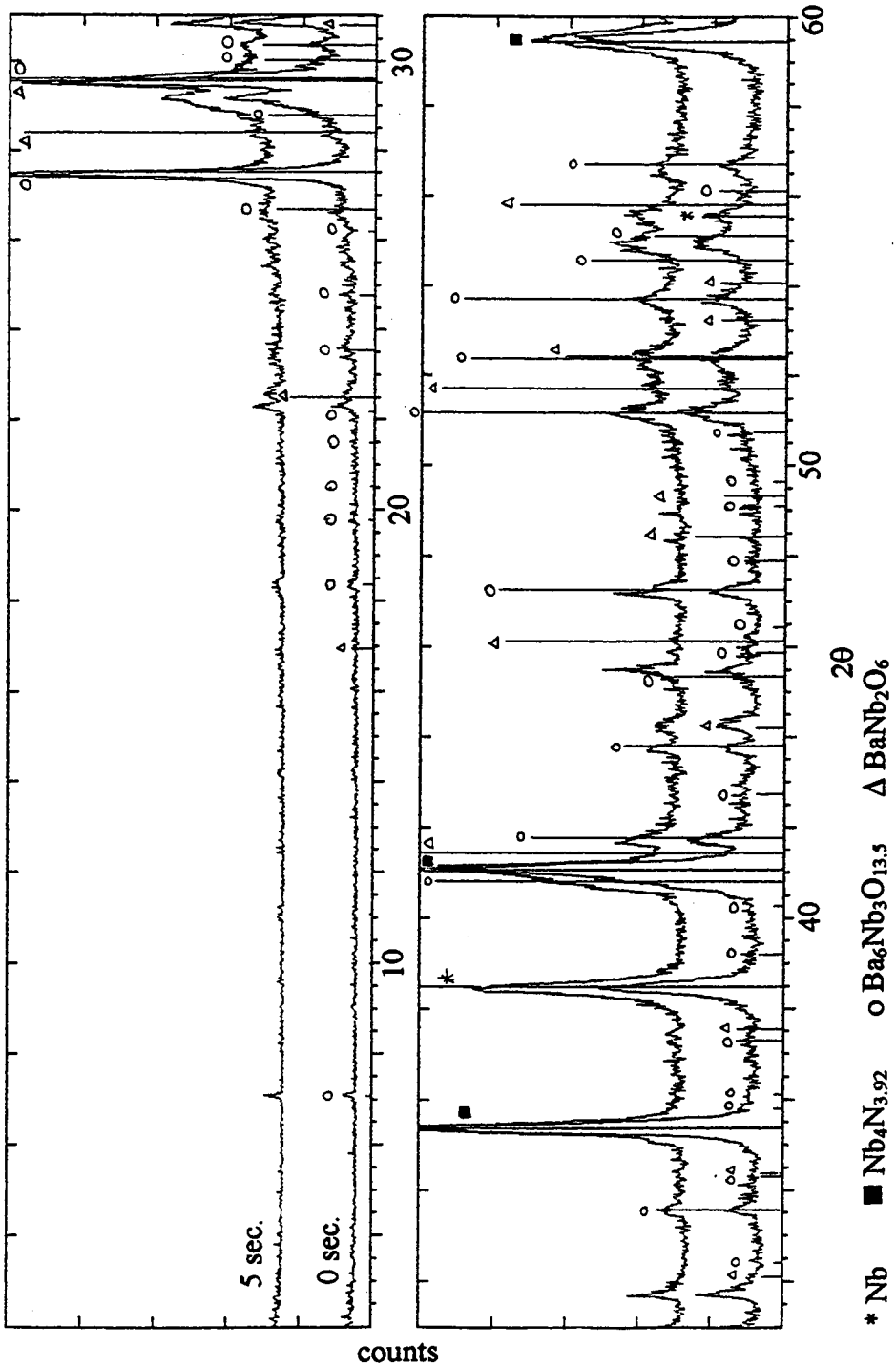

Figure 28: XRD of Nb and BaO_2 reacted in air

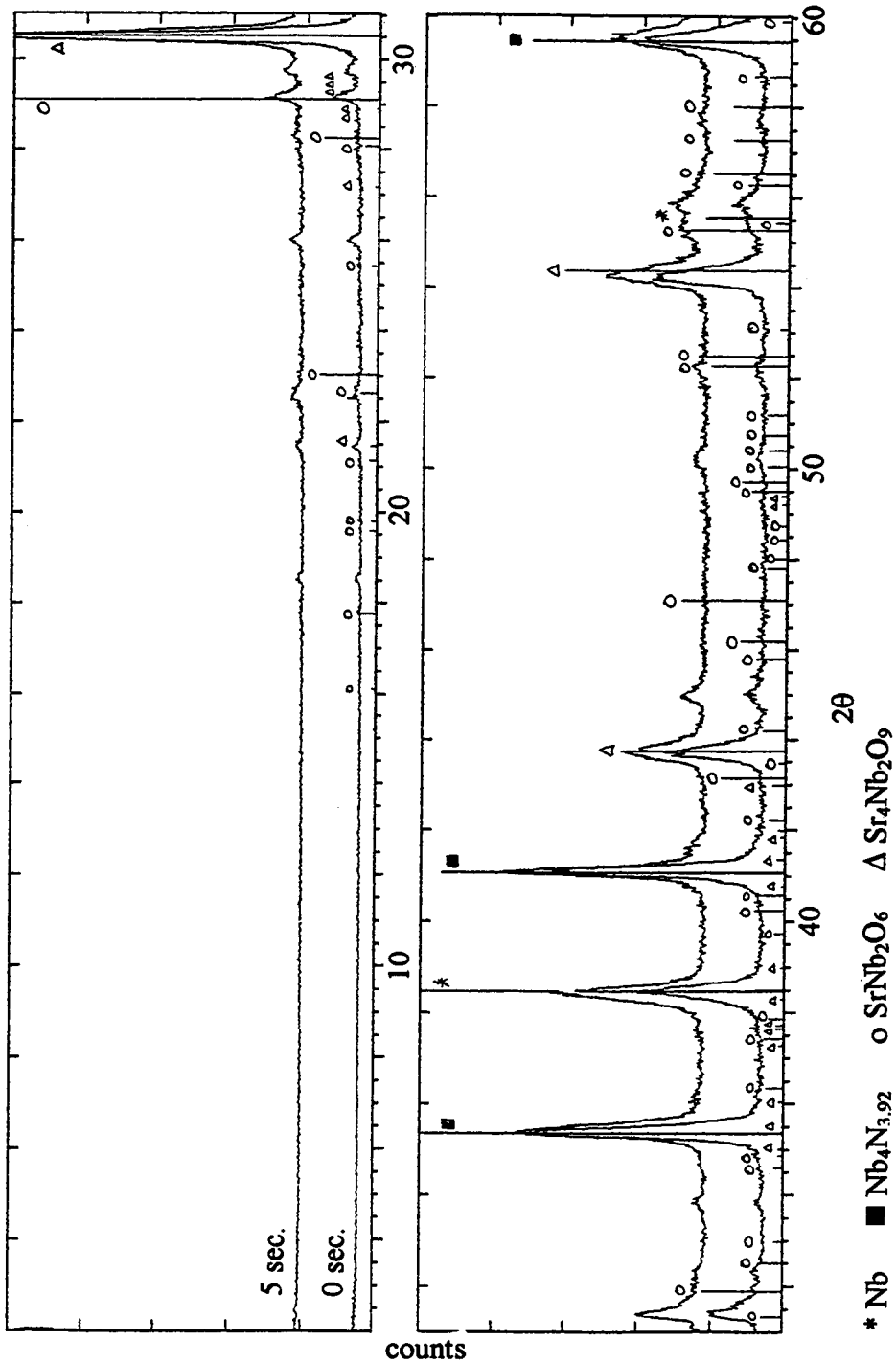

Figure 29: XRD of Nb and SrO_2 reacted in air

reported for NbN [48]. The x-ray results were essentially the same as those obtained by Gasparov et al..

When Nb is reacted by itself the only product is Nb_2O_5 and unreacted Nb (Fig. 30). Ti and BaO_2 mixtures yielded unreacted BaO_2 and Ti as well as Ba_2TiO_4 (Fig. 31). The reaction with Mo and BaO_2 produced unreacted Mo, Ba_2MoO_5, and $BaMoO_4$ (Fig. 32). W in place of Nb gives unreacted W, Ba_2WO_5, Ba_3WO_6, and $BaWO_4$ (Fig. 33). The reaction with Zr and BaO_2 was explosive and the pellet destroyed, but a mixture of Nb and Zr with BaO_2 produced predominantly $BaZrO_3$ with some $BaNb_2O_6$ and possibly $Nb_{0.20}Zr_{0.80}O_{2.10}$ and $ZrNb_{14}O_{37}$ (Fig. 34). In all of these reactions no nitride phase was observed.

The only other reaction of this kind that yielded a nitride phase was the reaction between Ta and BaO_2. The nitride phase found was Ta_2N along with $Ba_4Ta_2O_9$, $Ba_5Ta_4O_{15}$, and unreacted Ta (Fig. 35). The reaction with SrO_2 gave much weaker evidence for the presence of the nitride phase. Ta_2O_5 and SrO were also found in this sample (Fig 36).

Gasparov et al. used Auger analysis to examine their samples and found very little nitrogen in them. Based on this Auger work, the fact that Nb metal in air doesn't produce NbN under similar circumstances, probably the error in the reported lattice parameter for NbN in many literature sources, and the T_c for NbN of 16K which is lower than the 20K observed, all lead to the conclusion that NbN was not present in the sample.

The production of NbN in air under the conditions explained above could occur as follows. When the reaction starts the BaO_2 or SrO_2 may react with the Nb metal and more

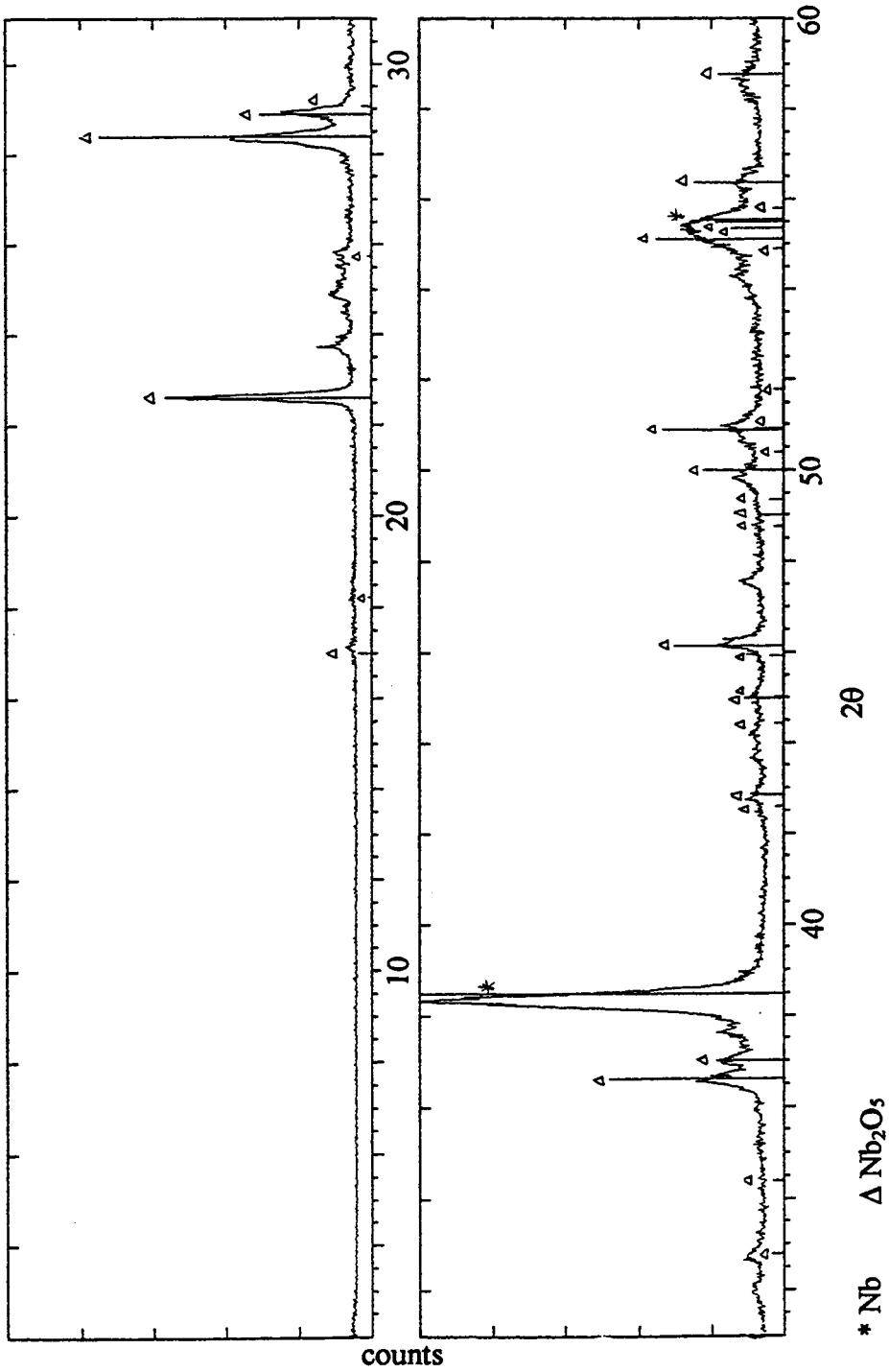

Figure 30: XRD of Nb in air

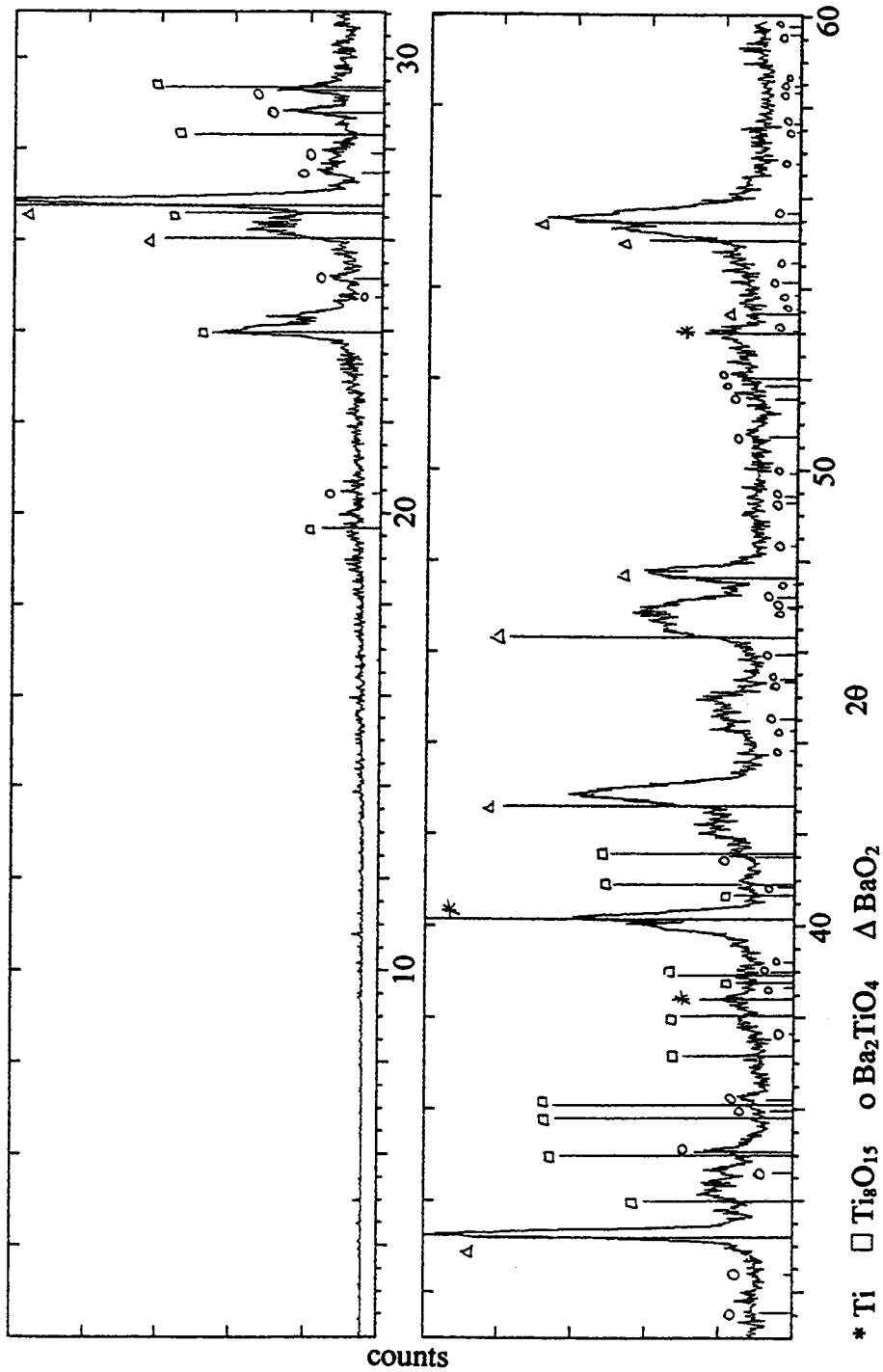

Figure 31: XRD of Ti and BaO_2 reacted in air

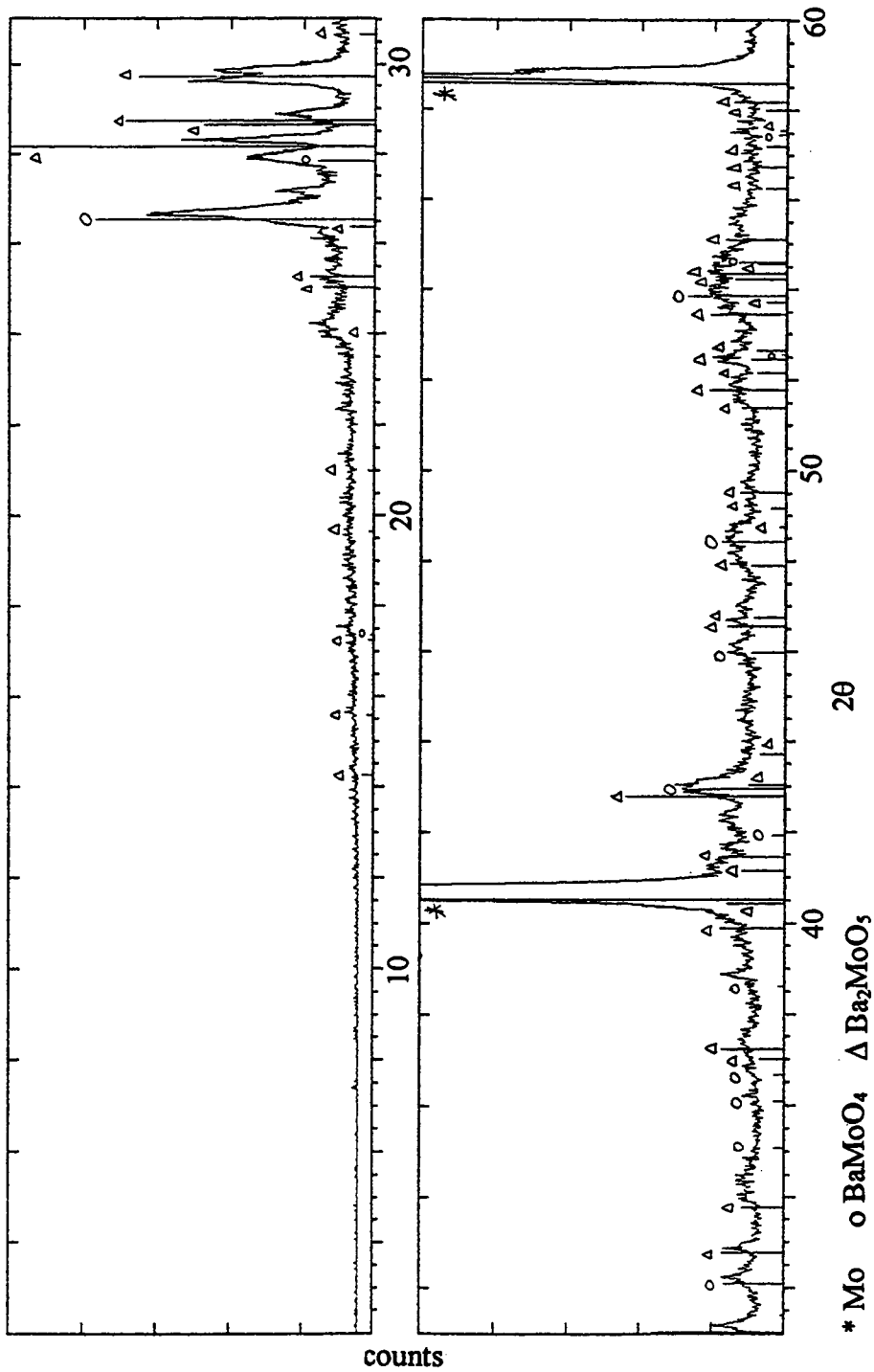

Figure 32: XRD of Mo and BaO_2 reacted in air

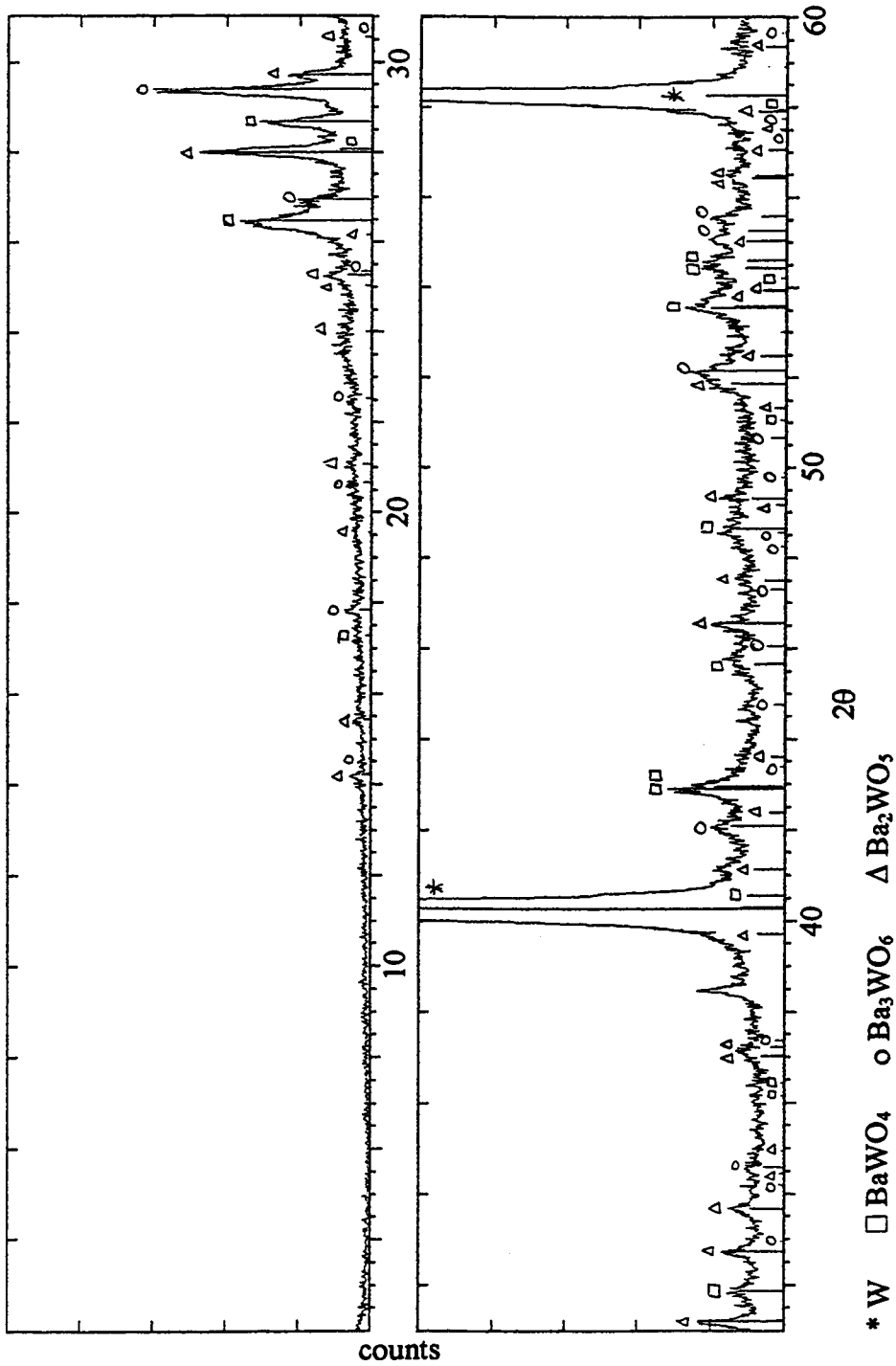

Figure 33: XRD of W and BaO_2 reacted in air

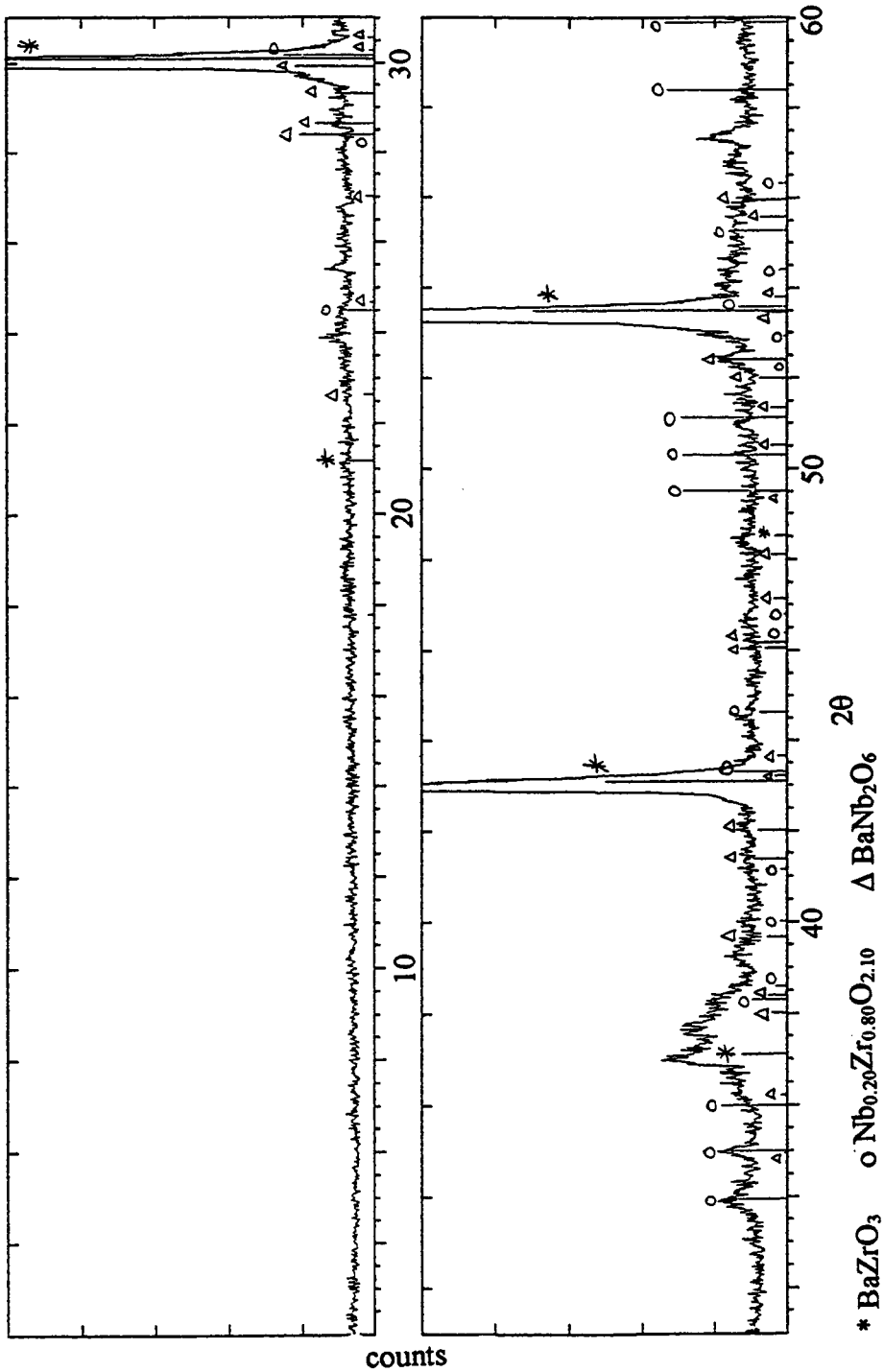

Figure 34: XRD of Zr, Nb and BaO_2 reacted in air

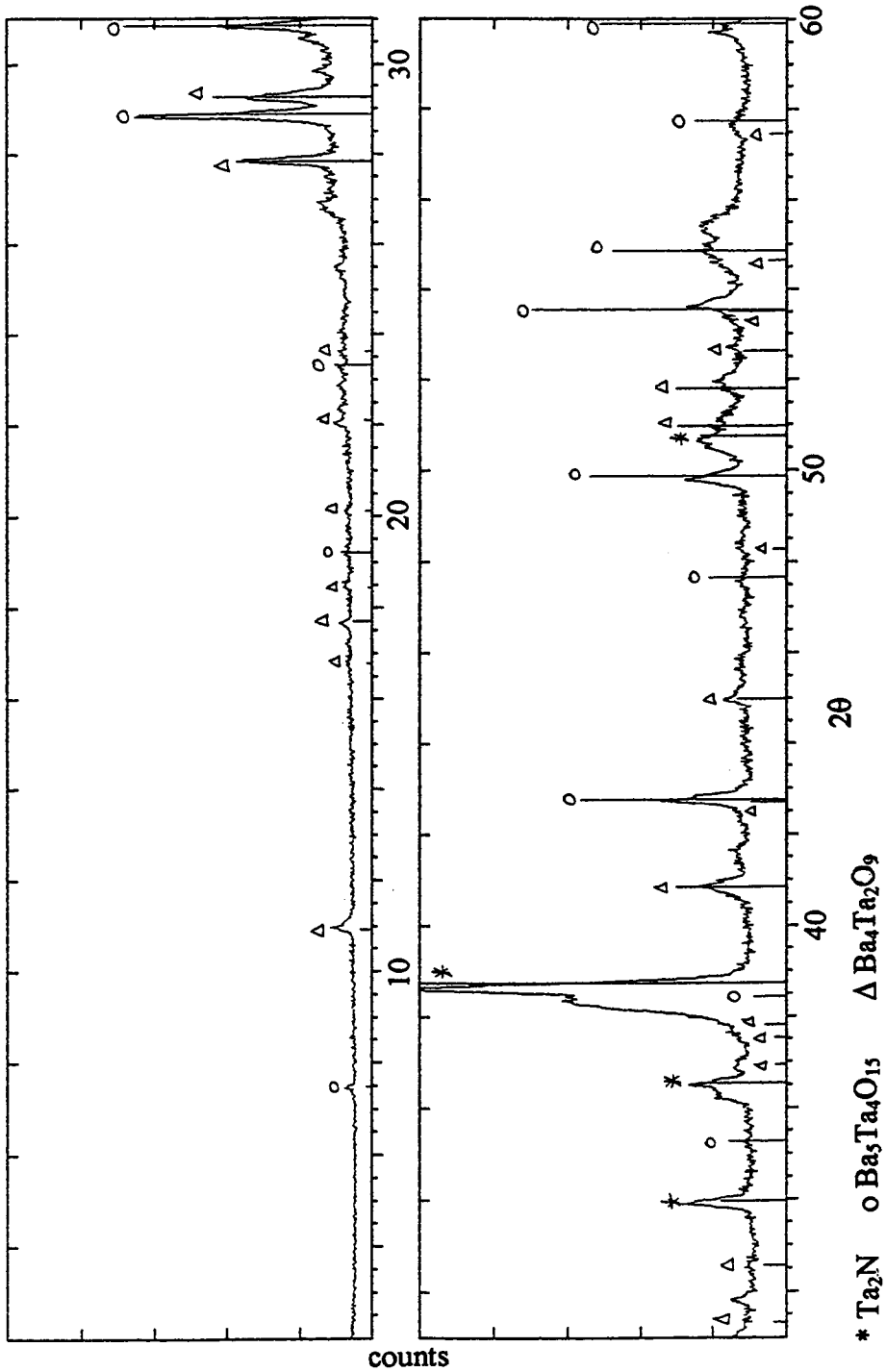

Figure 35: XRD of Ta and BaO_2 reacted in air

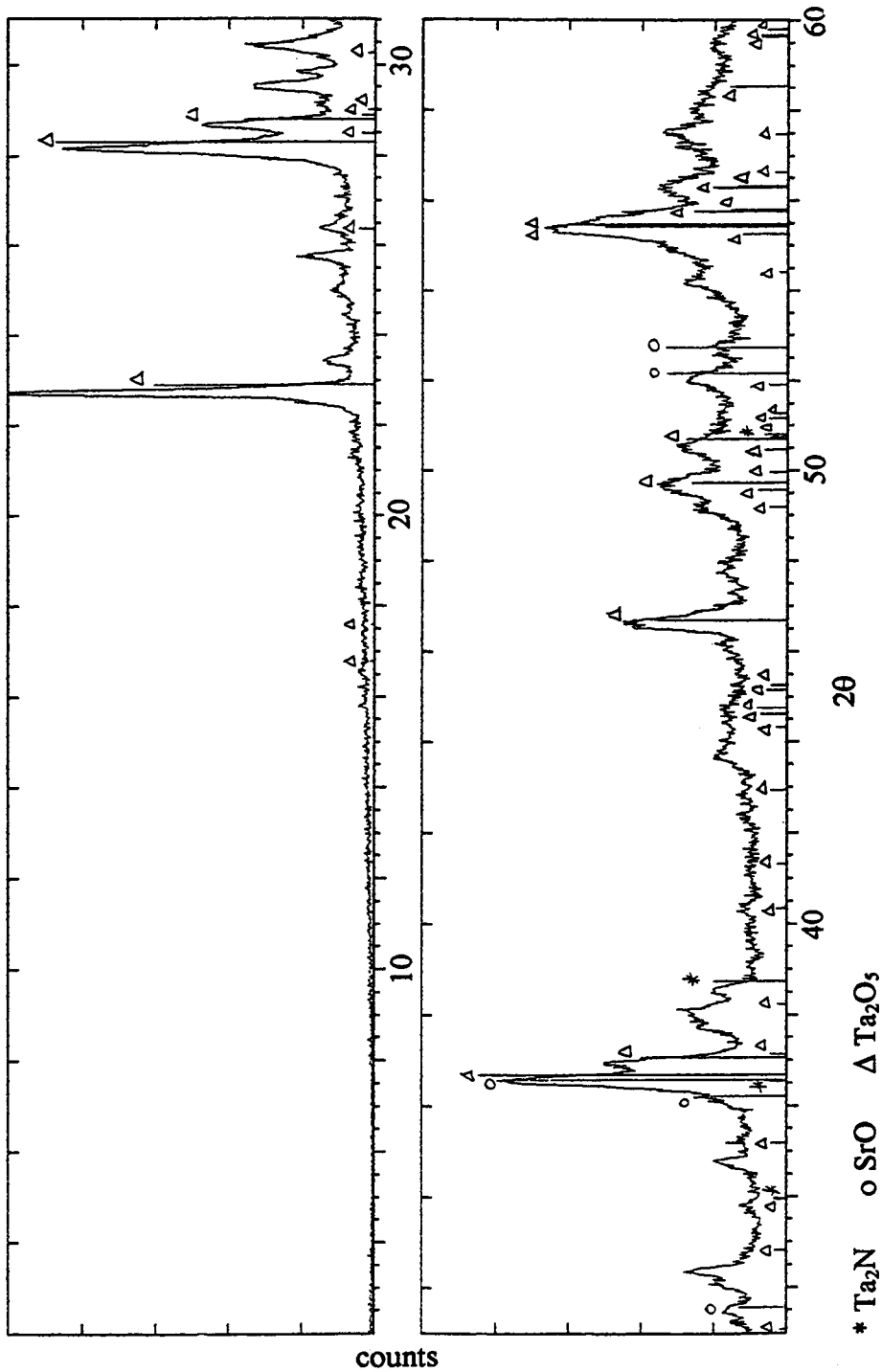

Figure 36: XRD of Ta and SrO_2 reacted in air

oxygen from the air to form barium/strontium niobium oxides. This reaction, if fast enough, would consume much of the local oxygen leaving a predominantly nitrogen atmosphere. The Nb metal then is exposed to this nitrogen atmosphere and forms NbN which is known to occur for Nb in N at these temperatures. NbN doesn't oxidize very rapidly at these temperatures so it is not subsequently converted to oxides.

J. G. Hou made ac susceptibility measurements on the samples of BaO_2/Nb and SrO_2/Nb prepared in our lab useing a Lakeshore ac susceptibility instrument. In both cases two T_cs were found. One was at 9K, indicative of the unreacted Nb in the samples, and the other was at 16K, which is what is expected for NbN. The Gasparov et al. result of a T_c of 20K may be due to carbon in the NbN which could give a T_c of around 18K. This carbon could have come from BaO_2 contaminated with carbonate.

R. L. Nielsen did electron microprobe analysis on our samples. To determine the quantitative amount of nitrogen in the sample, a synthetic multilayer diffracting crystal was used to separate the x-ray wavelengths coming off the sample for analysis. Regions of NbN were found in our samples as a reaction halo on the surface of the sample particles. The NbN regions are friable and can be knocked off and lost during analysis. This may be why Gasparov et al. did not see NbN in their Auger work.

Our results support the notion that the "unknown" fcc phase is in fact NbN. The phase matches that of NbN in the x-ray powder data file with a cell parameter of about 4.4Å. Electron microprobe shows the presence of NbN in the samples and ac susceptibility measurements show a transition temperature of 16K.

References

45.) P. E. Bacon, J. G. Hou, A. W. Sleight, and R. L. Nielsen, this work is currently in press.

46.) V. A. Gasparov, G. K. Strukova, and S. S. Khassanov, *Jour. Exper. Theor. Phys.*, **60,** 440, (1994).

47.) M. J. Geselbracht, T. J. Richardson, and A. M. Stacy, *Nature,* **345,** 324, (1990).

48.) A. Christensen, *Acta Chem. Scand. A,* **31,** 77, (1977).

VII. The Reaction of $YBa_2Cu_3O_6$ with Iodine

VII.1 Literature Review

When the high temperature superconductor $YBa_2Cu_3O_{7-\delta}$ (123-O_7) is annealed in vacuum or inert gas, it looses oxygen to form the insulator $YBa_2Cu_3O_6$ (123-O_6). At high temperatures (650°C) under oxygen the reverse process takes place with the reemergence of superconductivity. The oxygen that leaves or enters the structure is associated with the O(1) position in the Cu(1) chains of the structure (see Fig. 37).

If the deoxygenated 123-O_6 is exposed to halogen gases, superconductivity is observed in the resulting products. Transition temperatures of 90K, 80K, and 55K are typically observed for Cl, Br, and I samples respectively. In these experiments, the researchers wanted to replace oxygen with halogens to get information about the mechanism of high temperature superconductivity. Much debate ensued as to what the reaction products really were and whether the halogen ended up in the structure or in impurity phases. One side of the debate claimed that halogens substituted for oxygen at various sites in the 123 lattice. The other side claimed that iodine reacted with 123 to form impurity phases and that oxygen released in this process reoxygenated unreacted starting material.

The case in favor of iodine-oxygen isomorphism was first put forward by Ossipyan et al. in 1989. In this study, samples of 123 were made with 2 atomic % and 10 atomic % Fe in place of Cu so that Mössbauer studies could be conducted[49]. The Mössbauer technique probes the energy transitions in the nucleus and is limited to those

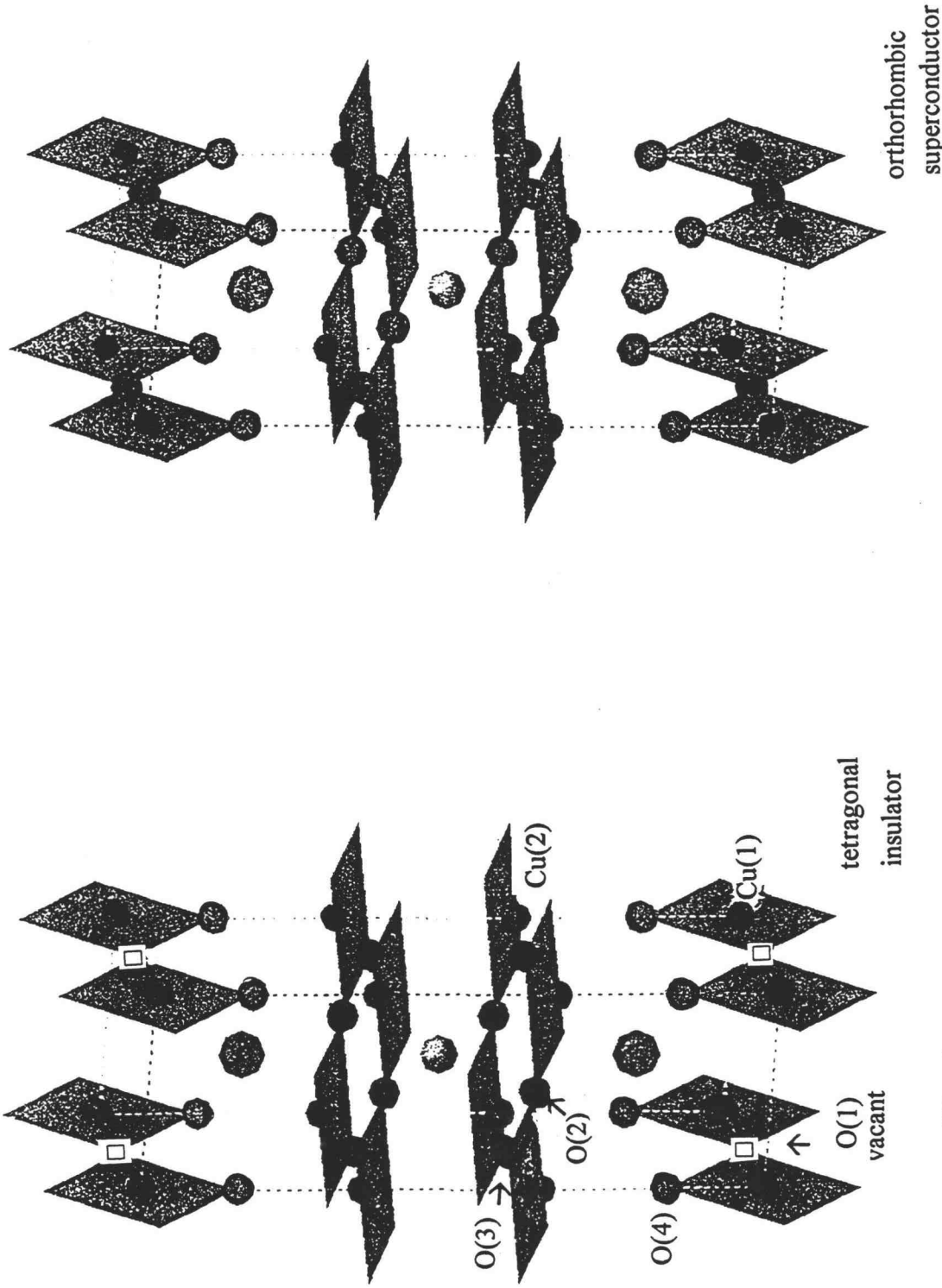

Figure 37: Structures of $YBa_2Cu_3O_6$ and $YBa_2Cu_3O_7$

atoms for which an available γ-ray source exists. The energy transitions are influenced by the oxidation state of the atom since the nuclear transitions are perturbed slightly by the chemical environment of the nucleus. Other influences on the spectrum are electric field gradients and magnetic interactions at the nucleus. From the results the claim is made that no oxygen enters the Cu(1) chains and that the iodine that does enter the chains is close to I^0. X-ray diffraction results gave lattice parameters close to those of 123-O_7 and impurity levels were estimated at ≤ 5%.

In another study Ossipyan and Zharikov report on the interaction of powder samples and single crystals with halogen gases [50]. Again orthorhombic products with lattice parameters close to 123-O_7 are observed. In addition, chlorinated samples were found to have substantial amounts of amorphous phases. It was claimed that the relative intensities of various reflections showed that iodine went into the structure but no details were given.

Ossipyan et al., in 1990, conducted iodine mössbauer experiments [51]. The iodine content of the samples was reported to be typically $YBa_2Cu_3O_{6.1}$ $I_{0.96}$. This included iodine in any byproducts of the reaction. The mössbauer results indicated the presence of I^- and a small amount of IO_6^{-5}. They also noted that elemental iodine was missing from their samples. An estimate of the charge on the iodine, based on the observed isometric shifts, was given as between -0.87 and 0.

In 1989, Pavlyukhin et al., also performed iodine and iron mössbauer work [52]. They found iodine in -1, +7, and +5 states. For the iron work, 1-3% Fe was used. There were two doublets assigned to Fe in the Cu(1) layer and one that corresponded to Fe in the

Cu(2) sheets. The increase in size of one of the $Fe_{Cu(1)}$ doublets was associated with an increase in coordination. In the case of Br it was found that much of the Fe was coordinated whereas in the I case there wasn't any increase in the coordination of the Cu(1) iron. Both spectra were different from that given by a 123-O_7 sample.

Another study by Ossipyan et al studied single crystals treated in Br or I [53]. The samples after treatment were found to have a lot of twinning in the crystals. The tetragonal starting material was covered with orthorhombic regions with lattice parameters of a = 3.836Å, b = 3.877Å, and c = 11.722Å. These lattice parameters, if in oxygenated material, would give $O_{6.4}$, $O_{6.75}$, and $O_{6.65}$ in the formula $YBa_2Cu_3O_y$. This discrepancy was claimed to indicate the incorporation of iodine into the structure.

Nuclear quadrupole resonance (NQR) and electron paramagnetic resonance (EPR) experiments were conducted on ceramic samples treated with iodine or bromine [54]. From the x-ray data, the authors reported single phase orthorhombic iodinated samples with lattice parameters a = 3.834Å, b = 3.884Å, and c = 11.73Å. The Br treated samples were found to be two phases; the tetragonal starting material and the orthorhombic phase with lattice parameters close to those found for the iodinated samples. The $^{63,65}Cu$ NQR spectrum for the iodinated samples was like those found for Cu(2), (the copper in the sheets), in 123-$O_{6.9}$. The brominated samples showed peaks characteristic of both 123-$O_{6.1}$ and 123-$O_{6.9}$. Both iodinated and brominated samples were missing the signal characteristic of Cu(1) (the chain copper). The authors suggested that this could be because there was no oxygen in the chains or that the halogen atoms were arranged around the Cu(1) in a nonuniform manner. From EPR measurements, it was found that

brominated samples behaved much like the starting material whereas the iodinated samples behaved differently. Their results indicated that no oxygen was entering the Cu(1) chains upon halogenation. This would show up if more and more Cu^{+} in Cu(1) positions was oxidized to Cu^{+2} (d^9), which has a unpaired electron. Since no increase of unpaired electrons was observed they concluded that oxygen was not entering the Cu(1) chains.

In a later paper on more ^{63}Cu NQR work, the practically identical behavior of spin-echo envelopes is observed between 123-$O_{6.9}$ and iodinated samples [55]. The results showed that the iodinated phase is not 123-$O_{6.5}$. 123-$O_{6.5}$ would have a T_c of around 50 - 60K similar to the T_c observed for iodine treated samples of 123.

Nemudry et al. calculated the changes in x-ray peak intensities for halogen in various positions in the 123 structure [56]. These calculations were compared with anomalous synchrotron x-ray scattering data and it was found that Br in the Cu(1) planes agreed within 15-20% to the experimental data. Extended x-ray absorption fine structure (EXAFS) and mössbauer were also conducted. The EXAFS spectra for the Y absorption edge were the same before and after bromination, indicating that there was no change in the environment of Y. EXAFS of the Br absorption edge was found to be consistent with the calculations based on Br in the Cu(1) planes. Fe mössbauer results indicated that the coordination number of Fe in the Cu(1) position increased when 123 was treated with Br.

Mokhtari et al. in 1992 conducted x-ray diffraction, SEM, and EDS analyses on brominated (using either Br_2 or CBr_4) samples of 123-O_y (y = 6,6.7, and 7) [57]. SEM investigations showed that bromine enriched microcrystals, probably $BaBr_2$ and $CuBr_2$, occurred only after several hours of treatment. In addition the grain size of the products

found to contain much larger amounts of impurity phases with lowered Y contents. Significant Br enrichment was observed near grain boundaries and only a small amount of Br in the center of crystallites. From T_c measurements several things were noticed. If 123-O_6 was the starting material only one T_c was ever observed over the course of the reaction, whereas for 123-$O_{6.7}$ T_c varied as treatment progressed. The superconducting volume was found to increase with halogen content for 123-O_6 but remained constant for 123-$O_{6.7}$ and 123-O_7.

Radousky et al. in 1990 did x-ray Rietveld analysis, raman spectroscopy, x-ray fluorescence microprobe, and thermal gravimetric analysis (TGA) on brominated 123 samples[58]. The x-ray results showed that the orthorhombic 123-O_7 structure best fit the results. Fully occupying the vacancies in the Cu(1) chains with Br caused the residuals to increase. Calculations with Br on other oxygen sites yielded only small amounts of Br, within experimental error and thus not significant. The authors suggest that Br is perhaps randomly situated on interstitial sites. X-ray fluorescence did show Br distributed throughout the entire sample, with increased Br content near the edges of particles. Peaks in the raman investigations were consistent with the 123-O_y structure. The apical oxygen vibration had the same value as found in 123-O_7. In general brominated samples gave broad peaks in the raman spectra. Diffuse infrared reflectivity measurements showed the same results as those for 123-O_7. The TGA results showed that no Br was lost from the sample even up to 1000°C. Annealing the samples in nitrogen, did however release oxygen and the T_c was seen to decrease. The idea that Br may displace some oxygen which then entered the Cu(1) chains was also put forward to explain these results.

sample even up to 1000°C. Annealing the samples in nitrogen, did however release oxygen and the T_c was seen to decrease. The idea that Br may displace some oxygen which then entered the Cu(1) chains was also put forward to explain these results.

Kemnitz et al. also proposed a similar idea [59]. They postulate that the halogens (specifically Cl in this case) attack the 123-O_6 causing the release of oxygen. This liberated oxygen then interacts with some untouched 123-O_6 to form superconducting 123-O_7. In their samples they observe an orthorhombic phase that is identical with that of 123-$O_{6.9}$. As more Cl is added the x-ray patterns become more diffuse indicating the rise of amorphous products. Superconductivity is lost in samples with high Cl content. They also note that the final product is the same in both cases of 123-$O_{6.1}$ and 123-$O_{6.9}$ as starting materials. From weight increases in their samples, they found that the maximum amount of Cl would give a formula of "$YBa_2Cu_3O_{6.1}Cl_{7.4}$".

Nemudry et al. used electron microscopic studies (SEM, TEM, and electron diffraction), selective dissolution (SD), differentiating dissolution (DS), and magnetic susceptibility measurements on iodinated samples of 123 [60,61]. The electron microscopic studies showed that when iodine reacts with 123-O_6, the surface layers are destroyed. This is accompanied by the formation of barium and copper iodides as well as amorphous yttrium compounds. SD studies were conducted using N, N -dimethylformamide (DMFA) which does not dissolve 123. The reacted samples were washed with DMFA to dissolve the iodide products. The resulting solutions were analyzed for Y, Cu, Ba, and I. The copper content was found to exceed that expected from the 3:2 Cu-Ba ratio of the starting material indicating that the orthorhombic 123 compound from the reaction was deficient in

Cu. 60-80% of the iodine also turned up in solution. DD was used to get the individual phases into solution for elemental analysis. The results showed BaI_2, $YBa_2Cu_{3-x}O_yI_z$, $YBa_2Cu_3O_y$, and CuI (oxygen could not be determined).

These same authors wrote another paper on SEM, TEM, and electron diffraction results in the iodinated 123 system[62]. Both powders and single crystals were investigated and several stages of the reaction were presented. The first stage is the formation of a thin layer of the primary reaction product. Next the primary product crystallizes and CuI crystals are produced. In stage three needle-like BaI_2 crystals grow in. Acetone washes removed the BaI_2 and DMFA was used to dissolve off the CuI. The washed product consists of a cracked surface covered by a thin film of amorphous material probably containing Y_2O_3, YOI, $Y_2Cu_2O_5$, and possibly others. It was proposed that Cu^+ diffused out of the matrix as the oxidation by iodine progressed. This Cu^+ combined with I^- to form CuI. The Cu was depleted from the underlying 123 leading to decomposition into various oxides. These oxides then reacted with iodine to form BaI_2 crystals and amorphous yttrium compounds.

E. B. Amitin et al. have used ^{35}Cl NMR, Cu K x-ray absorption near edge structure (XANES), and x-ray Cu Lα fluorescence on chlorinated samples of 123-$O_{6.9}$[63]. Samples were washed prior to analysis and the formula from chemical analysis was $YBa_{2.01}Cu_{2.92}O_{6.54}Cl_{0.61}$. The NMR results gave three peaks with intensity integrals of 1:3.6:1.8. This corresponds to 16% of Cl in one position, 56% in another, and 28% in the last. Three clear peaks would not be observed if the Cl were distributed randomly throughout interstitial sites in the sample. Positions in the Cu(1) chains, the apical oxygen

in the Cu pyramids, and in the Y plane were suggested for the iodine. Using synchrotron radiation, absorption spectra were obtained in the K edge regions of Y and Cu. The EXAFS spectrum of 123-$O_{6.9}$ had a few more satellite peaks than the chlorinated sample and because of this the authors claimed that 123-O_7 was not produced.

In 1993, Olesch et al. conducted auger electron spectroscopy (AES) on chlorinated samples [64]. X-ray diffraction saw no difference between starting material and chlorinated samples, with the exception of an increasing diffuse background with increased chlorine exposure. From the auger work some chlorine was seen to enter the bulk. Chlorine concentrations were highest at the surface and approached concentrations typical of pure metal chlorides. The authors claimed this excluded the possibility of Cl entering the 123 lattice. The fact that the Cu/Ba ratio near the surface is lower than in the bulk leads them to the conclusion that volatile copper chlorides or oxychlorides probably got lost from the system. Raman studies were also done. The observed raman peak corresponds to a 123-$O_{6.4}$ phase and it is noted that Cl in the structure should have lead to more dramatic shift.

Infrared spectroscopy on halogenated 123-O_6 showed a slight difference between the halogenated samples and the oxygenated 123 [65]. One vibration at 640 cm^{-1} is not observed in intermediate halogenated compounds whereas in intermediate oxygenated 123 it is observed. No extra vibrations were observed that could be related to the presence of halogens in the lattice and the spectra behaved much like those obtained for the 123 oxides.

Micro-raman data obtained by Faulques et al. on some needles found in 123/I samples indicated the presence of I_5^- and I_3^- [66]. XPS analysis showed the presence of I_5^- and I_3^- on the surface and two other large peaks. These other peaks were postulated to be from one of two things, either from iodine atoms at interstitial positions or from secondary phases formed in the reaction with iodine.

Mokhtari et al. used extended hückel tight-binding calculations to find which sites should be preferred by the halogens[67]. These calculations indicated that Br and Cl preferred the Cu(1) oxygen site. Despite this preference, no difference has been observed by anybody in the x-ray diffraction patterns of halogenated and oxygenated 123.

VII. Experimental

Samples of 123-O_7 were reduced in flowing N_2 to form the insulating 123-O_6 phase. Appropriate amounts of this 123-O_6 and I_2 were sealed in silica tubes. The end of the tube was submersed in liquid nitrogen while the tube was sealed to keep iodine from leaving the system. Two molar ratios of reactants were used, either an I/123 ratio of 1:1 or 0.5:1. Reactions were carried out in a muffle furnace for different lengths of time at either 250°C or 400°C. Times ranged from three to twenty hours. When the products were removed from the tubes solid iodine was almost always found in the end opposite the sample.

X-ray powder diffraction and magnetic susceptibility measurements were performed on the samples. The diffraction patterns are given in figure 38 for the 1:1 reactions. Some impurity peaks could be seen in some samples and were close to those

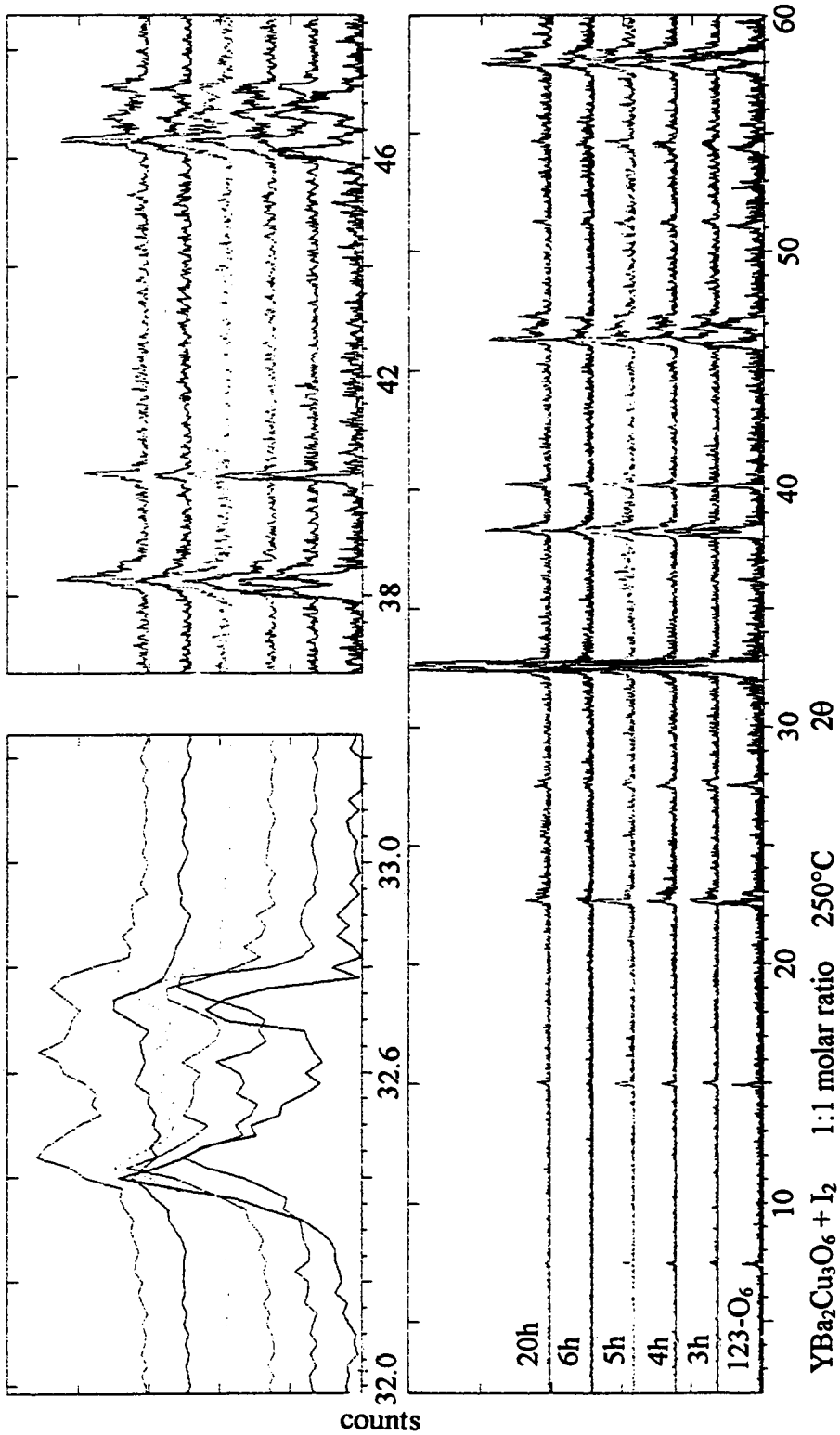

Figure 38: XRD of $YBa_2Cu_3O_6$ reacted with iodine for various times

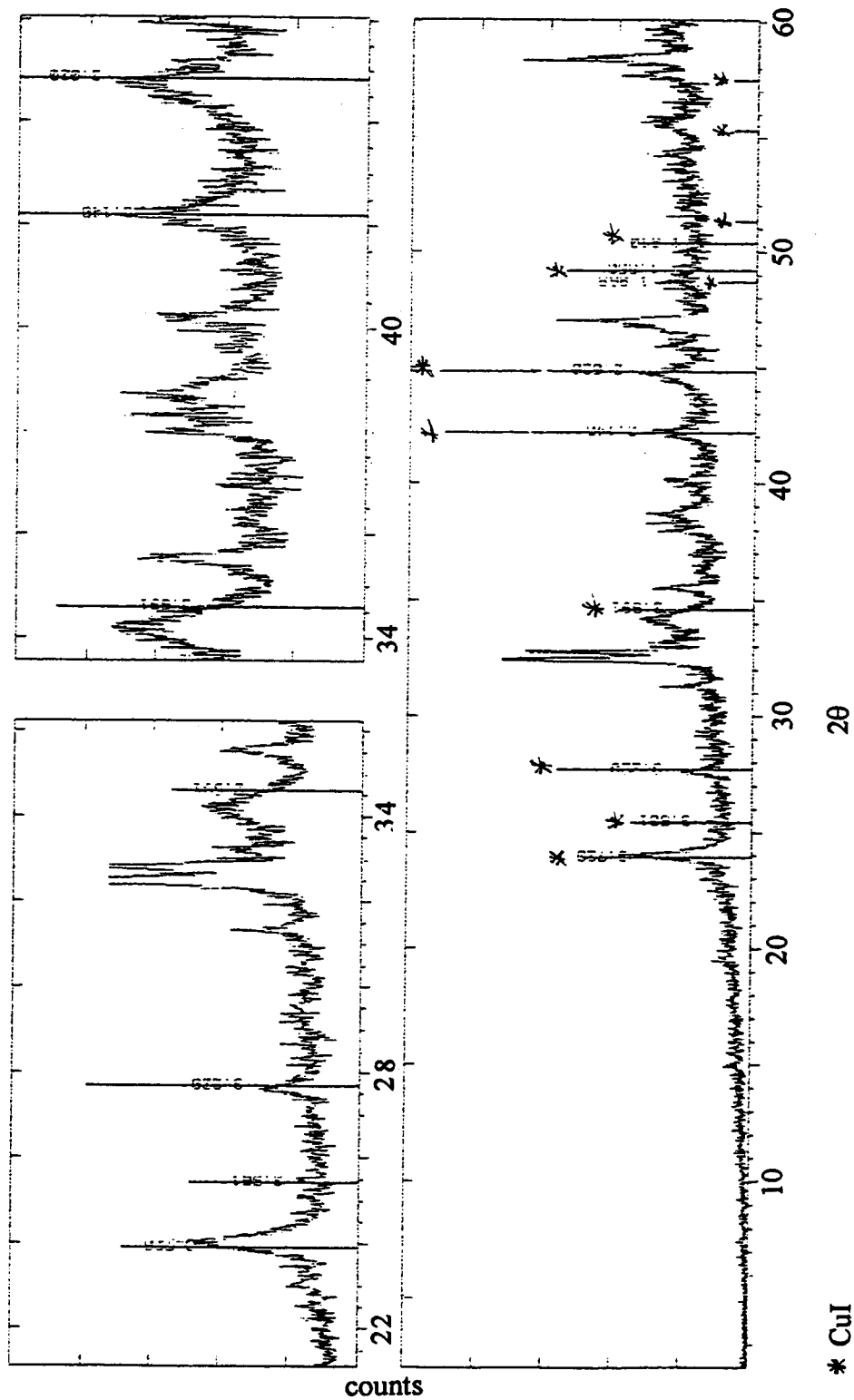

Figure 39: XRD of a sample showing impurity peaks

obtained from CuI (Fig 39), but in general any impurity peaks could not be matched. The magnetic susceptibility measurements gave results similar to those reported in the literature. Transitions were observed between 50 and 60 K (Fig 40).

Microprobe analysis was also attempted on these samples but was not very revealing. The samples had small particle sizes (on the order of a couple micrometers)and were heterogeneous (Fig.41). This made them hard to analyze, as the electron beam was averaging over entire particles.

We were unable to shed any more light on the reaction between $YBa_2Cu_3O_6$ and I_2. X-ray powder data and susceptibility measurements gave results similar to those found in the literature. It was hoped that electron microprobe analysis would be able to show a change in iodine concentrations with depth, but due to small particle size these efforts didn't yield any new insight.

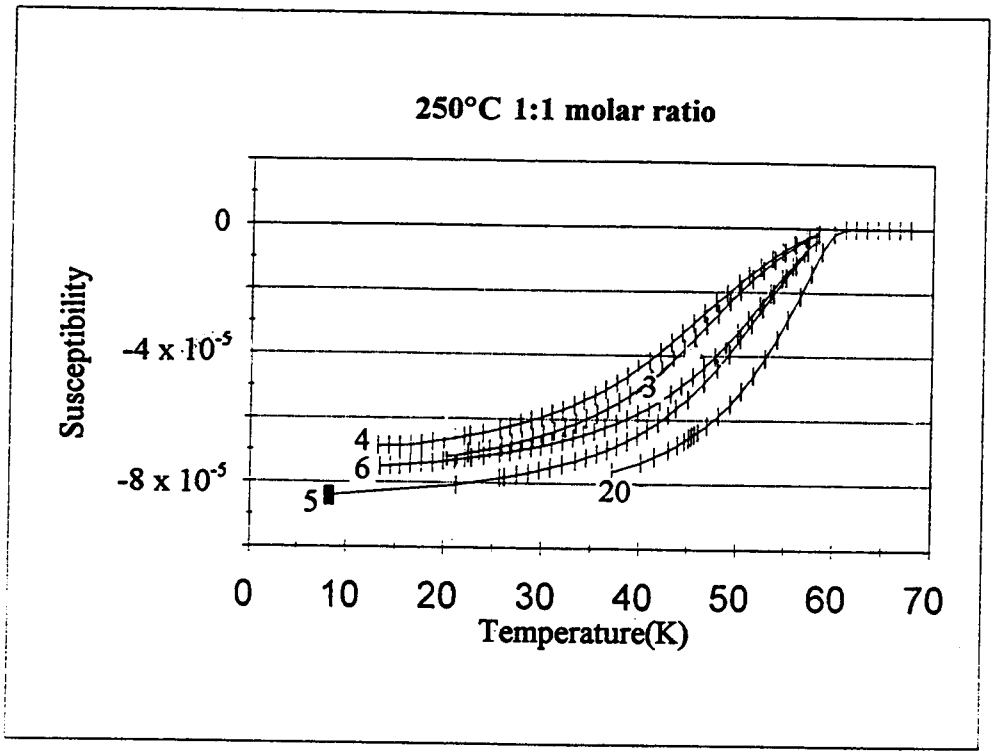

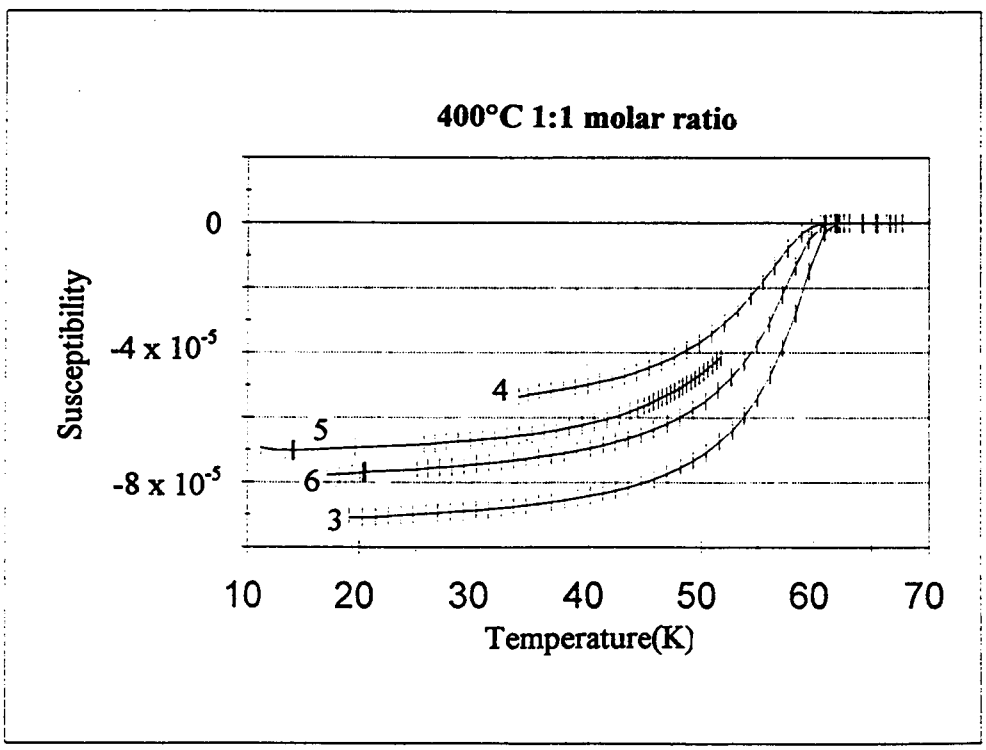

Figure 40: Magnetic susceptibility data

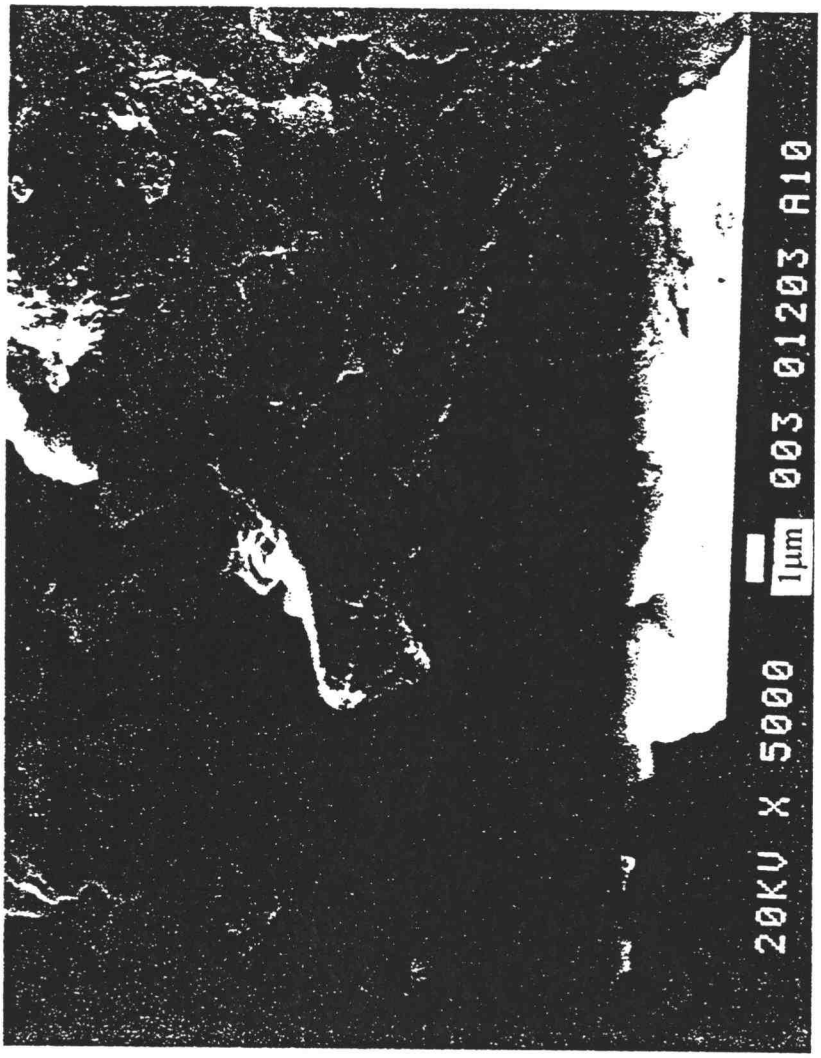

Figure 41: Scanning electron microscopy (SEM) picture of small particle size

References

49.) Yu. A. Osipyan, O. V, Zharikov, G. V. Novikov, N. S. Sidorov, V. I. Kulakov, L. V. Sypavina, R. K. Nikolaev, and A. M. Gromov, *Physica C,* **159,** 137-140 (1989).

50.) Yu. A. Ossipyan and O. V. Zharikov, *Physica C,* **162-164,** 79-80, (1989).

51.) Yu. A. Ossipyan, O. V. Zharikov, A. M. Gromov, V. K. Kulakov, R. K. Nikolaev, N. S. Sidorov, Yu. S. Grushko, Yu. V. Ganzha, M. F. Kovalev, L. I. Molkanov, E. F. Makarov, and A. T. Maylybaev, *Physica C,* **171,** 311-314, (1990).

52.) Yu. T. Pavlyukhin, A. P. Nemudry, N. G. Khainovsky, and V. V. Boldyrev, *Solid State Comm.,* **72,** 107-112, (1989).

53.) Yu. A. Ossipyan, O. V. Zharikov, G. Yu. Logvenov, N. S. Sidorov, V. I. Kulakov, I. M. Shmytko, I. K.. Bdikin, and A. M. Gromov, *Physica C,* **165,** (1990).

54.) Yu. A. Ossipyan, Yu. S. Greznev, V. L. Matukhin, I. A. Safin, N. S. Sidorov, G. B. Teitelbaum, and O. V. Zharikov, *Solid State Comm.,* **74,** 617-619, (1990).

55.) V. L. Matukhin, I. A. Safin, V. N. Anashkin, O. V. Zharikov, and Yu. A. Ossipyan, *Solid State Comm.,* **79,** 1063-1065, (1991).

56.) A. P. Nemudry, Yu. T. Pavlukhin, N. G. Hainovsky, and V. V. Boldyrev, *J. Solid State Chem.,* **93,** 1-8, (1991).

57.) M. Mokhtari, C. Perrin, O. Peña, A. Perrin, and M. Sergent, *Material Lett.,* **13,** 241-253 (1992).

58.) H. B. Radousky, R. S. Glass, P. A. Hahn, M. J. Fluss, R. G. Meisenheimer, B. P. Bonner, C. I. Mertzbacher, E. M. Larson, K. D. McKeegan, J. C. O'Brien, J. L. Peng, R. N. Shelton, and K. F. McCarty, *Physical Rev. B,* **41,** 11140-11148, (1990).

59.) E. Kemnitz, T. Olesch,and N. Pruss, *Mat. Res. Bull.,* **25,** 1019-1024, (1990).

60.) A. P. Nemudry, B. B. Bokhonov, S. S. Shatskaya, V. V. Boldyrev, I. G. Vasilyeva, and N. F. Zakharchuk, *Physica C,* **211,** 366-374, (1993).

61.) A. P. Nemudry, I. I. Gainutdinov, Yu. T. Pavlyukhin, and V. V. Bodyrev, *Physica C,* **211,** 375-379, (1993).

62.) B. B. Bokhonov, A. P. Nemudry, Yu. T. Pavlukhin, and V. V. Boldyrev, *Materials Letters,* **16,** 53-56, (1993).

66E63.) B. . Amitin, N. V. ausck, S. A. Gromilov, S. G. Kozlova, N. K. Moroz, L. N. Mazalov, V. N. Naumov, P. P. Samoilov, S. A. Slobodjan, M. A. Starikov, V. B. Fedorov, G. I. Frolova, and S. . Brenburg, *Physica C,* **209,** 407-414, (1993).

64.) T. Olesch, B. Kemnitz, A. M. Gas'kov, T. A. Kouznetsova, and G. N. Maso, *Physica C,* **218,** 443-448, (1993).

65.) . Gacel, P. Caillet, M. Mokhtari, and C. Perrin, *Physica C,* **235-240,** 849-850, (1994).

66.) B. Faulques, P. Molinié, P. erdahl, T. P. Nguyen, and J. -L. Mansot, *Physica C,* **219,** 297-314, (1994).

67.) M. Mokhtari, C. Perrin, M. Sergent, B. Furet, J. -F. Halet, J. -Y Saillard, B. Ressouche, and P. urlet, *Solid State Comm.,* **93,** 487-492, (1995).

VIII. Conclusion

This thesis has shown that a new series of compounds with the formula Ca_xNbO_3 has been discovered. The range of composition varies from x = 0.66 to about x = 0.86. The structure of $Ca_{0.66}NbO_3$ is orthorhombic, possibly space group Pnma, with a = 5.518Å, b = 7.824Å, and c = 5.516Å. Both the initial sample and the refined structure had a calcium content of 0.66. Samples with the starting composition of $Ca_{0.96}NbO_3$ are monoclinic, space group $P2_1/m$, with a = 5.520Å, b = 7.884Å, c = 5.608Å, β = 90.013°, and a refined calcium content of 0.86.

A good quality crystal was obtained from a sample of initial composition of $Ca_{0.76}NbO_3$. The crystal refined as cubic, space group Pm-3m with a cell edge of 7.828Å to an R value of 2.26% and weighted R of 4.09%. The calcium content refined to a value of 0.75. The crystal shows evidence of A site cation and vacancy ordering which is not common in perovskite structures. Additional film work indicated the presence of a much larger cell with an edge of eight times the simple perovskite unit cell edge.

In other work in this thesis it was shown that NbN was responsible for the superconducting transition observed in the products of the ignition reactions of Nb metal, barium or strontium peroxide, in air. No new barium niobium oxide was found in this system. Of other metals tried, only Ta was found to also produce a nitride phase.

Reactions of $YBa_2Cu_3O_6$ and I_2 were studied, but no new insight was gained in these reactions. X-ray powder diffraction and magnetic susceptibility data replicated results found in the literature. Electron microprobe analysis was unable to determine the

location of iodine in the samples due to the heterogeneous nature and small particle size of the reaction products.

Bibliography

1.) M. J. Geselbracht, T. J. Richardson, and A. M. Stacy, *Nature*, **345**, 324 (1990).

2.) J.Bardeen, L. N. Cooper, and J. R. Schrieffer, *Phys. Rev.*, **B108**, 1175-1204 (1957).

3.) A. Metha, A. Navrotsky, N. Kumada, and N. Kinomura, *J. Solid State Chem.*, **102**, 213-225 (1993).

4.) M. E. Lines and A. M. Glass, Principles and Applications of Ferroelectrics and Related Materials, Clarendon Press, Oxford, 1977.

5.) S. C. Abrahams and P. Marsh, *Acta Cryst.*, **B42**, 61-68 (1986).

6.) N. Kumada, S. Muramatu, F. Muto, N. Kinomura, S. Kikkawa, and M. Koizumi, *J. Solid State Chem.*, **73**, 33-39 (1988).

7.) A. C. Sakowski-Cowley, K. Lukaszewicz, and H. D. Megaw, *Acta Cryst.*, **B25**, 851-865, (1969).

8.) M. Ahtee, A. M. Glazer, and H. D. Megaw, *Phil. Mag.*, **26**, 995-1014, (1972).

9.) A. M. Glazer and H. D. Megaw, *Phil. Mag.*, **25**, 1119-1135, (1972).

10.) M. H. Francombe and B. Lewis, *Acta Cryst.*, **11**, 175-178, (1958).

11.) L. Katz and H. D. Megaw, *Acta Cryst.*, **22**, 639-648, (1967).

12.) M. Serafin and R. Hoppe, *J. Less-Common Metals*, **76**, 299-316, (1980).

13.) G. Meyer and R. Hoppe, *Z. anorg. allg. Chem.*, **436**, 75-86, (1977).

14.) G. Meyer, R. Hoppe, and M. Jansen, *Naturwissenschaften*, **63**, 386, (1976).

15.) J. Sieler, B. Kreßner, and H. Holzapfel, *Z. Chem.*, **8**, 33, (1968).

16.) A. M. Abakumov, R.V. Shpanchenko, and E.V. Antipov, *Mat. Res. Bull.*, **30**, 97-103, (1995).

17.) J. Sturm and R. Gruehn, *Naturwissenschaften*, **62**, 296, (1975).

18.) K. Ishikawa, G. Adachi, and J. Shiokawa, *Mat. Res. Bull.*, **18**, 653-661, (1983).

19.) M. T. Casais, J. A. Alonso, I. Rasines, and M. A. Hidalgo, *Mat. Res. Bull.*, **30,** 201-208, (1995).

20.) G. Svensson and P. Werner, *Mat. Res. Bull.*, **25,** 9-14, (1990).

21.) R. R. Kreiser and R. Ward, *J. Solid State Chem.*, **1,** 368-371, (1970).

22.) B. Hessen, S. A. Sunshine, T. Siegrist, and R. Jimenez, *Mat. Res. Bull.*, **26,** 85-90, (1991).

23.) D. Ridgley and R. Ward, *Am. Chem. Soc.*, **77,** 6132-6136, (1955).

24.) K. Isawa, J. Sugiyama, K. Matsuura, A. Nozaki, and H. Yamauchi, *Phys. Rev. B,* **47,** 123-127, (1993).

25.) V. J. Tennery, *J. Am. Ceramic Soc.*, **51,** 183-186, (1968).

26.) A. Molak, M. Pawelczyk, and J. Kwapulinski, *J. Phys.:Condens. Matter,* **6,** 6833-6842, (1994).

27.) C. Manolikas, G. Van Tendeloo, and S. Amelinckx, *Solid State Comm.*, **58,** 845-849, (1986).

28.) K. Isawa, R. Itti, J. Sugiyama, N. Koshizuka, and H. Yamamauchi, *Phys. Rev. B.*, **48,** 7618-7623, (1993).

29.) H. Brusset, H. Gillier-Pandraud, and P. Rajaonera, *Mat. Res. Bull.*, **10,** 209-216, (1975).

30.) P. B. Jamieson, S. C. Abrahams, and J. L. Bernstein, *J. Chem. Phys.*, **48,** 5048- 5057, (1968).

31.) J. Akimitsu, J. Amano, H. Sawa, O. Hagase, K. Gyoda, and M. Kogai, *Jpn. J. Appl. Phys.*, **30,** L1155-L1156, (1991).

32.) S. Y. Istomin, O. G. D'yanchenko, E. V. Antipov, *Mat. Res. Bull.*, **29,** 743-749, (1994).

33.) A. Nakamura, *Jpn. J. Appl. Phys.*, **33,** L583-L586, (1994).

34.) V. A. Gasparov, G. K. Strukova, and S. S. Khassanov, *Jour. Exper. Theor. Phys.*, **60,** 440-444, (1994).

35.) S. J. Reed, Electron Microprobe Analysis 2nd ed.,Cambridge University Press, 1993.

36.) S. Geller, *J. Chem. Phys.*, **24,** 1236-1239, (1950).

37.) A. M. Glazer, *Acta Cryst.*, **B28,** 3384-3392, (1972).

38.) Suggested modifications of Glazer by Pat Woodward

39.) B. Hessen, S. A. Sunshine, T. Siegrist, and R. Jimenez, *Mat. Res. Bull.*, **26,** 85-90, (1991).

40.) A. M. Abakumov, R. V. Shpanchenko, and E. V. Antipov, *Mat. Res. Bull.*, **30,** 97-103, (1995).

41.) P. N. Iyer and A. J. Smith, *Acta Cryst.*, **23,** 740-746, (1967).

42.) Y. Torii, *Chem. Lett.*, **1979,** 1215-1218.

43.) M. Abe and K. Uchino, *Mat. Res. Bull.*, **9,** 147-156, (1974).

44.) Instruction Manual, Model 7000 AC Susceptometer, 1989, Lake Shore Cryotronics, Inc.

45.) P. E. Bacon, J. G. Hou, A. W. Sleight, and R. L. Nielsen, this work is currently in press.

46.) V. A. Gasparov, G. K. Strukova, and S. S. Khassanov, *Jour. Exper. Theor. Phys.*, **60,** 440, (1994).

47.) M. J. Geselbracht, T. J. Richardson, and A. M. Stacy, *Nature*, **345,** 324, (1990).

48.) A. Christensen, *Acta Chem. Scand. A*, **31,** 77, (1977).

49.) Yu. A. Osipyan, O. V, Zharikov, G. V. Novikov, N. S. Sidorov, V. I. Kulakov, L. V. Sypavina, R. K. Nikolaev, and A. M. Gromov, *Physica C*, **159,** 137-140 (1989).

50.) Yu. A. Ossipyan and O. V. Zharikov, *Physica C*, **162-164,** 79-80, (1989).

51.) Yu. A. Ossipyan, O. V. Zharikov, A. M. Gromov, V. K. Kulakov, R. K. Nikolaev, N. S. Sidorov, Yu. S. Grushko, Yu. V. Ganzha, M. F. Kovalev, L. I. Molkanov, E. F. Makarov, and A. T. Maylybaev, *Physica C*, **171,** 311-314, (1990).

52.) Yu. T. Pavlyukhin, A. P. Nemudry, N. G. Khainovsky, and V. V. Boldyrev, *Solid State Comm.*, **72,** 107-112, (1989).

53.) Yu. A. Ossipyan, O. V. Zharikov, G. Yu. Logvenov, N. S. Sidorov, V. I. Kulakov, I. M. Shmytko, I. K.. Bdikin, and A. M. Gromov, *Physica C*, **165,** (1990).

54.) Yu. A. Ossipyan, Yu. S. Greznev, V. L. Matukhin, I. A. Safin, N. S. Sidorov, G. B. Teitelbaum, and O. V. Zharikov, *Solid State Comm.*, **74,** 617-619, (1990).

55.) V. L. Matukhin, I. A. Safin, V. N. Anashkin, O. V. Zharikov, and Yu. A. Ossipyan, *Solid State Comm.*, **79,** 1063-1065, (1991).

56.) A. P. Nemudry, Yu. T. Pavlukhin, N. G. Hainovsky, and V. V. Boldyrev, *J. Solid State Chem.*, **93,** 1-8, (1991).

57.) M. Mokhtari, C. Perrin, O. Peña, A. Perrin, and M. Sergent, *Material Lett.*, **13,** 241-253 (1992).

58.) H. B. Radousky, R. S. Glass, P. A. Hahn, M. J. Fluss, R. G. Meisenheimer, B. P. Bonner, C. I. Mertzbacher, E. M. Larson, K. D. McKeegan, J. C. O'Brien, J. L. Peng, R. N. Shelton, and K. F. McCarty, *Physical Rev. B,* **41,** 11140-11148, (1990).

59.) E. Kemnitz, T. Olesch,and N. Pruss, *Mat. Res. Bull.*, **25,** 1019-1024, (1990).

60.) A. P. Nemudry, B. B. Bokhonov, S. S. Shatskaya, V. V. Boldyrev, I. G. Vasilyeva, and N. F. Zakharchuk, *Physica C,* **211,** 366-374, (1993).

61.) A. P. Nemudry, I. I. Gainutdinov, Yu. T. Pavlyukhin, and V. V. Bodyrev, *Physica C,* **211,** 375-379, (1993).

62.) B. B. Bokhonov, A. P. Nemudry, Yu. T. Pavlukhin, and V. V. Boldyrev, *Materials Letters,* **16,** 53-56, (1993).

63.) E. B. Amitin, N. V. Bausck, S. A. Gromilov, S. G. Kozlova, N. K. Moroz, L. N. Mazalov, V. N. Naumov, P. P. Samoilov, S. A. Slobodjan, M. A. Starikov, V. E. Fedorov, G. I. Frolova, and S. B. Erenburg, *Physica C,* **209,** 407-414, (1993).

64.) T. Olesch, E. Kemnitz, A. M. Gas'kov, T. A. Kouznetsova, and G. N. Maso, *Physica C,* **218,** 443-448, (1993).

65.) B. Gacel, P. Caillet, M. Mokhtari, and C. Perrin, *Physica C,* **235-240,** 849-850, (1994).

66.) E. Faulques, P. Molinié, P. Berdahl, T. P. Nguyen, and J. -L. Mansot, *Physica C,* **219,** 297-314, (1994).

67.) M. Mokhtari, C. Perrin, M. Sergent, E. Furet, J. -F. Halet, J. -Y Saillard, E. Ressouche, and P. Burlet, *Solid State Comm.*, **93,** 487-492, (1995).